TESE DE DOUTORAMENTO

GOLD(I)-CATALYZED ENANTIOSELECTIVE ADDITION AND CYCLOADDITION REACTIONS

Jaime Fernández Casado

DECLARACIÓN DO AUTOR DA TESE

Gold(I)-catalyzed enantioselective addition and
cycloaddition reactions

D. Jaime Fernández Casado

Presento miña tese, seguindo o procedemento adecuado ao Regulamento, e declaro que:

1) A tese abarca os resultados da elaboración do meu traballo.

2) No seu caso, na tese se fai referencia as colaboracións que tivo este traballo.

3) A tese é a versión definitiva presentada para a súa defensa e coincide ca versión enviada en formato electrónico.

4) Confirmo que a tese non incorre en ningún tipo de plaxio de outros autores nin de traballos presentados por min para a obtención de outros títulos.

En Santiago de Compostela, 16 de Maio de 2018

Asdo. Jaime Fernández Casado

AUTORIZACIÓN DO
DIRECTOR / TITOR DA TESE

Gold(I)-catalyzed enantioselective addition and cycloaddition reactions

D. José Luis Mascareñas Cid
D. Fernando José López García

INFORMAN:

Que a presente tese, correspóndese co traballo realizado por D. Jaime Fernández Casado, baixo a miña dirección, e autorizo a súa presentación, considerando que reúne os requisitos esixidos no Regulamento de Estudos de Doutoramento da USC, e que como director desta non incorre nas causas de abstención establecidas na Lei 40/2015.

En Santiago de Compostela, 16 de Maio de 2018

Asdo. José Luis Mascareñas Cid   Asdo. Fernando José López García

Table of contents

Disclaimer

Throughout this thesis, when referring to cycloadditions we use the Huisgen notation, using parenthesis, where the numbers refer to the atoms involved in the forming ring (for instance in (4+3), (4+2), (2+2) cycloadditions) to distinguish from the Woodward-Hoffman notation, using brackets, where the numbers refer to the electrons involved in bonding changes.[1] However, in some specific examples we use the brackets notation that is also acceptable.

---

[1] (a) R. Huisgen, *Angew. Chemie Int. Ed.* **1968**, *7*, 321. (b) J. Limanto, K. S. Khuong, K. N. Houk, M. L. Snapper, *J. Am. Chem. Soc.* **2003**, *125*, 16310.

Abbreviations and acronyms

Ac	Acetyl/CH₃CO-	DTBM-	(6,6'-dimethoxy-[1,1'-
BArᶠ	Tetrakis[3,5-bis(trifluoromethyl)phenyl]borate	BIPHEP	biphenyl]-2,2'-diyl)bis(bis(3,5-di-tert-butyl-4-methoxyphenyl)phosphane)
BINAP	2,2'-Bis(diphenylphosphino)-1,1'-binaphthalene	DETBM-SEGPHOS	5,5'-Bis[di(3,5-di-tert-butyl-4-methoxyphenyl)phosphino]-4,4'-bi-1,3-benzodioxole
BINOL	1,1'-Bi(2-naphthol)	DTBP	2,6-di-*tert*-butyl pyridine
bmim	1-Butyl-3-methylimidazolium	DuPhos	(−)-1,2-Bis[(2*R*,5*R*)-2,5-dimethylphospholano]benzene
Bn	Benzyl/C₆H₅CH₂		
Boc	*tert*-Butyloxycarbonyl		
bpy	2,2'-bipyridine		
br	Broad	DuanPhos	(1R,1'R,2S,2'S)-2,2'-Di-tert-butyl-2,3,2',3'-tetrahydro-1H,1'H-(1,1')biisophosphindolyl
Bz	Benzoyl/C₆H₅CO-		
BzOH	Benzoic acid		
CAN	Ceric ammonium nitrate		
COD	1,5-cyclooctadiene	EBX	Ethynyl Benziodoxolone
Cy	Cyclohexyl	EDG	Electron donating group
d	Doublet	ee	Enantiomeric excess
dd	Double doublet	eq/equiv	Equivalents
ddd	Doublet of doublet of doublets	er	Enantiomeric ratio
		ESI	Electrospray
dq	Doublet of quartet	EWG	Electron withdrawing group
dt	Doublet of triplets	fluorenone	4,5-Diazafluoren-9-one
dba	dibenzylideneacetone	GC-MS	Gas chromatography mass spectrometry
DAD	Diode array detector		
DBM	2,2-dimethylbutane	HOMO	Highest occupied molecular orbital
DBU	1,8-Diazabicyclo[5.4.0]undec-7-ene	HPLC	High performance liquid chromatography
DCE	1,2-dichloroethane	HRMS	High resolution mass spectra
DET	Diethyl tartrate	IMes	1,3-Bis(2,4,6-trimethylphenyl)imidazol-2-ylidene
DFT	Density functional theory		
DMAP	4-dimethylaminopyridine		
DME	Dimethoxy ethane	IPr	1,3-Bis(2,6-diisopropylphenyl)imidazol-2-ylidene
DMF	*N,N*-dimethyl formamide		
DMSO	Dimethyl sulfoxide		
DPP	Diphenyl phosphoric acid	JohnPhos	(2-Biphenyl)di-tert-butylphosphine
dppm	Bis(diphenylphosphino)methane		
		LRMS	Low resolution mass spectra
dppp	1,3-Bis(diphenylphosphino)propane	LUMO	Lowest unoccupied molecular orbital
		m	Multiplet
d.r.	Diastereomeric ratio	min	Minute/s

Ms	Methanesulfonyl		THP	Tetrahydropyran
MS	Molecular sieves		TIPS	Triisopropylsilyl
MTBE	Methyl-*tert*-butyl ether		TLC	Thin layer chromatography
nOe	Nuclear Overhauser effect		TMS	Trimethylsilyl
NTf₂	bis(trifluoromethanesulfonyl)imide		Tol	Tolyl
NHC	*N*-heterocyclic carbene		TPS	Triphenylsilyl
NMR	Nuclear magnetic resonance		Ts	*para*-toluenesulfonyl/Tosyl
PDC	Pyridinium dichromate		TunePhos	(R)-1,13-Bis(diphenylphosphino)-7,8-dihydro-6H-dibenzo[f,h][1,5]dioxonin
PG	Protecting group			
PhanePhos	(*R*)-(–)-4,12-Bis(diphenylphosphino)-[2.2]-paracyclophan			
			UHPLC	Ultra-high performance liquid chromatography
phen	1,10-phenanthroline		VAPOL	2,2'-Diphenyl-(4-biphenanthrol)
Piv	Pivaloyl/(CH₃)₃CCO-			
P(O-*o*-biPh)₃	tris(2-phenylphenyl)phosphite		VANOL	3,3'-Diphenyl-2,2'-bi-1-naphthalol
PTAD	2-((3r,5r,7r)-adamantan-1-yl)-2-(1,3-dioxoisoindolin-2-yl)acetate		Xantphos	4,5-Bis(diphenylphosphino)-9,9-dimethylxanthene
			XPhos	2-Dicyclohexylphosphino-2',4',6'-triisopropylbiphenyl
p-TsOH	*para*-toluenesulfonic acid			
Pyrr	Pyrrolidine			
q	Quartet			
rt	Room temperature			
RuPhos	2-Dicyclohexylphosphino-2',6'-diisopropoxybiphenyl			
s	Singlet			
SOMO	Singly occupied molecular orbital			
SPhos	2-Dicyclohexylphosphino-2',6'-dimethoxybiphenyl			
SPINOL	2,2',3,3'-tetrahydro-1,1'-spirobi[indene]-7,7'-diol			
SYNPHOS	6,6'-Bis(diphenylphosphino)-2,2',3,3'-tetrahydro-5,5'-bibenzo[b][1,4]dioxine			
t	Triplet			
t	time			
td	Triple doublet			
T	Temperature			
TA	Triazole			
TBDPS	*tert*-butyldiphenylsilyl			
TBS	*tert*-butyldimethylsilyl			
TFA	Trifluoroacetic acid			
Tf	Trifluoromethanesulfonyl			
THF	Tetrahydrofuran			

Introduction

Chemistry is defined as the science that studies the structure, properties and transformations of matter from its molecular composition and along with biology, physics and medicine, constitutes one of the pillars of the well-fare and the technological progress of our society. From molecular biology to molecular computing, molecular medicine, molecular (nano) technology and even molecular gastronomy, science is becoming increasingly integrated and "molecularized".[2]

This growing molecular perspective of most branches of science increases the need to have molecules of synthetic origin. Chemists have been laying out the foundations for this molecular revolution for the past two centuries, where organic synthesis emerges as a central and fundamental branch of knowledge, allowing chemists to design, manipulate and construct complex molecules from atoms and/or simpler derivatives.[3]

Many natural products with relevant biological properties present relatively complex molecular structures featuring different type of polycyclic skeletons and a number of stereogenic centers (Figure 1). Despite the huge amount of methods and new reactions discovered by chemists over the last century, our ability to build this type of skeletons is still very limited. In the 21st century, synthetic chemistry still faces many challenges and new methodologies are needed to allow a rapid and practical access to these complex structures in an efficient manner.[4,5]

strychnine
R. B. Woodward (1954)

taxol
K. C. Nicolaou (1994)

endiandric acid A
K. C. Nicolaou (1982)

tetrodotoxin
Y. Kishi (1972)

progesterone
W. S. Johnson (1971)

(-)-englerin A
J. L. Mascareñas & F. López (2016)
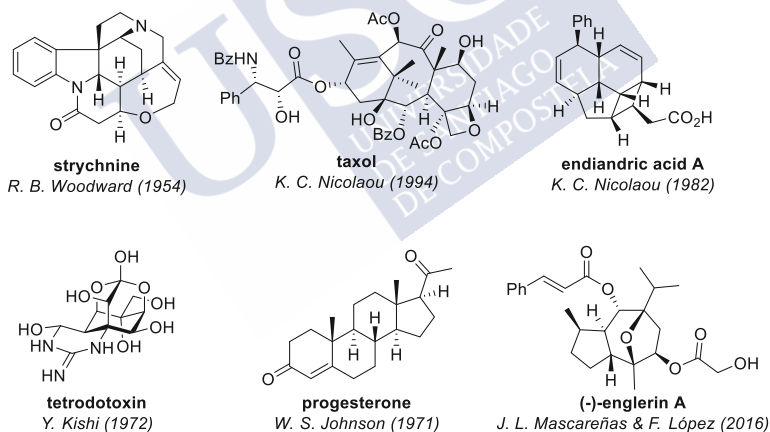
Figure 1. Examples of cyclic natural products with an important biological activity.

Not only is the preparation of this type of natural products needed. Often, subtle modifications on the core of these natural products, or entirely new designed molecules, can have superior properties and interesting new functions. Therefore, a major goal in

[2] P. A. Wender, B. L. Miller, *Nature* **2009**, *460*, 197.

[3] C. A. Kuttruff, M. D. Eastgate, P. S. Baran, *Nat. Prod. Rep.* **2014**, *31*, 419.

[4] (a) K. C. Nicolaou, E. J. Sorensen, *Classics in Total Synthesis: targets, strategies, methods*, Wiley-VCH, **1996**. (b) K. C. Nicolaou, S. A. Snyder, *Classics in Total Synthesis II: more targets, strategies, methods*, Wiley-VCH, **2003**. (c) E. J. Corey, J. J. Li, *Total Synthesis of Natural Products: At the Frontiers of Organic Chemistry*, Springer, **2012**.

[5] R. Nelson, M. Gulías, J. L. Mascareñas, F. López, *Angew. Chemie - Int. Ed.* **2016**, *55*, 14359.

organic synthesis is the development of new methodologies that allow access to complex molecular skeletons in few steps from commercially available and inexpensive precursors and reagents, with high efficiency and minimizing the amount of waste.[6]

In this context, the development of **catalytic processes** is particularly appealing. Since its origins, catalysis has experienced exponential growth, and nowadays, we seldom find a synthetic route that does not have a step that entails a catalytic process. There are different catalytic strategies depending on the type of molecules used as catalysts. These include simple bases and acids, enzymes (biocatalysis),[7] organic molecules (organocatalysis)[8] or metal complexes (**organometallic catalysis**).[9] Moreover, in recent years, the development of new synthetic methods that combine two or more different types of catalysts (i.e. **cooperative and synergistic catalytic processes**),[10] has experienced an important growth, facilitating the catalytic and stereoselective access to complex structures from simple molecules.

1. Transition metal catalysis and multicatalytic processes

Transition metals, due to their coordination abilities, range of electronegativities and the ability to change their oxidation state, offer many possibilities to generate reactive intermediates under mild conditions. Thus, they are powerful tools to promote organic transformations that usually are difficult to accomplish under thermal or photochemical conditions.

The impact of organometallic chemistry in organic synthesis is reflected in the fact that several synthetic methodologies, involving the use of transition metal catalysts, have deserved the Nobel Prize recognition (Figure 2). In 2001, B. Sharpless was awarded for his work on asymmetric epoxidation of allylic alcohols and W. Knowles and R. Noyori for their work on asymmetric hydrogenation of unsaturated systems.[11] In 2005, Y. Chauvin, R. Grubbs and R. Schrock were recognized with the Nobel Prize for the development of the alkene metathesis, that entails the metal-promoted redistribution of fragments of olefins by the scission and regeneration of carbon-carbon double bonds. [12] In 2010, Pd-catalyzed cross-couplings, which are among the most practical methods for C-C bond construction, were recognized with the Nobel Prize award to R. Heck (C-C coupling between aryl halides and activated alkenes), E. Negishi (C-C coupling between

---

[6] P. A. Wender, *Tetrahedron* **2013**, *69*, 7529

[7] K. Drauz, H. Waldmann, *Enzyme Catalysis in Organic Synthesis*, 2nd Ed. Wiley-VCH, **2002**.

[8] M. T. Reetz, B. List, S. Jaroch, H. Weinmann, *Organocatalysis*, Springer-Verlag, **2008**.

[9] (a) L. S. Hegedus, B. C. G. Söderberg, *Transition Metals in the Synthesis of Complex Organic Molecules*, 2nd Ed. University Science Books: Sausalito, California, **1999**. (b) D. Astruc, *Organometallic Chemistry and Catalysis*, Springer-Verlag, **2007**.

[10] (a) Z. Du, Z. Shao, *Chem. Soc. Rev.* **2013**, *42*, 1337. (b) A. E. Allen, D. W. C. MacMillan, *Chem. Sci.* **2012**, *3*, 633.

[11] https://www.nobelprize.org/nobel_prizes/chemistry/laureates/2001/

[12] https://www.nobelprize.org/nobel_prizes/chemistry/laureates/2005/

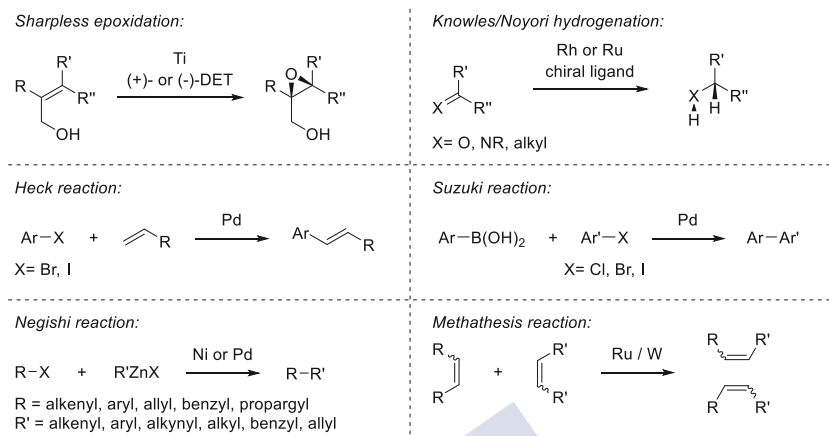organozinc compounds with various halides), and A. Suzuki (C-C coupling between organoboronic acids and halides).[13]

Figure 2. Transition metal catalyzed reaction awarded with a Nobel Prize.

These, and many other transition metal catalyzed methods involve the participation of a single metal catalyst. However, in recent years, the development of catalytic processes combining the participation of two or even more catalysts (dual or multiple catalytic processes) have steadily increased and contributed to improve the power of catalysis. In these processes, the transition metal catalyst is combined with other metal catalyst or alternatively with an organocatalyst, to promote a process which otherwise would not be feasible. As an illustrative example (Figure 3), dual catalysis might involve the simultaneous activation of both a nucleophile and an electrophile using distinct catalysts. Thus, creating two reactive species, one with a higher HOMO and the other with a lower LUMO in comparison to the respective ground state starting materials.
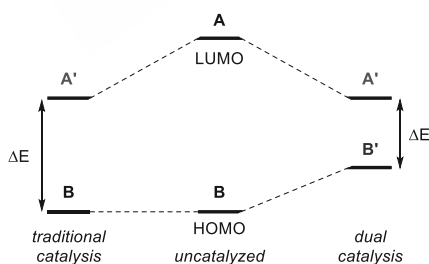

**Figure 3**. The concept of dual (or multi) catalysis.

These multicatalytic processes are generally classified as (a) cooperative, (b) synergistic, and (c) sequential (or relay catalysis).[10]

---

[13] https://www.nobelprize.org/nobel_prizes/chemistry/laureates/2010/

In <u>cooperative catalysis</u>, both catalysts are directly involved in the same catalytic cycle, working cooperatively to afford the product (Scheme 1a). [14]

<u>Synergistic catalysis</u> is considered when the two substrates are simultaneously activated in separate catalytic cycles and, upon the formation of the reactive intermediates, the two catalytic cycles are directly integrated leading to the formation of the corresponding product (Scheme 1b). [15]

In <u>sequential or relay catalysis</u>, the two catalysts are operating in series; the first catalyst activates the substrates towards the formation of a reactive intermediate, which is subsequently transformed in the next catalytic cycle with the aid of the second catalyst, that delivers the product (Scheme 1c). The differences between sequential and relay catalysis relies on the fact that in the first one the addition of another catalyst, reagent or change in reaction conditions is needed after the first catalytic process; while in relay catalysis there is no change in the reaction conditions, so both catalytic processes are directly coupled.
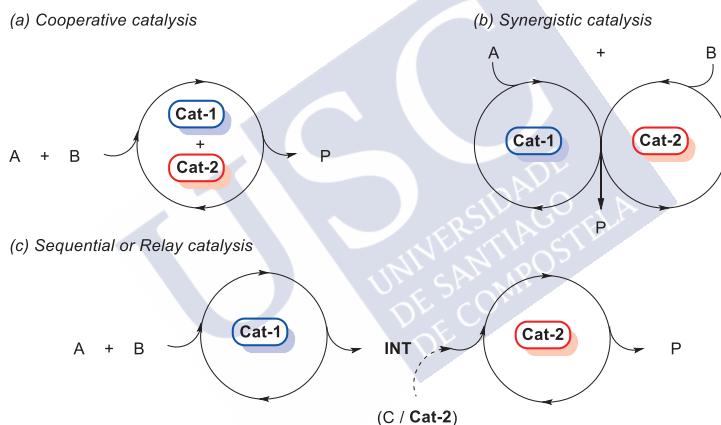
**Scheme 1**. Different types of dual catalysis.

As a representative example of a synergistic process, in 2016 the group of Lee reported a Pd(0)/Rh(II) dual catalytic transformation based on the interceptive coupling of π-allyl Pd(II) complexes **I** with α-imino Rh(II) carbenoids **II**, to afford *N*-allylated (*Z*)-amino vinyl carboxylates. The Pd(0) and Rh(II) catalysts selectively activate each substrate to generate intermediates **I** and **II**, which could get together through the coordination of the pendant α-amine with the Pd atom, facilitating the nucleophilic carboxylate transfer to the carbonic carbon to afford the Rh/Pd zwitterionic intermediate **III**. The elimination of

[10] (a) Z. Du, Z. Shao, *Chem. Soc. Rev.* **2013**, *42*, 1337. (b) A. E. Allen, D. W. C. MacMillan, *Chem. Sci.* **2012**, *3*, 633.

[14] Y. J. Park, J.-W. Park, C.-H. Jun, *Acc. Chem. Res.* **2008**, *41*, 222.

[15] (a) A. E. Allen, D. W. C. MacMillan, *Chem. Sci.* **2012**, *3*, 633. (b) A. Gualandi, L. Mengozzi, C. M. Wilson, P. G. Cozzi, *Chem. - An Asian J.* **2014**, *9*, 984. (c) Y. Deng, S. Kumar, H. Wang, *Chem. Commun.* **2014**, *50*, 4272.

the Rh(II) catalyst gives the carbonyl-coordinated intermediate **IV**, which most likely undergoes reductive *N*-allylation to afford the corresponding product (Scheme 2).[16]
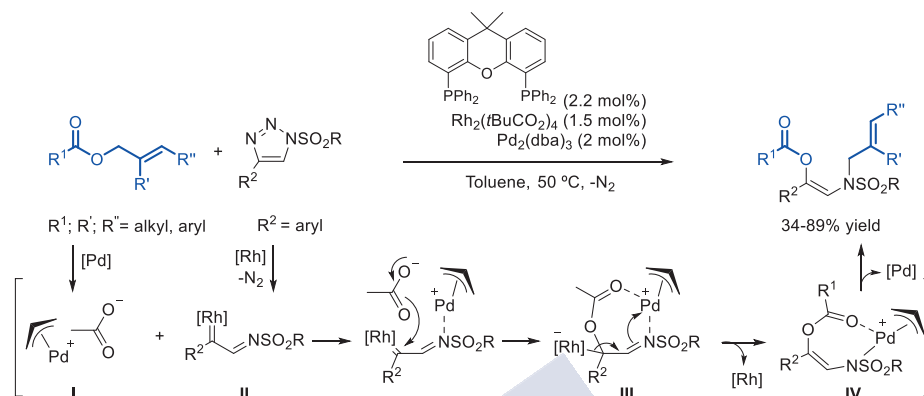
Scheme 2. Synergistic Pd(0)/Rh(II) dual catalysis reported by Lee.

2. Cycloaddition reactions

While the development of metal-promoted methods to make single carbon-carbon or carbon-heteroatom bonds is extremely important in synthetic chemistry, the invention of **annulation/cycloaddition** technologies can be even of higher interest, owing to the innumerable amount of natural products that exhibit cyclic skeletons. In this context, cycloaddition reactions allow the construction of at least one cycle and two bonds in a single synthetic operation from two or more simpler fragments, thus promoting an important rapid increase in structural complexity. In addition, they usually take place with a great atom economy and with excellent selectivity.[17]

In a simplified way, cycloadditions can be classified as forbidden or permitted processes taking into consideration Woodward-Hoffman rules[18] and Fukui's frontier molecular orbital theory.[19] Permitted reactions, *a priori*, may occur spontaneously or by heating, while those forbidden need photochemical conditions, radical initiators or other promoters.[20] Definitely, Diels-Alder reaction is the most relevant cycloaddition, as it

---

[16] Z.-S. Chen, L.-Z. Huang, H. J. Jeon, Z. Xuan, S.-G. Lee, *ACS Catal.* **2016**, *6*, 4914.

[17] (a) S. Kobayashi, K. A. Jørgensen, *Cycloaddition Reactions in Organic Synthesis*, Wiley-VCH, **2001**. (b) P. A. Wender, *Chem. Rev.* **1996**, *96*, 1.

[18] R. Hoffmann, R. B. Woodward, *Acc. Chem. Res.* **1968**, *8*, 781.

[19] S. Inagaki, H. Fujimoto, K. Fukui, *J. Am. Chem. Soc.* **1976**, *98*, 4693.

[20] M. Lautens, W. Klute, W. Tam, *Chem. Rev.* **1996**, *96*, 49.

provides a direct access to six-membered rings from very simple precursors, and has the ability to generate up to four contiguous stereogenic centers in a single step (Scheme 3).[21]
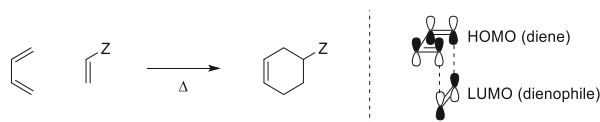
Scheme 3. Diels-Alder reaction.

An example of the usefulness of Diels-Alder reaction and of the increase in structural complexity that can be achieved in a single synthetic step, can be seen in the total synthesis of panepophenanthrin developed by Baldwin's group. As shown in Scheme 4, the reaction provides only one diastereoisomer and allows the generation of four stereogenic centers in one step (Scheme 4).[22]
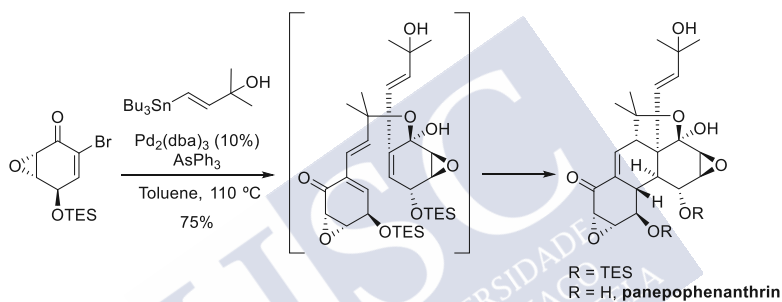
Scheme 4. Total synthesis of Panepophenanthrin.

Despite the versatility of cycloaddition reactions, many of them require the reaction partners to be electronically matched, by incorporating electron-donating or electron-withdrawing groups. In general, the reactivity of inactivated olefins, dienes, and acetylenes is usually very low, and harsh conditions or special methods are needed to promote their cycloadditions.

In this context, transition metal catalysis offers an appealing opportunity to induce such reactivity, because the coordination of transition metal to the unsaturated systems of alkenes, dienes or alkynes significantly modifies their electronic properties. Therefore, the use of transition metal complexes has allowed the development of cycloadditions that otherwise could not be achieved.[23] Moreover, by incorporating chiral ligands at the metal center, it is even possible to achieve enantioselective transformations.[24]

[21] (a) O. Diels, K. Alder, *Justus Liebigs Ann. Chem.* **1928**, *460*, 98. For representative reviews see: (b) F. Fringuelli, A. Taticchi, The Diels-Alder Reaction: Selected Practical Methods; Wiley, **2002**. (c) J. P. Miller, Advances in Chemistry Research. Volume 18 - Recent Advances in Asymmetric Diels-Alder Reactions; Taylor, J. C., Ed.; Nova Science Publishers, Inc., **2013**, 18, 179. (d) K. P. C. Vollhardt, N. E. Schore, Organic Chemistry, W.H. Freeman & Co Ltd, **1998**.

[22] J. E. Moses, L. Commeiras, J. E. Baldwin, R. M. Adlington, *Org. Lett.* **2003**, *5*, 2987.

[23] A. C. Jones, J. A. May, R. Sarpong, B. M. Stoltz, *Angew. Chemie - Int. Ed.* **2014**, *53*, 2556.

[24] E. N. Jacobsen, A. Pfaltz, H. Yamamoto, *Comprehensive Asymmetric Catalysis I-III*, Springer-Verlag, **2000**.

A representative example of the potential of transition metal catalysis in cycloaddition reactions is the Reppe annulation of acetylene to give cyclooctatetraene. The classic synthesis of this product required 13 steps and takes place with a very low overall yield.[25] However, using nickel catalysis, it is possible to make cyclooctatetraene from acetylene in 90% yield, and in only one step.[26]
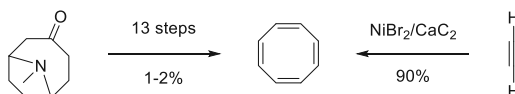

Scheme 5. General scheme of a catalytic reaction with a metal complex.

The Wender's group published in 1986 one of the pioneering examples of a metal-promoted intramolecular cycloaddition. In particular, they discovered a formal (4+4) cycloaddition between two conjugated dienes that does not take place thermally (since it is not allowed) but can effectively proceed at low temperatures if a nickel(0) catalyst is present (Scheme 6).[27]
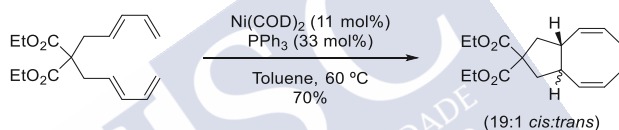
Scheme 6. Wender's nickel-catalyzed (4+4) cycloaddition reaction.

Another example described by Wender that nicely exemplifies the potential of transition metal catalysis for promoting cycloadditions of inactivated systems, consists of a (4+2) Diels-Alder type annulation between alkynes and tethered non-activated dienes. In the absence of catalyst, this cycloaddition only occurs at temperatures higher than 150 °C. However, in presence of a nickel catalyst the reaction proceeds at room temperature, with excellent yield and stereoselectivity (Scheme 7).[28]
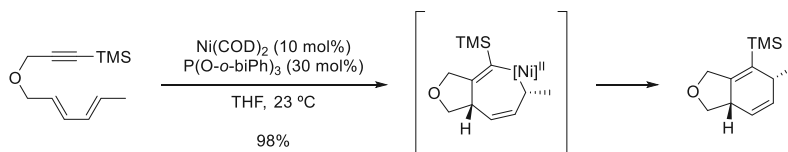
**Scheme 7**. Ni-catalyzed (4+2) cycloaddition reaction.

---

[25] Willstätter, R.; Waser, E. *Berichte der Dtsch. Chem. Gesellschaft* **1911**, *44*, 3423.

[26] W. Reppe, O. Schlichting, K. Klager, T. Toepel, *Justus Liebigs Ann. Chem.* **1948**, *560*.

[27] P. A. Wender, N. C. Ihle, *J. Am. Chem. Soc.* **1986**, *108*, 4678.

[28] P. A. Wender, T. E. Jenkins, *J. Am. Chem. Soc.* **1989**, *111*, 6432.

A more recent example of the potential of metal catalysis in cycloaddition reactions from our own laboratory is shown in Scheme 8.[29] In this case, it was possible to promote a thermally forbidden (2+2) intramolecular annulation between allenes and dienes using a ruthenium catalyst under mild conditions.
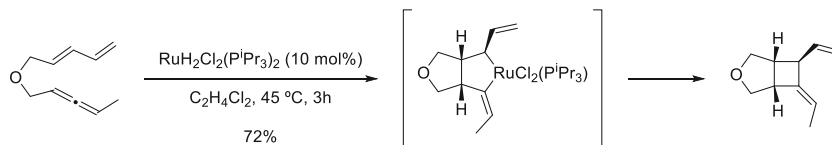

Scheme 8. Ru-catalyzed (2+2) cycloaddition occurring via ruthenacycle intermediate.

Another advantage of the power of transition metal catalysts in cycloaddition chemistry has to do with the use of precursors with strained rings such as alkylidenecyclopropanes. The reactivity of these systems stems from the easiness of an initial oxidative addition step, that releases ring strain and affords a metalacyclic intermediate that can subsequently engage in migratory insertions of cycloadditions partners.[30] Based on this concept, our group has explored the use of alkylidenecyclopropanes as 3C components in several types of (3+2) and (4+3) cycloadditions, promoted by palladium or ruthenium catalysts (Scheme 9).[31] Moreover, it is also possible to perform multicomponent (3+2+2) annulations, as can be seen in a recent example also developed in our laboratory (Scheme 10).[32]
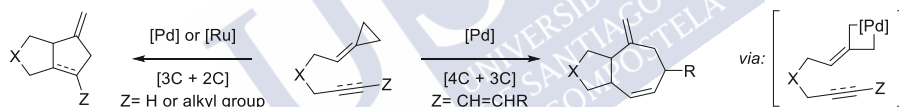
Scheme 9. Transition metal-catalyzed cycloaddition reactions with alkylidenecyclopropanes.
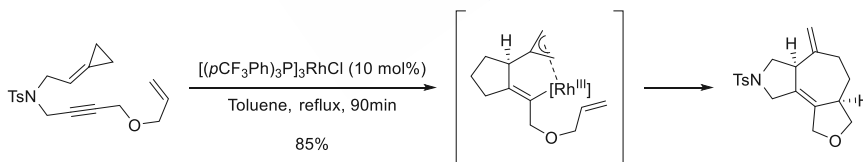
Scheme 10. Rh(I)-catalyzed (3+2+2) cycloaddition.

[29] M. Gulías, A. Collado, B. Trillo, F. López, E. Oñate, M. A. Esteruelas, J. L. Mascareñas, *J. Am. Chem. Soc.* **2011**, *133*, 7660.

[30] P.-H. Chen, B. A. Billett, T. Tsukamoto, G. Dong, *ACS Catal.* **2017**, *7*, 1340.

[31] (a) A. Delgado, J. R. Rodríguez, L. Castedo, J. L. Mascareñas, *J. Am. Chem. Soc.* **2003**, *125*, 9282. (b) F. López, A. Delgado, J. R. Rodríguez, L. Castedo, J. L. Mascareñas, *J. Am. Chem. Soc.* **2004**, *126*, 10262. (c) M. Gulías, R. García, A. Delgado, L. Castedo, J. L. Mascareñas, *J. Am. Chem. Soc.* **2006**, *128*, 384. (d) M. Gulías, J. Durán, F. López, L. Castedo, J. L. Mascareñas, *J. Am. Chem. Soc.* **2007**, *129*, 11026.

[32] M. Araya, M. Gulías, I. Fernández, G. Bhargava, L. Castedo, J. L. Mascareñas, F. López, *Chem. Eur. J.* **2014**, *20*, 10255. For a review on transition metal-catalyzed cycloaddition reactions see also: M. Gulías, F. López, J. L. Mascareñas, *Pure Appl. Chem.* **2011**, *83*, 495.

In general, most of the metal catalyzed cycloaddition reactions so far reported involve the use of late transition metals such as cobalt, nickel, ruthenium, rhodium or palladium. These transition metals are prone to undergo redox processes (oxidative additions, reductive eliminations and β-hydride eliminations). Accordingly, as exemplified in Scheme 7-10, the annulations often proceed through metalacyclic intermediates. After different migratory insertions, the final cycloadduct is obtained through a final reductive elimination.[33]

In recent years, it has been extensively shown that carbophilic transition metals such as platinum and gold, which do not easily undergo redox processes like oxidative additions or reductive eliminations, can also promote annulation processes. Therefore, and contrary to the abovementioned annulations promoted by Ru, Ni or Pd, these cycloadditions do not proceed through metalacyclic intermediates. Some examples, relevant to this PhD work, will be described in the following section.

3. Catalysis by gold

3.1. General features of their reactivity. Selected examples with alkynes

The first report in the literature on the catalytic use of a gold salt was described by H. Erdmann and P. Köthner over a century ago.[34] However, despite the great development of transition metal catalysis over the 20th century, the catalytic properties of gold complexes received only modest attention, probably due to the notion that gold is an inert metal. It is in the last decade when homogeneous catalysis with this carbophilic metal, in particular with gold(I) complexes, has experienced an exponential growth.[35]

The particular reactivity and characteristics of gold (and also of platinum complexes) are attributed to the so called "relativistic effects". It has been postulated that the contraction of the *6s* orbital and the expansion of the *5d* are two consequences of these relativistic effects that confer special and differentiating attributes to these metals.[36] The higher retention of the *5d* electrons could be the reason why both Au and Pt do not easily participate in redox-based catalytic cycles, including oxidative additions and reductive eliminations, which are very common with other metals like Ni, Ru, Rh or Pd. In addition, the contraction of the *6s* orbitals leads to a relatively lower energy LUMO, and hence a better ability to coordinate unsaturated systems. Such coordination triggers the reactivity usually by generating carbocationic reaction intermediates from alkynes, alkenes or allenes.

---

[33] For examples on oxidative addition/reductive elimination strategies with transition metal catalysis see: P. A. Wender, J. A. Love, in *Advances in Cycloaddition*, Vol. 5; M. Harmata, Ed.; JAI Press: Greenwich, **1999**.

[34] H. Erdmann, P. Köthner, *Anorg. Chemie* **1898**, *18*, 48.

[35] A. S. K. Hashmi, F. D. Toste, *Modern Gold Catalyzed Synthesis*, Wiley-VCH, **2012**.

[36] (a) D. J. Gorin, F. D. Toste, *Nature* **2007**, *446*, 395. (b) A. Fürstner, P. W. Davies, *Angew. Chemie - Int. Ed.* **2007**, *46*, 3410.
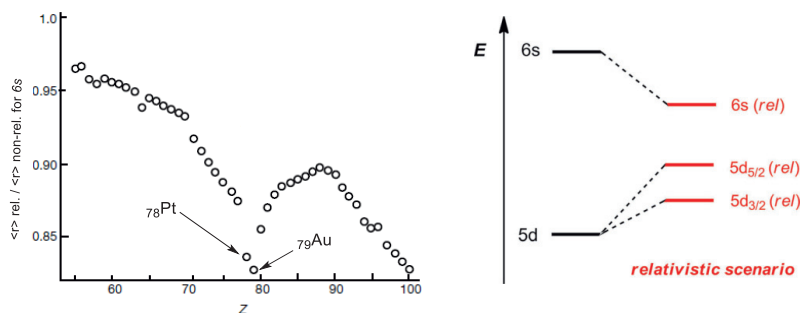
Figure 4. Calculation of the relativistic contraction of *6s* orbitals. Figure produced from ref. 30a.

The current, great popularity of this field is also due to the simplicity associated to the use of these gold salts and complexes as catalysts. Initially, simple salts like AuCl or AuCl$_3$ were employed. However, gold(I) complexes of type LAuCl proved to be much more versatile, since the properties and reactivity of the catalyst can be modulated by the type of ancillary ligand (L), which might be a phosphine, a *N*-heterocyclic carbene, a phosphite or a pyridine, among others. The orbital characteristics of Au(I) complexes favors the formation of two-coordinate linear complexes, such as that observed for the complex PPh$_3$AuCl indicated in Figure 5. [36]
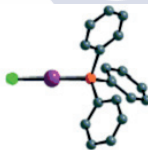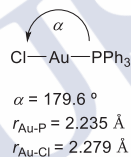

α = 179.6 º
r_{Au-P} = 2.235 Å
r_{Au-Cl} = 2.279 Å

**Figure 5**. Schematic and crystal structure representation of Ph$_3$PAuCl. Figure produced from ref. 30b.

A consequence of the linear coordination mode of neutral Au(I) complexes such as LAuCl, is the need to abstract the chloride atom to allow an efficient coordination of the substrate to the gold(I) center. Indeed, most gold(I)-catalyzed processes promoted by LAuCl complexes require the addition of equimolar amounts of a scavenger, such as a silver(I) salt, to remove the chloride and allow the coordination to the organic moiety. This type of activation introduces some limitations, since silver salts are not always catalytically innocent,[37] and some of them are highly hygroscopic and difficult to handle. To solve this issue, Gagosz and coworkers introduced bis(trifluoromethanesulfonyl)imide (NTf$_2$-) gold complexes of type LAuNTf$_2$ as an alternative. These complexes do not need activation by ligand abstraction, whereas they can be stored under air at room temperature without decomposition.[38] Alternatively,

[36] (a) D. J. Gorin, F. D. Toste, *Nature* **2007**, *446*, 395. (b) A. Fürstner, P. W. Davies, *Angew. Chemie - Int. Ed.* **2007**, *46*, 3410

[37] (a) C. Nevado, A. M. Echavarren, *Chem. Eur. J.* **2005**, *11*, 3155. (b) A. Homs, I. Escofet, A. M. Echavarren, *Org. Lett.* **2013**, *15*, 5782.

[38] N. Mézailles, L. Ricard, F. Gagosz, *Org. Lett.* **2005**, *7*, 4133.

other groups developed catalysts that incorporate nitrogen-based molecules coordinated to gold, in order to provide stability while keeping enough catalytic power. These are the cases of the acetonitrile gold complexes developed by Echavarren,[39] or the triazole-gold complexes developed by Shi (Scheme 11).[40]
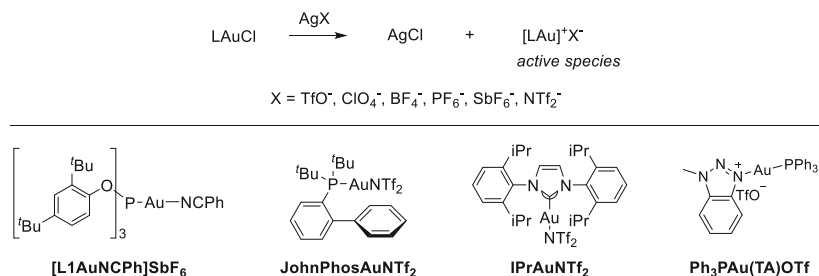
Scheme 11. General formation of active gold(I) species and some of the most common gold(I) catalysts.

Most of the catalytic applications of gold complexes are based on the activation of triple C-C bonds, although many examples based on the activation of allenes have also been introduced in recent years. Both alkynes and allenes, once activated by these metals, may undergo attack by diverse types of nucleophiles, such as hydroxyl groups, water, nitrogenous nucleophiles, or π electrons of unsaturated systems such as dienes or alkenes.

It is well accepted that most gold-catalyzed additions take place through nucleophilic attack on a $[LAu]^+$-alkyne (or alkene/allene) leading to a *trans*-alk(en)yl gold complex intermediate (stage 1);[41] the resulting vinyl (or alkyl) gold complex reacts via protodeauration with an electrophile (usually a proton) and regenerates the cationic-like gold species (stage 2). The reactive gold(I) species can undergo a decay or deactivation by disproportionation, as indicated in the Scheme 12 (stage 3).[42] It is important to note that while it is commonly written LAu^+, the real species most probably contains another labile ligand or a solvent molecule coordinated to the gold atom.

[39] (a) P. De Frémont, E. D. Stevens, M. R. Fructos, M. M. Díaz-Requejo, P. J. Pérez, S. P. Nolan, *Chem. Commun.* **2006**, 2045. (b) E. Herrero-Gómez, C. Nieto-Oberhuber, S. López, J. Benet-Buchholz, A. M. Echavarren, *Angew. Chemie - Int. Ed.* **2006**, *45*, 5455.

[40] H. Duan, S. Sengupta, J. L. Petersen, N. G. Akhmedov, X. Shi, *J. Am. Chem. Soc.* **2009**, *131*, 12100.

[41] E. Jiménez-Núñez, A. M. Echavarren, *Chem. Rev.* **2008**, *108*, 3326.

[42] (a) M. Kumar, G. B. Hammond, B. Xu, *Org. Lett.* **2014**, *16*, 3452. (b) A. Grirrane, E. Álvarez, H. García, A. Corma, *Angew. Chemie - Int. Ed.* **2014**, *53*, 7253.
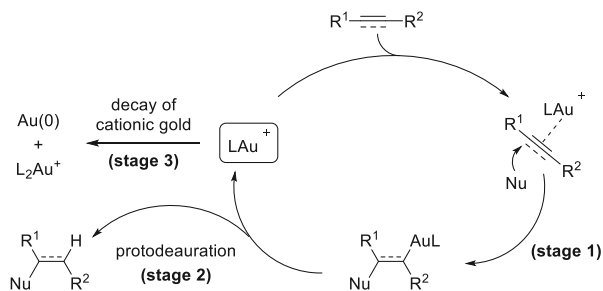
Scheme 12. Activation of triple or double C-C bonds by gold(I) complexes.

The ancillary ligands at gold play a significant role by tuning the catalyst reactivity. In 2012, the group of Hammond outlined general aspects about the structure and electronic properties of the ligand and how they affect the reactivity of the metal,[43] concluding that gold complexes with electron-poor ligands favor the activation of the substrate; while electron-rich ligands accelerate the protodeauration step. They also propose that biphenyl phosphine gold complexes, like JohnPhosAuNTf$_2$, present a higher stability and therefore retard the decay or deactivation processes.

On the other hand, gold(I) complexes might also have good affinity to impurities such as halides or Lewis bases. Thus, in the last years, research was also focused on finding new strategies to improve the efficiency of gold-catalyzed processes, via new ways to reactivate the catalyst with Lewis acids (Cu^I, Cu^{II}, Zn^{II}, In^{III}, Si^{IV}, Bi^{III}, Ga^{III});[44,45] or by exploring different counterions that help to modulate their catalytic behavior (TFA$^-$. BF$_4^-$, BAr^{F-}, OAc$^-$, OTs$^-$, OTf$^-$, SbF$_6^-$, PF$_6^-$, NTf$_2^-$).[46]

Besides the use of gold complexes in simple addition reactions, these carbophilic metals have also been used in recent years for the development of **novel annulation or cycloaddition protocols**. One of the very first examples of a gold-catalyzed cycloaddition was reported by Hashmi in the year 2000 and consists of a (4+2) annulation of furyl-tethered alkynes to give phenols. The authors proposed that the reaction proceeds by an initial cyclization which provides the cyclopropyl carbene intermediate **III**. Split of the cyclopropane bond, followed by and opening of the dihydrofuran and a tandem cyclization/aromatization yields the phenolic products (Scheme 13).[47]

---

[43] W. Wang, G. B. Hammond, B. Xu, *J. Am. Chem. Soc.* **2012**, *134*, 5697.

[44] (a) J. Han, N. Shimizu, Z. Lu, H. Amii, G. B. Hammond, B. Xu, *Org. Lett.* **2014**, *16*, 3500. (b) Y. Xi, D. Wang, X. Ye, N. G. Akhmedov, J. L. Petersen, X. Shi, *Org. Lett.* **2014**, *16*, 306.

[45] (a) A. Guérinot, W. Fang, M. Sircoglou, C. Bour, S. Bezzenine-Lafollée, V. Gandon, *Angew. Chemie - Int. Ed.* **2013**, *52*, 5848. (b) W. Fang, M. Presset, A. Guérinot, C. Bour, S. Bezzenine-Lafollée, V. Gandon, *Chem. Eur. J.* **2014**, *20*, 5439.

[46] (a) M. Jia, G. Cera, D. Perrotta, M. Monari, M. Bandini, *Chem. Eur. J.* **2014**, *20*, 9875. (b) G. Ciancaleoni, L. Belpassi, D. Zuccaccia, F. Tarantelli, P. Belanzoni, *ACS Catal.* **2015**, *5*, 803.

[47] (a) A. S. K. Hashmi, T. M. Frost, J. W. Bats, *J. Am. Chem. Soc.* **2000**, *122*, 11553. (b) A. S. K. Hashmi, M. Rudolph, J. P. Weyrauch, M. Wölfle, W. Frey, J. W. Bats, *Angew. Chemie - Int. Ed.* **2005**, *44*, 2798.
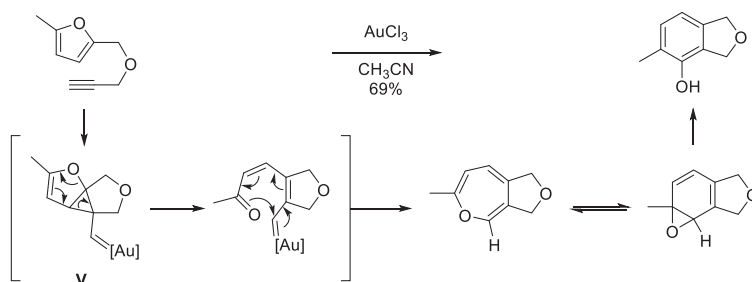
Scheme 13. Gold-catalyzed synthesis of phenols.

Among all the gold-catalyzed reactions of alkynes, cycloisomerizations of enynes are among the most studied.[48] Indeed, the richness of gold chemistry is well manifested in these reactions, since several types of products can be divergently obtained depending on the conditions, additives, substituents or ligands at gold. The Au(I) species usually activates the alkyne promoting a nucleophilic addition of the alkene. In the case of terminal alkynes, this addition occurs by the *exo* mode (5-*exo*-dig, **VIa**), whereas, enynes incorporating substituted alkynes or heteroatoms at the connecting tether usually undergo a 6-*endo*-dig pathway (Scheme 14, **VIIa**). This is a general tendency; the real picture is much more complex and sometimes is difficult to predict the outcome of the reactions.
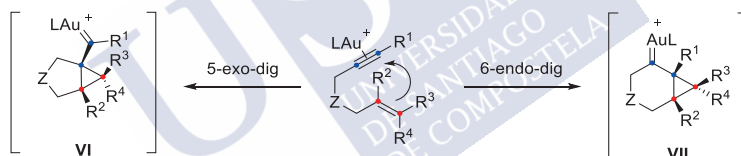

Scheme 14. Activation of enynes by a gold catalyst.

The variety of products that can be obtained from gold catalyzed enyne cycloisomerizations can be further extended, simply by the addition of an external nucleophile. For instance, those enynes that react with gold catalysts via the 5-*exo*-dig pathway to give gold carbenes **VI**, might react with alcohols, amines or aromatic compounds to give products of type **1** or **2** (Scheme 15).[49]

---

[48] E. Jímenez-Núñez, A. M. Echavarren, *Chem. Commun.* **2007**, 333.

[49] (a) C. Nieto-Oberhuber, M. P. Muñoz, S. López, E. Jímenez-Núñez, C. Nevado, E. Herrero-Gómez, M. Raducan, A. M. Echavarren, *Chem. Eur. J.* **2006**, *12*, 1677. (b) P. Y. Toullec, E. Genin, L. Leseurre, J.-P. Genêt, V. Michelet, *Angew. Chemie - Int. Ed.* **2006**, *45*, 7427.
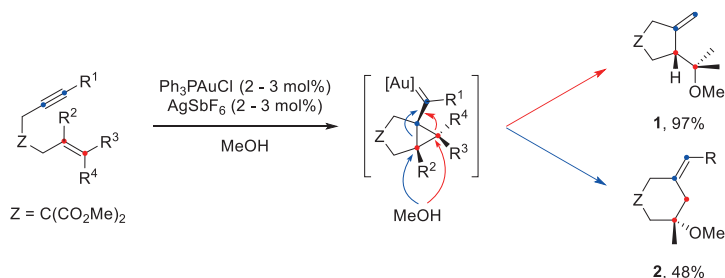
Scheme 15. Alkoxycyclization of enynes with gold catalysis.

On the other hand, in the absence of nucleophiles, enynes react with gold(I) catalysts under mild conditions to give products of skeletal rearrangement (Scheme 16, left arrow); or, less commonly, cyclobutenes resulting from ring expansions (Scheme 16, right arrow).[41, 50]
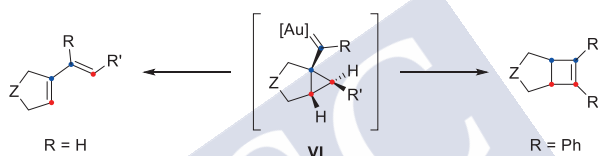

Scheme 16. Gold(I)-catalyzed cyclizations of 1,6-enynes.

Echavarren also reported that, under the same reaction conditions, similar 1,6-enynes undergo a formal (4+2) cycloaddition. DFT calculations and deuterium labeling at the aromatic ring support a stepwise mechanism initiated by the formation of a cyclopropyl gold(I)-carbene **VIa**, that evolves to carbocation **VIII**. Rearomatization and a final protodeauration afford the cycloadduct **8** (Scheme 17).[51]

[41] E. Jiménez-Núñez, A. M. Echavarren, *Chem. Rev.* **2008**, *108*, 3326.

[50] (a) C. Nieto-Oberhuber, M. P. Muñoz, E. Buñuel, C. Nevado, D. J. Cárdenas, A. M. Echavarren, *Angew. Chemie - Int. Ed.* **2004**, *43*, 2402. (b) C. Nieto-oberhuber, S. López, M. P. Muñoz, D. J. Cárdenas, E. Buñuel, C. Nevado, A. M. Echavarren, *Angew. Chemie - Int. Ed.* **2005**, *44*, 6146.

[51] C. Nieto-Oberhuber, P. Pérez-Galán, E. Herrero-Gómez, T. Lauterbach, C. Rodríguez, S. López, C. Bour, A. Rosellón, D. J. Cárdenas, A. M. Echavarren, *J. Am. Chem. Soc.* **2008**, *130*, 269.
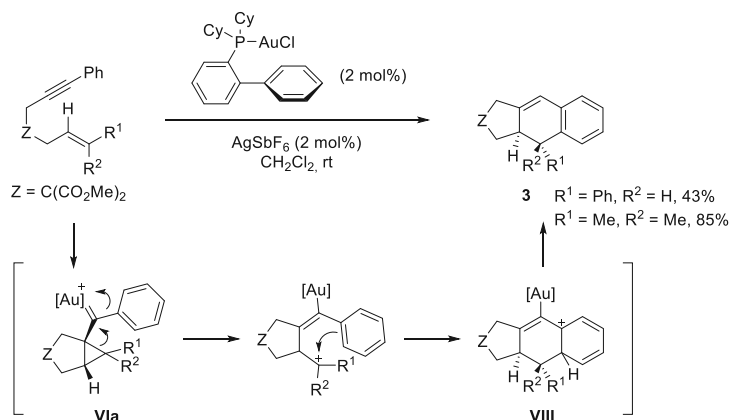
Scheme 17. (4+2) cycloaddition of 1,6-enynes.

More related to the content of this PhD thesis, Ueda has recently reported an intramolecular cycloaddition cascade that constitutes the first reported example of a gold-catalyzed cycloaddition using oxime ethers. The proposed mechanism starts with the attack of the nitrogen atom of the oxime on the gold-activated alkyne leading to an azomethine ylide that features a gold-carbene. This species, undergoes an intramolecular (3+2) cycloaddition to give intermediate **IX,** followed by a double-bond migration and a protodeauration. Then, a thermally ring-opening reaction gives **4**, that undergoes a second (3+2) intramolecular cycloaddition to provide the highly fused aza-bridged polycyclic system **5** (Scheme 18).[52]
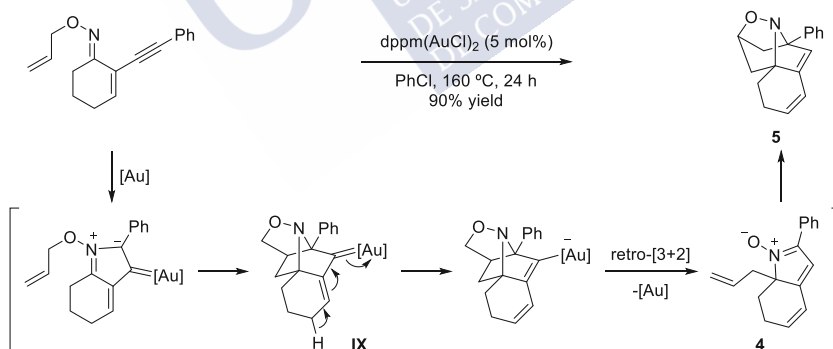
Scheme 18. Gold-catalyzed cycloaddition reaction involving oxime ethers.

A particular case of gold activation of alkynes occurs when these are part of a propargylic ester like in **6**. These systems can undergo a 6-*endo*-dig cyclization generating an allenyl acetate **A** (1,3-migration) or a 5-*exo*-dig cyclization to form intermediate **X**, which upon ring opening forms carbene **B**, representing a formal 1,2-acyloxy migration (Scheme 19). Usually, if the propargylic systems have an electronically

---

[52] S. Sugita, N. Takeda, N. Tohnai, M. Miyata, O. Miyata, M. Ueda, *Angew. Chemie - Int. Ed.* **2017**, *56*, 2469.

unbiased internal alkyne (R^2 ≠ H), the 1,3-acyloxy migration takes place. Alternatively, with terminal alkynes (R^2 = H), the 1,2-acyloxy migration is preferred. However, other factors such as the type of catalyst, the substitution pattern at the propargylic moiety, and the temperature, can influence the regiochemical outcome of these reactions.[53,35]
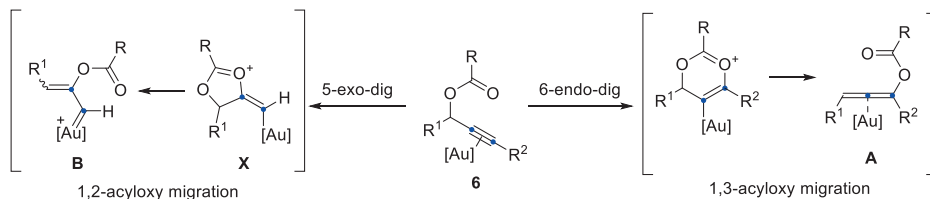

Scheme 19. Competitive 1,2- or 1,3-migration of propargylic esters.

The reactivity of the allenic intermediates generated from the 1,3-acyloxy migration was initially exploited by L. Zhang in the development of formal (3+2) and/or (2+2) annulations of propargylic indole-3-acetates. Interestingly, in the presence of Ph$_3$PAuCl/AgSbF$_6$, the (2+2) cycloaddition was favored, furnishing 2,3-indole-fused cyclobutanes (upper arrow, Scheme 20).[54] However, when PtCl2 (under CO atmosphere) was used, 2,3-indoline-fused cyclopentenes, which arise from a formal (3+2) cycloaddition, were obtained as major products (lower arrow, Scheme 20)[55]
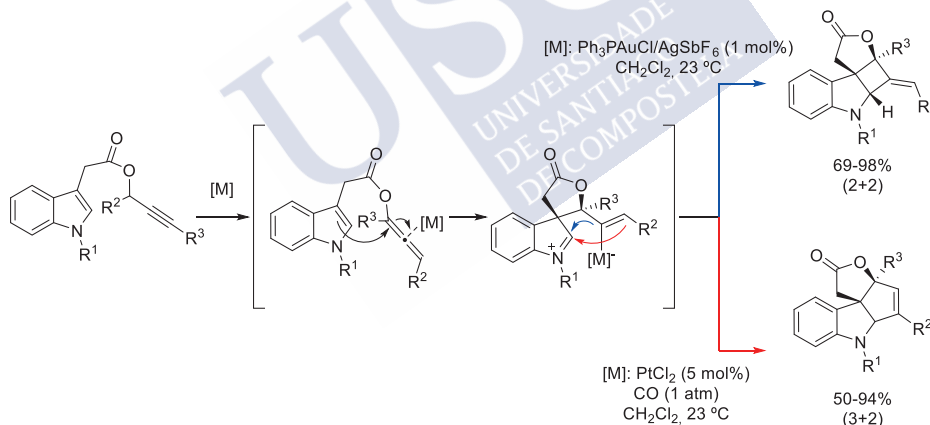
Scheme 20. Gold(I)-catalyzed (2+2) and platinum(II)-catalyzed (3+2) cycloadditions of indole-3-acetates.

---

[53] R. K. Shiroodi, V. Gevorgyan, *Chem. Soc. Rev.* **2013**, *42*, 4991.

[35] A. S. K. Hashmi, F. D. Toste, *Modern Gold Catalyzed Synthesis*, Wiley-VCH, **2012**.

[54] L. Zhang, *J. Am. Chem. Soc.* **2005**, *127*, 16804.

[55] G. Zhang, V. J. Catalano, L. Zhang, *J. Am. Chem. Soc.* **2007**, *129*, 11358.

## 3.2. Reactions with allenes and derivatives

Allenes

Although the activation of alkynes by gold has been dominant in the last years, an important number of processes involving the activation of allenes have also been developed. The coordination of the metal to the allene can lead to different types of structures that, according to computational studies of Malacria and coworkers, can be categorized in two groups (Scheme 21).[56] The η^2 complexes **A**, which involve one of the two double bonds are the most intuitive. Depending on the substitution of the allene, the contribution of the carbon atoms to the coordination might be not strictly equivalent, leading to distorted structures of type **A'** or **A''**. The presence of electron-donating groups on the allene stabilizes **A'**, while electron-withdrawing groups would favor **A''**. The second category comprises species in which the metal fragment is coordinated to the central allene carbon only. Along with σ-allylic cations **B**, there are alternatives, such as zwitterionic carbenes **B'** or η^1-coordinated bent allenes **B''**.
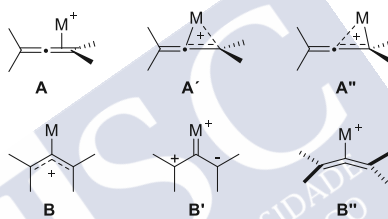
Scheme 21. Various coordination modes of allenes.

As mentioned before, these activated allenes are prone to undergo nucleophilic attacks. Widenhoefer published several examples of gold catalyzed intramolecular hydroamination and hydroalkoxylation reactions of allenes. These reactions allowed for instance heterocycles like **7/7'** to be obtained in good yields and excellent stereospecificity (Scheme 22).[57]
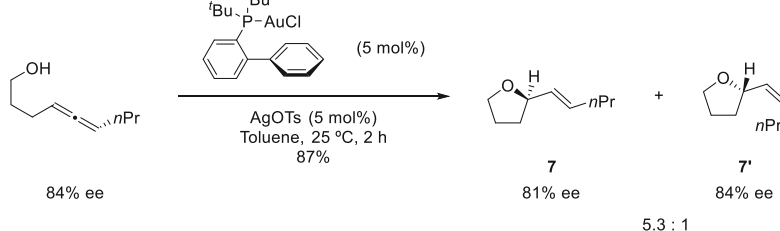
Scheme 22. Hydroalkoxylation of allenyl alcohols with chirality transfer.

In 2006, Yamamoto and coworkers developed a gold(III)-catalyzed intermolecular hydroamination of allenes, which proceeds smoothly at room temperature affording

---

[56] V. Gandon, G. Lemière, A. Hours, L. Fensterbank, M. Malacria, *Angew. Chemie - Int. Ed.* **2008**, *47*, 7534.

[57] Z. Zhang, C. Liu, R. E. Kinder, X. Han, H. Qian, R. A. Widenhoefer, *J. Am. Chem. Soc.* **2006**, *128*, 9066.

allylic amines in good yields and, again, with transference of chirality of the allene moiety to the product (Scheme 23).[58]
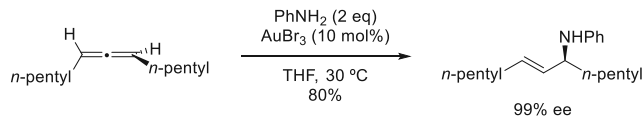
Scheme 23. Gold(III)-catalyzed hydroamination of allenes.

Later, the group of Widenhoefer reported a regio- and stereoselective gold(I)-catalyzed intermolecular hydroalkoxylation of allenes to form alkyl allylic ethers at room temperature and in good yields using a gold catalyst bearing a *N*-heterocyclic carbene (NHC) ligand (**IPrAuCl**, Scheme 24).[59]

Scheme 24. Gold(I)-catalyzed hydroalkoxylation of allenes.

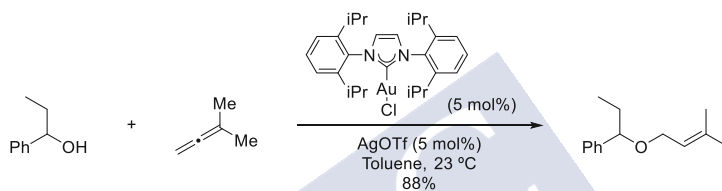Toste and coworkers reported a strategy for the synthesis of substituted cyclopentadienes from vinylallenes using gold(I) catalysts.[60] The reaction, which resembles the Nazarov cyclization, is fast and can be carried out with a catalyst load of 2 mol%. The reaction proceeds through a final 1,2-migration which, depending on the allene substituents, could be a hydrogen or alkyl shift (Scheme 25).
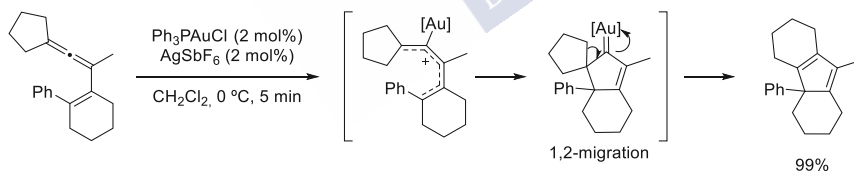
Scheme 25. Gold(I)-catalyzed synthesis of functionalized cyclopentadienes.

The same group developed in 2007 an interesting gold(I)-catalyzed (2+2) cycloaddition of 1,6-allenenes to afford alkylidene cyclobutene products.[61a] The mechanism, proposed in 2011 on the basis of DFT calculations,[61b] would involve the generation of a gold(I)-allyl cation, which undergoes a cyclization to give a new carbocationic species in which the

[58] N. Nishina, Y. Yamamoto, *Angew. Chemie - Int. Ed.* **2006**, *45*, 3314.

[59] Z. Zhang, R. A. Widenhoefer, *Org. Lett.* **2008**, *10*, 2079.

[60] J. H. Lee, F. D. Toste, *Angew. Chemie - Int. Ed.* **2007**, *46*, 912.

[61] (a) M. R. Luzung, P. Mauleón, F. D. Toste, *J. Am. Chem. Soc.* **2007**, *129*, 12402. For computational analysis on the Au(I)-catalyzed cycloadditions of allenenes, see: (b) A. Z. González, D. Benitez, E. Tkatchouk, W. A. Goddard, III, F. D. Toste, *J. Am. Chem. Soc.* **2011**, *133*, 5500.

gold center establishes a stabilizing electrostatic interaction with the benzylic carbocation. A subsequent ring closure provides the observed bicyclo[3.2.0]heptanes (Scheme 26).
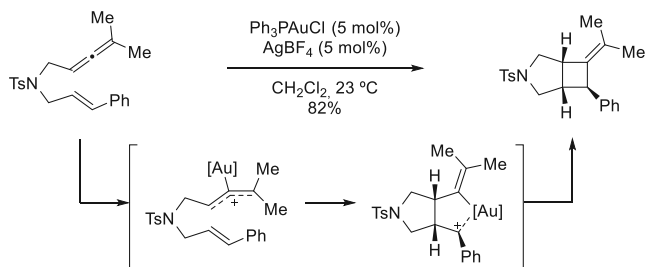
Scheme 26. Gold(I)-catalyzed (2+2) cycloaddition of allenenes.

On the other hand, our group demonstrated in 2008 the possibility of using allenes as three-carbon components in formal (4+3) intramolecular cycloadditions of allenedienes promoted by Pt and Au catalysts. The (4+3) process can be achieved with PtCl₂,[62] or with cationic Au(I) catalysts containing a σ-donor *N*-heterocyclic carbene ligand (like **IPrAuCl**), which allows these reactions to proceed under mild conditions (Scheme 27).[63] Later, Toste reported similar results using a highly donating biaryl phosphine ligand (like **JohnPhosAuCl**).[64]

$Z = C(CO_2Me)_2$

PtCl₂ (10 mol%): 92%
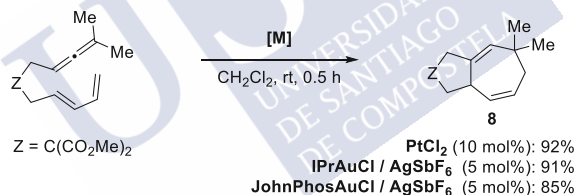**IPrAuCl / AgSbF₆** (5 mol%): 91%
JohnPhosAuCl / AgSbF₆ (5 mol%): 85%

Scheme 27. Gold(I) catalyzed (4+3) cycloadditions of allenedienes.

Remarkably, when allenes are dialkylated at the distal position, the appropriate selection of the gold catalyst allows to obtain either the (4+3) adducts or formal (4+2) cycloadducts. Thus, if these substrates are treated with a gold(I) precatalyst bearing a π-acceptor ligand, such as a triarylphosphite (**L1AuCl**), (4+2) cycloadducts like **9** are obtained (Scheme 28).[65,64]

[62] B. Trillo, F. López, M. Gulías, L. Castedo, J. L. Mascareñas, *Angew. Chemie - Int. Ed.* **2008**, *47*, 951.

[63] B. Trillo, F. López, S. Montserrat, G. Ujaque, L. Castedo, A. Lledós, J. L. Mascareñas, *Chem. Eur. J.* **2009**, *15*, 3336.

[64] P. Mauleón, R. M. Zeldin, A. Z. González, F. D. Toste, *J. Am. Chem. Soc.* **2009**, *131*, 6348.

[65] I. Alonso, B. Trillo, F. López, S. Montserrat, G. Ujaque, L. Castedo, A. Lledós, J. L. Mascareñas, *J. Am. Chem. Soc.* **2009**, *131*, 13020.
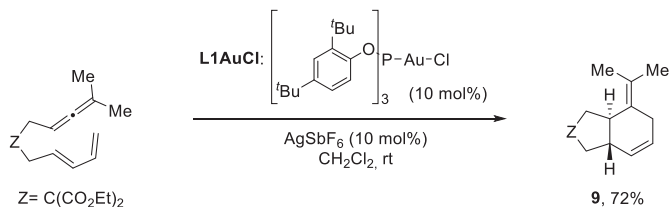
Scheme 28. Gold(I)-catalyzed (4+2) cycloaddition of allenedienes.

Combined experimental and theoretical data suggests that both processes share the initial formation of a metal allyl cation which undergoes a concerted $[4C(4\pi) + 3C(2\pi)]$ cycloaddition with the diene moiety, leading to a cycloheptanic carbene intermediate (Scheme 29). At this point, the process becomes divergent: while σ-donor ligands at the gold atom or the use of PtCl$_2$, favor a 1,2-hydrogen shift leading to seve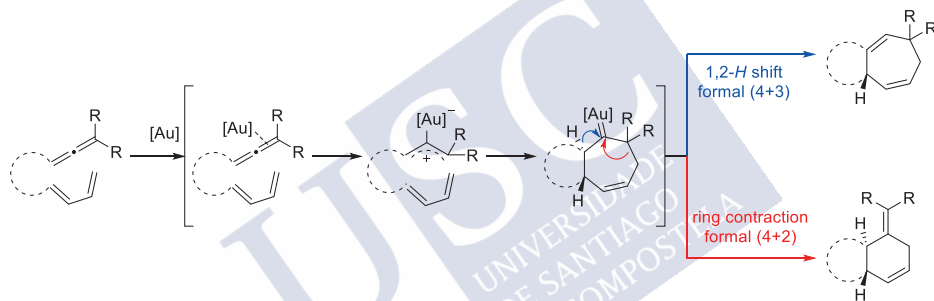n-membered cycloadducts, a gold(I) catalyst bearing a π-acceptor ligand favors a 1,2-alkyl shift (ring contraction, red pathway) affording the formal (4+2) cycloadducts.

Scheme 29. Divergent pathways for the (4+3) and (4+2) gold catalyzed cycloadditions of allenedienes

Recently, Sigman and Toste suggested that it can be established a correlation between the selectivity of the (4+3)/(4+2) cycloaddition of allenedienes and the distance of the Au-Cl bond in gold complexes containing phosphorous ligands. This distance would be determined not only by the electronic influence of the ligand at gold, but also by its steric properties. Thus, both factors determine the divergent outcome of the reaction. Specifically, the ring contraction is favored at a shorter distance of the Au-Cl bond, as depicted in Scheme 30 using phosphite ligand **L1** (distance of 2.300 Å). On the other hand, the (4+3) cycloaddition is favored when the Au-Cl bond is larger, such as with RuPhos ligand (distance of 2.335 Å, Scheme 30).[66] It is reasonable that the distance is also correlated with the π-acceptor and σ-donor character of the ligand.

[66] A. H. Christian, Z. L. Niemeyer, M. S. Sigman, F. D. Toste, *ACS Catal.* **2017**, *7*, 3973.
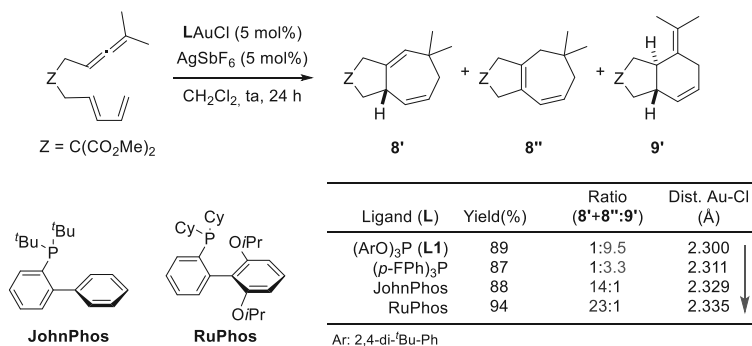
Scheme 30. Correlation between the Au-Cl distance and the selectivity in the (4+3)/(4+2) cycloaddition.

Based on the mechanistic hypothesis for the (4+3) and (4+2) cycloadditions of allenedienes (Scheme 29), Toste revisited the gold(I)-catalyzed reaction of allenenes to determine whether the ligand could also be employed to get a divergent access to both the (2+2) and the (3+2) adduct (see Scheme 26, page 33).[61] Indeed, the use of a gold catalyst such as JohnPhosAuCl/AgSbF$_6$, led to exclusive formation of cyclopentene cycloadducts resulting from the (3+2) cycloaddition (Scheme 31).[64]
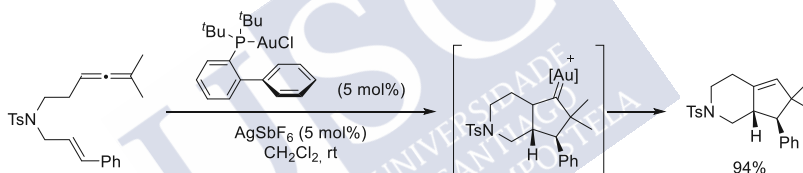
Scheme 31. Gold(I)-catalyzed (3+2) cycloaddition of allenenes.

Allenamides

In recent years, our group and others have demonstrated that allenamides, a type of heteroatom-substituted allenes, are excellent partners in gold catalyzed processes.[67,68] The π-donating ability of the nitrogen atom make allenamines more electron-rich than simple allenes, therefore predisposing them to electrophilic activations. However, allenamines are highly sensitive towards hydrolysis and exhibit a great tendency to polymerize, even at low temperatures (Scheme 32a). In this context, allenamides emerge as an attractive variant since delocalization of the nitrogen lone-pair into the electron-

[61] (a) M. R. Luzung, P. Mauleón, F. D. Toste, *J. Am. Chem. Soc.* **2007**, *129*, 12402. (b) A. Z. González, D. Benitez, E. Tkatchouk, W. A. Goddard, III, F. D. Toste, *J. Am. Chem. Soc.* **2011**, *133*, 5500.

[64] P. Mauleón, R. M. Zeldin, A. Z. González, F. D. Toste, *J. Am. Chem. Soc.* **2009**, *131*, 6348.

[67] For examples of gold-catalyzed hydroamination of allenamides see: (a) A. M. Manzo, A. D. Perboni, G. Broggini, M. Rigamonti, *Tetrahedron Lett.* **2009**, *50*, 4696. (b) A. W. Hill, M. R. J. Elsegood, M. C. Kimber, *J. Org. Chem.* **2010**, *75*, 5406.

[68] For examples of gold-catalyzed hydroarylation of allenamides see: (a) T. Watanabe, S. Oishi, N. Fujii, H. Ohno, *Org. Lett.* **2007**, *9*, 4821. (b) M. C. Kimber, *Org. Lett.* **2010**, *12*, 1128. (c) S. Singh, M. R. J. Elsegood, M. C. Kimber, *Synlett* **2012**, *23*, 565. (d) Z.-X. Ma, S. He, W. Song, R. P. Hsung, *Org. Lett.* **2012**, *14*, 5736.

withdrawing carbonyl group diminishes its donating ability, enhancing their stability (Scheme 32b).[69]

Allenamines
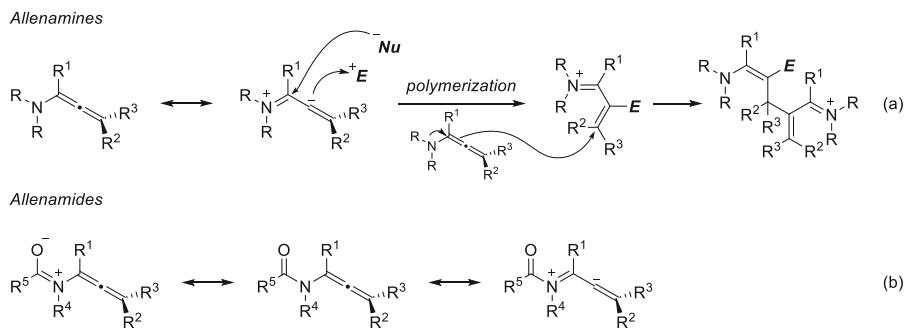
Allenamides

Scheme 32. Allenamine and allenamide resonance forms.

This stability, combined with their electron rich nature, allowed allenamides to be used as useful building blocks in several types of synthetic methodologies, including some mediated by transition metals, such as Ru (reductive coupling of sulfonamide allenes and aldehydes under ruthenium-catalyzed transfer hydrogenation);[70] or Pd (annulation reactions of heteroatom-substituted allenes),[71] among others. However, their use under gold catalysis is relatively recent. Broggini and coworkers reported a gold(III)-catalyzed intramolecular hydroamination of allenamides like **10**. A proposed mechanism starts with the activation of the allene moiety by the gold complex, which triggers the intramolecular nucleophilic attack by the amino group yielding the cyclic vinyl-gold intermediate. A final protonolysis gives the corresponding 2-vinylimidazolidinone and regenerates the catalyst (Scheme 33).[67a]
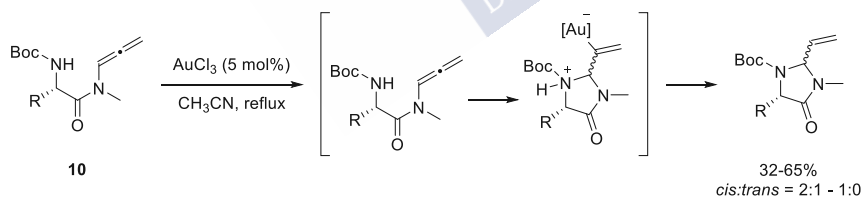
Scheme 33. Gold(III)-catalyzed intramolecular hydroamination of α-amino allenamides.

In 2010, the group of Kimber disclosed an intermolecular gold-catalyzed hydroamination of allenamides using arylamines, stereoselectively affording the allylamino *E*-enamides in high yields. The proposed mechanism involves the formation of the key gold zwitterionic species that undergoes the addition of the nucleophile, followed by a subsequent protodeauration that yields the *E*-enamides (Scheme 34).[72]

[69] T. Lu, Z. Lu, Z. X. Ma, Y. Zhang, R. P. Hsung, *Chem. Rev.* **2013**, *113*, 4862.

[70] E. Skucas, J. R. Zbieg, M. J. Krische, *J. Am. Chem. Soc.* **2009**, *131*, 5054.

[71] K. Inamoto, A. Yamamoto, K. Ohsawa, K. Hiroya, T. Sakamoto, *Chem. Pharm. Bull.* **2005**, *53*, 1502.

[72] A. W. Hill, M. R. J. Elsegood, M. C. Kimber, *J. Org. Chem.* **2010**, *75*, 5406.
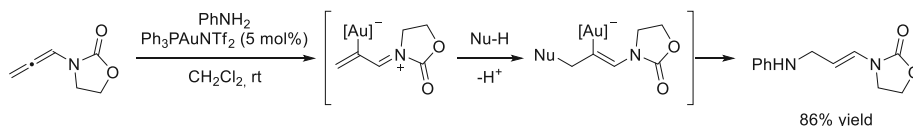
Scheme 34. Gold-catalyzed intermolecular hydroamination of allenamides.

Almost simultaneously, our group developed the first gold-catalyzed cycloaddition of allenamides, in particular an intermolecular (4+2) cycloaddition between allenamides and conjugated dienes.[73] AuCl resulted to be the most suitable catalyst affording the corresponding cyclohexenes in good yields at room temperature. However, in some cases, a significant improvement of the yield could be observed when IPrAuCl was employed. The process is highly regio- and stereoselective, exclusively obtaining the products with *Z* configuration at the *exo*-enamide moiety (Scheme 35).

Scheme 35. Gold(I)-catalyzed intermolecular (4+2) cycloaddition of allenamides developed in our group.
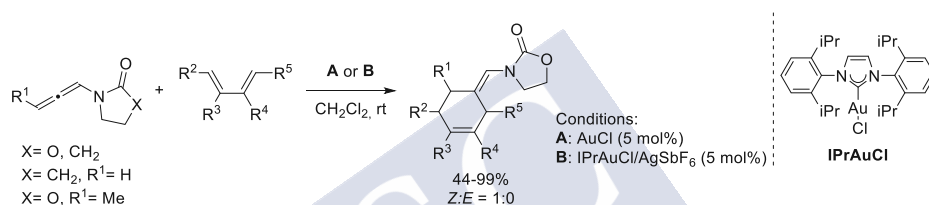
The mechanistic scenario for this process was investigated through experimental and computational studies, resulting in three possible pathways depending on the type of diene (neutral *vs* electron-rich) and on the catalysts employed (AuCl *vs* **IPrAuCl**/AgSbF$_6$).[74] All three pathways have in common the easy activation of the allenamides by the catalyst leading to the zwitterionic gold complex **XI**. The cycloadduct is formed by a concerted (4+2) cycloaddition when a neutral diene like isoprene and **IPrAuCl** are used (pathway **B**). However, when AuCl is employed the mechanisms becomes more complex. DFT calculations suggest that, in the presence of a neutral diene, the formation of the product can go through a concerted (4+2) process (pathway **B**), or through a concerted (4+3) cycloaddition followed by a ring contraction (pathway **A**). Indeed, a stabilizing interaction between the carbocation and the gold atom is reflected in the calculations for the intermediate **XII'**, whose energy values are more stable than for the intermediate **XII''**. This interaction is the same that Toste described in his gold(I)-catalyzed (2+2) cycloaddition of allenenes (Scheme 26, page 33). On the other hand, the calculations suggest a step-by-step mechanism in the presence of AuCl when an electron-rich diene like methoxydiene is used, going through cationic key intermediate of type **XII**. In this case, the methoxy group is able to stabilize the positive charge and seems to disfavor a concerted process (Scheme 36).

---

[73] H. Faustino, F. López, L. Castedo, J. L. Mascareñas, *Chem. Sci.* **2011**, *2*, 633.

[74] S. Montserrat, H. Faustino, A. Lledós, J. L. Mascareñas, F. López, G. Ujaque, *Chem. Eur. J.* **2013**, *19*, 15248.
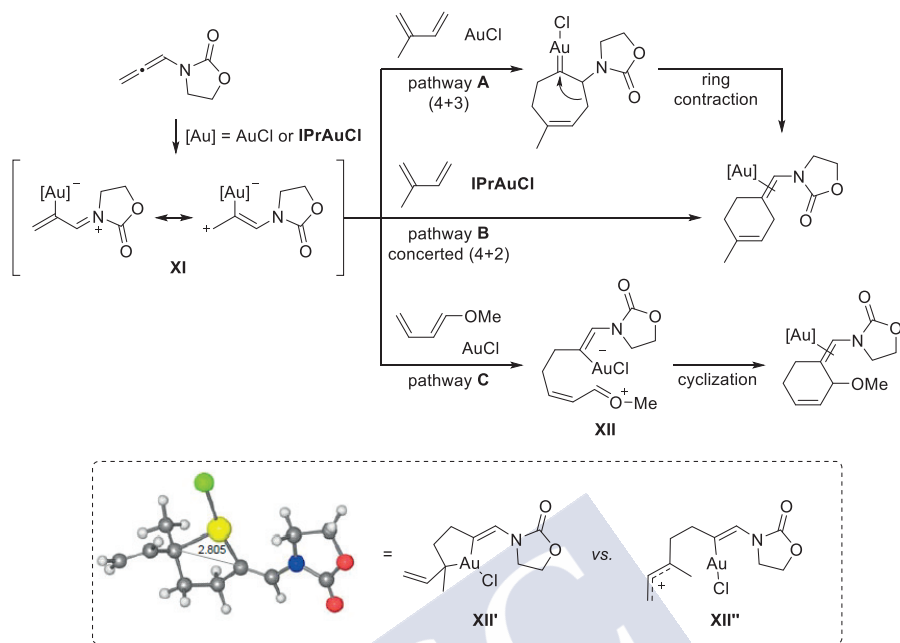
Scheme 36. Mechanistic proposal for the intermolecular (4+2) cycloaddition of allenamides.

During the study of this (4+2) cycloadditions between allenamides and dienes with different gold-catalysts, the formation of a side product, a cyclic compound resulting from a (2+2) cycloaddition between the allenamide and the most substituted double bond of the diene, could be observed (Scheme 37).
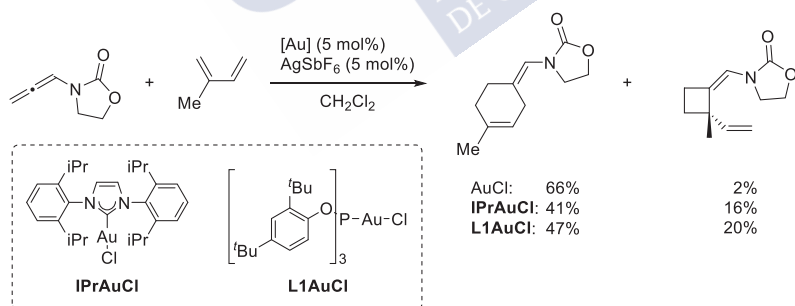
Scheme 37. Intermolecular (4+2)/(2+2) cycloaddition of allenamides.

On these basis, our group demonstrated in 2012 the feasibility of a (2+2) process between allenamides and alkenes such as styrenes or enamides, using the phosphite gold catalyst **L1AuCl**/AgSbF$_6$. As a result, different cyclobutanes were obtained with high regioselectivities and good to excellent yields.[75a] The proposed mechanism involves the

---

[75] (a) H. Faustino, P. Bernal, L. Castedo, F. López, J. L. Mascareñas, *Adv. Synth. Catal.* **2012**, *354*, 1658. For other related examples of gold(I)-catalyzed (2+2) processes between allenamides and alkenes see: (b) X. Li, L. Zhu, W. Zhou, Z. Chen, *Org. Lett.* **2012**, *14*, 436. (c) S. Suárez-Pantiga, C. Hernández-Díaz, M. Piedrafita,

formation of the zwitterionic intermediate **XI**, which undergoes an intermolecular attack of the olefin to form intermediate **XIII**. A subsequent intramolecular attack of the vinyl-gold on the carbocation would close the cycle (Scheme 38). Almost simultaneously, the groups of Chen and González reported the same process, with very related scopes.
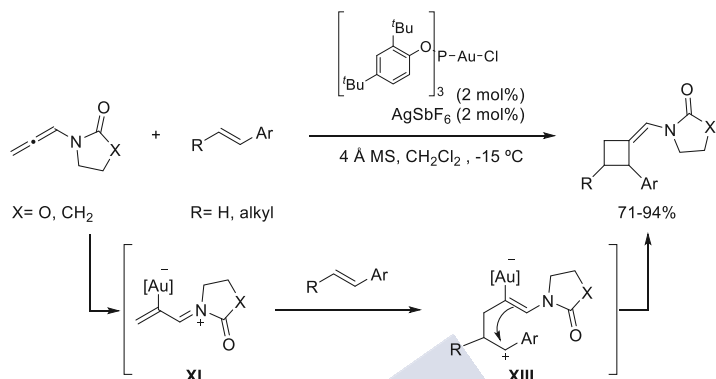
Scheme 38. Intermolecular (2+2) cycloaddition between allenamides and alkenes developed in our group.

During the development of this (2+2) cycloaddition reaction, it was observed that in the absence of an appropriate alkene, the allenamide reacts with a second allenamide unit (which acts as alkene partner), providing a (2+2) homodimerization product **11**. These (2+2) products were also observed by the groups of Chen and González, which reported their isolation in good yields (Scheme 39).[75b, 75c]

Recently, the group of González described the (2+2+2) cyclotrimerization of sulfonylallenamides. They reasoned that lowering the temperature might offer a proper element of control, allowing the incorporation of the third allene unit, herein favoring the cyclotrimerization over the (2+2) homodimerization.[76]
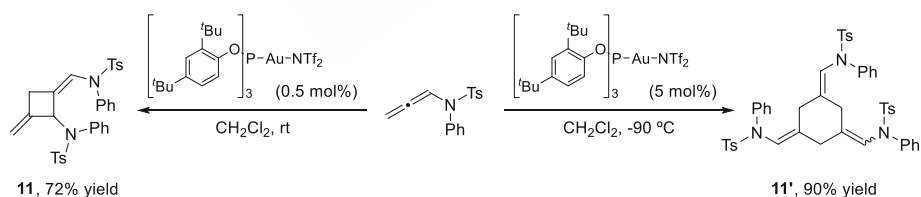
Scheme 39. Gold(I)-catalyzed (2+2) homodimerization and (2+2+2) cyclotrimerization of allenamides.

E. Rubio, J. M. González, *Adv. Synth. Catal.* **2012**, *354*, 1651. For a previous example of a gold(I)-catalyzed (2+2) process between alkynes and alkenes see: (d) V. López-Carrillo, A. M. Echavarren, *J. Am. Chem. Soc.* **2010**, *132*, 9292.

[76] C. Hernández-Díaz, E. Rubio, J. M. González, *European J. Org. Chem.* **2016**, 265.

3.3. Enantioselective Gold(I) catalysis

Additions and cyclizations

The rapid rise of gold catalysis has been accompanied by significant efforts to develop enantioselective variants that could further increase the synthetic utility of these gold-catalyzed transformations.[77,78] However, the linear nature of gold(I) complexes makes very difficult the design of catalysts that can provide highly asymmetric transformations. The first enantioselective gold(I) catalyzed reaction was developed by Hayashi and coworkers in 1986 and consists of an asymmetric aldol condensation promoted by a chiral ferrocenylphosphine-gold(I) complex (Scheme 40).[79]
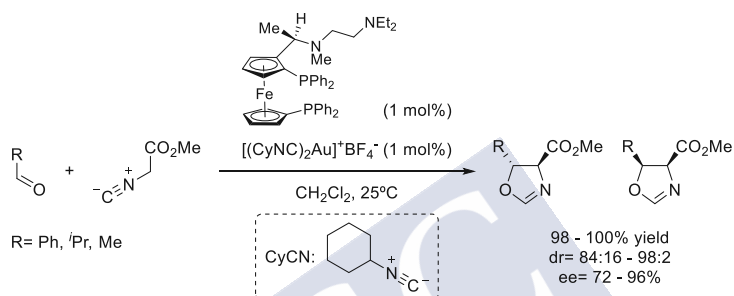
Scheme 40. Reaction of aldehydes with isocyanoacetate catalyzed by a chiral gold(I) complex.

Despite the importance of this report, it was not until two decades later when gold enantioselective catalysis was again investigated. In 2005, Carretero and Echavarren reported the gold(I)-catalyzed alkoxycyclization of 1,6-enynes to yield methylenecyclopentanes.[80] After screening several chiral phosphorous ligands, the authors found that the best enantioselectivies (up to 94 %ee) were obtained with an enyne containing a phenyl group in the terminal position of the alkyne (R=Ph) and a chiral digold(I) complex derived from Tol-BINAP **Au1** (Scheme 41). Unfortunately, the scope of the process was quite limited.
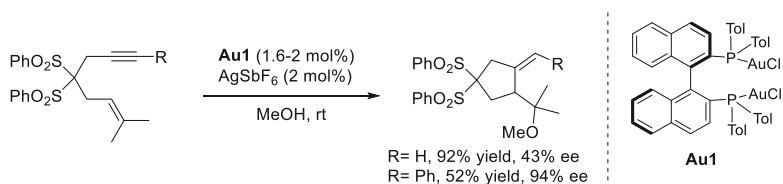
Scheme 41. Gold(I)-catalyzed enantioselective alkoxycyclization.

[77] Y. Wang, A. D. Lackner, F. D. Toste, *Acc. Chem. Res.* **2014**, *47*, 889.

[78] Reviews on enantioselective gold catalysis: (a) R. A. Widenhoefer, *Chem. Eur. J.* **2008**, *14*, 5382. (b) A. Pradal, P. Y. Toullec, V. Michelet, *Synthesis (Stuttg)*. **2011**, *10*, 1501. (c) F. López, J. L. Mascareñas, *Beilstein J. Org. Chem* **2013**, *9*, 2250. (d) E. Manoni, M. Bandini, *Eur. J. Org. Chem.* **2016**, 3135. (e) Y. Li, W. Li, J. Zhang, *Chem. Eur. J.* **2017**, *23*, 467.

[79] Y. Ito, M. Sawamura, T. Hayashi, *J. Am. Chem. Soc.* **1986**, *108*, 6405.

[80] M. P. Muñoz, J. Adrio, J. C. Carretero, A. M. Echavarren, *Organometallics* **2005**, *24*, 1293.

Chiral digold complexes of bisphosphine ligands were also successfully employed in asymmetric intramolecular hydroarylation[81] or hydroamination[82] of allenes developed by Widenhoefer and coworkers. They obtained very high enantioselectivities using the digold complex prepared from (*S*)-MeO-DTBM-BIPHEP (Scheme 42).
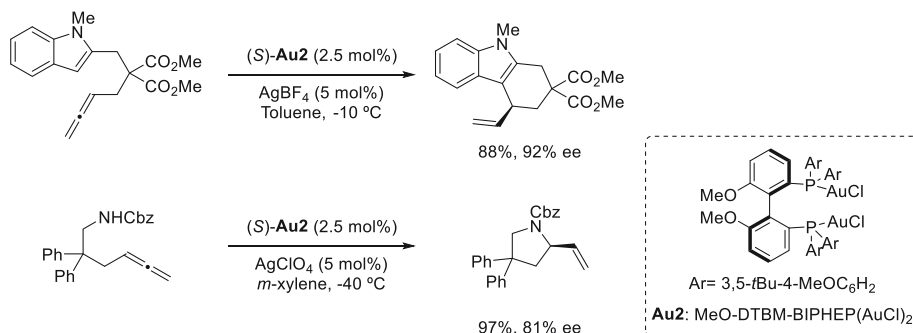
Scheme 42. Intramolecular gold(I)-catalyzed enantioselective hydroarylation and hydroamination.

Gagné carried out the enantioselective cycloisomerization of γ-allenenes to give vinylcyclohexenes.[83] In this case, the best enantiomeric excesses were obtained by using a digold(I) complex derived from BINAP, although the results were modest (Scheme 43). The X-ray analysis of a crystal of the digold(I) complex showed the presence of π-π stacking interactions between the two P-bound aryl groups, something similar to what was previously observed by Carretero and Echavarren. Gagné suggested that this type of interactions may lend the structure a degree of rigidity and thus establishes a well-defined chiral environment around the gold atom.
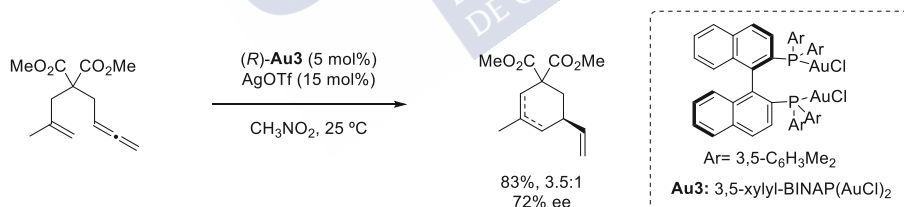
Scheme 43. Gold(I)-catalyzed enantioselective cycloisomerization of γ-allenenes.

In 2012, the group of Widenhoefer reported the first enantioselective intermolecular hydroamination of allenes with carbamates generating a tertiary stereocenter in high yields and enantioselectivities, also using a chiral bisphosphine digold(I) complex (Scheme 44).[84]

---

[81] C. Liu, R. A. Widenhoefer, *Org. Lett.* **2007**, *9*, 1935.

[82] Z. Zhang, C. F. Bender, R. A. Widenhoefer, *Org. Lett.* **2007**, *9*, 2887.

[83] M. A. Tarselli, A. R. Chianese, S. J. Lee, M. R. Gagné, *Angew. Chemie - Int. Ed.* **2007**, *46*, 6670.

[84] K. L. Butler, M. Tragni, R. A. Widenhoefer, *Angew. Chemie - Int. Ed.* **2012**, *51*, 5175.
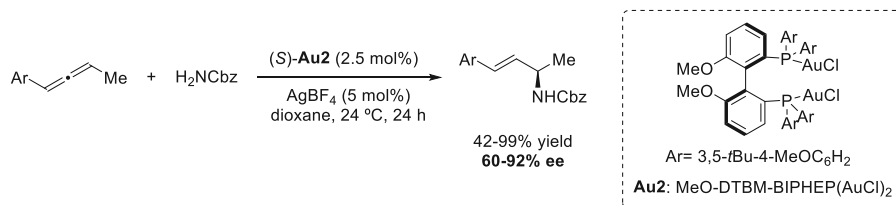
Scheme 44. Gold(I)-catalyzed intermolecular enantioselective hydroamination of allenes.

Cycloadditions

As can be deduced from the above cases, successful asymmetric inductions involve chiral digold complexes with phosphines carrying large aromatic groups attached to the phosphorous atom, probably because of a better transmission of the chiral information from the ligand to the product.

The fact that these bisphosphine-based digold complexes dominate the field is probably due to the notion that monodentate chiral ligands could not overcome the intrinsic limitation of the linear coordination of gold(I) complexes. Indeed, gold complexes of monodentate chiral ligands had provided very poor enantioselectivities (<2% ee). [80]

This notion changed in 2009, when our group found that BINOL-derived phosphoramidites featuring large aryl substituents at the 3 and 3' position of the binaphthol unity (e.g. anthracenyl groups, (*R*,*R*,*R*)-**Au4**) were excellent ligands for the asymmetric gold(I)-catalyzed (4+2) cycloaddition of allene-dienes, providing excellent yields and enantioselectivities above 91%. It is noteworthy that the chemoselectivity of the processes was also very high in favor of the (4+2) adduct over the (4+3). The enantiomeric excess of the major (4+2) cycloadduct was virtually identical to that of the minor (4+3) products regardless of the chiral gold catalyst and temperature employed, which supports the mechanistic proposal shown in Scheme 29 (page 34) involving a common cycloheptanic carbene intermediate. This report constituted the first example of a highly enantioselective process promoted by a mononuclear gold catalyst (Scheme 45). [65]

Later, Toste reported similar results using related phosphoramidites like **Au5**. Additionally, these authors reported a gold(I) precatalyst based on a H8-BINOL derived ligand (**Au6**), that was able to provide the (4+2) cycloadduct with excellent enantiomeric excess. [85] Fürstner and coworkers developed a chiral phosphoramidite-gold complex based on the Taddol backbone (**Au7**), which proved to be effective in these (4+2) cycloadditions and also in other asymmetric gold-catalyzed processes, such as in the

---

[80] M. P. Muñoz, J. Adrio, J. C. Carretero, A. M. Echavarren, *Organometallics* **2005**, *24*, 1293.

[65] I. Alonso, B. Trillo, F. López, S. Montserrat, G. Ujaque, L. Castedo, A. Lledós, J. L. Mascareñas, *J. Am. Chem. Soc.* **2009**, *131*, 13020.

[85] A. Z. González, F. D. Toste, *Org. Lett.* **2010**, *12*, 200.

(2+2) cycloadditions of allenenes, cycloisomerizations of *O*-tethered enynes or hydrofunctionalization of allenes.[86]

Z	n	R^1	R^2	[Au]	yield	ee
NTs	1	Me	Me	**Au4**	93%	92%
NTs	1	Me	Me	**Au5**	83%	99%
NTs	1	Me	Me	**Au7**	90%	91%
NTs	1	-(CH$_2$)$_5$-		**Au4**	88%	97%
NTs	2	Me	Me	**Au4**	90%	91%
C(CO$_2$Me)$_2$	1	Me	Me	**Au6**	87%	92%[a]

[a] benzene, rt
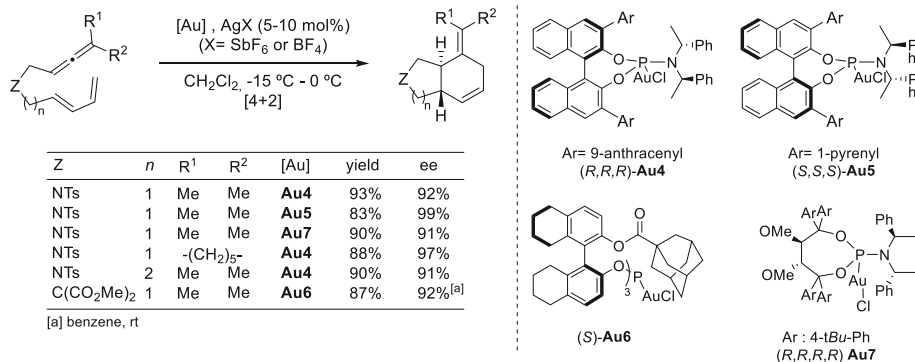
Scheme 45. Gold(I)-catalyzed enantioselective (4+2) cycloadditions of allenedienes.

In 2011, our group demonstrated that these chiral mononuclear phosphoramidite-gold complexes are also good catalysts for the (4+3) cycloaddition, provided that the allenes are monosubstituted at the distal position. Thus, optically active 5,7- and 6,7-fused bicyclic systems were obtained with good yields, complete diastereocontrol and excellent enantioselectivities (Scheme 46).[87] Interestingly, while the disubstitution at the distal position of the allene favors the formation of (4+2) cycloadducts, the presence of a substituent at the internal position, instead of the terminal one, is compatible with the (4+3) cycloaddition, allowing access to 5,7-fused bicyclic systems with chiral carbon quaternary stereocenter at the ring fusion, with excellent enantioselectivities (Scheme 46, R ≠ H).
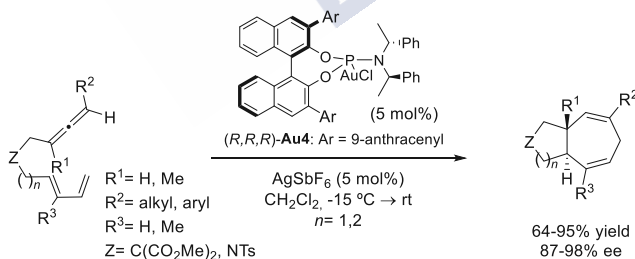
Scheme 46. Gold(I)-catalyzed (4+3) enantioselective cycloaddition of allenedienes.

Recently, the group of Echavarren developed an enantioselective synthesis of cyclobutanes by intermolecular (2+2) cycloaddition of alkynes with alkenes using non-C$_2$ symmetric digold catalysts in good yields and enantioselectivities. They postulate that only one of the gold(I) centers is directly involved in the activation of the alkyne,

---

[86] (a) H. Teller, S. Flügge, R. Goddard, A. Fürstner, *Angew. Chemie - Int. Ed.* **2010**, *49*, 1949. (b) H. Teller, M. Corbet, L. Mantilli, G. Gopakumar, R. Goddard, W. Thiel, A. Fürstner, *J. Am. Chem. Soc.* **2012**, *134*, 15331.

[87] I. Alonso, H. Faustino, F. López, J. L. Mascareñas, *Angew. Chemie - Int. Ed.* **2011**, *50*, 11496.

although the second one is required to induce the enantioselectivity due to a combination of stabilizing π-stacking and unfavorable steric effects (Scheme 47).[88]
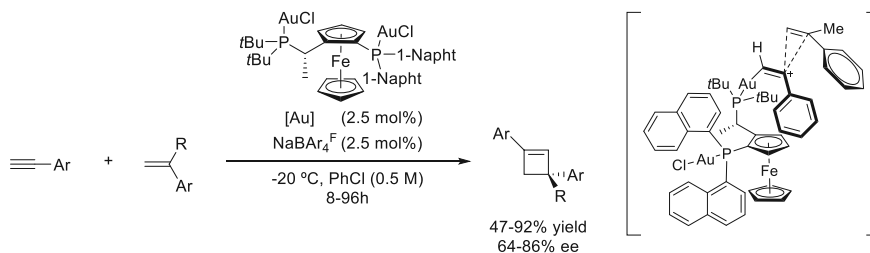
Scheme 47. Intermolecular gold(I)-catalyzed (2+2) enantioselective synthesis of cyclobutanes by Echavarren.

Enantioselective gold catalysis with allenamides

During the last years, several enantioselective reactions promoted by chiral gold complexes involved the use of allenamides as key components. The first examples were reported in 2012 by our group, in collaboration with the group of J. M. Lassaletta and R. Fernández. In particular, we demonstrate that a new class of chiral NHC-Au(I) complexes bearing a chiral triazole ligand embedded in a rigid axially chiral cyclic frame, were excellent catalysts for promoting the abovementioned intermolecular (4+2) cycloaddition between allenamides and dienes (Scheme 35, page 37). The catalyst afforded the (4+2) cycloadducts in good yields and excellent enantioselectivities (up to 99%). This method also constituted the first example of a highly enantioselective intermolecular (4+2) cycloaddition between any type of allenes and dienes (Scheme 48).[89]
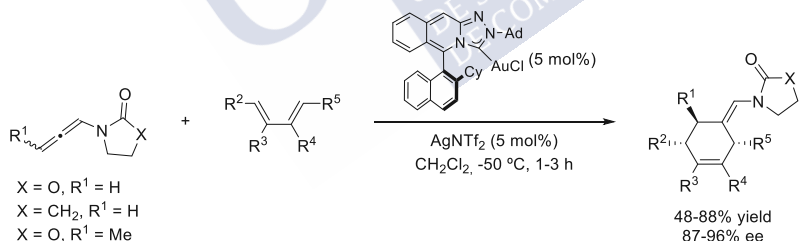
Scheme 48. Intermolecular gold(I)-catalyzed (4+2) enantioselective cycloaddition between allenamides and dienes.

The same year, González and coworkers reported the first asymmetric (2+2) cycloaddition between sulfonylallenamides and vinylarenes in the presence of chiral

---

[88] C. García-Morales, B. Ranieri, I. Escofet, L. López-Suárez, C. Obradors, A. I. Konovalov, A. M. Echavarren, *J. Am. Chem. Soc.* **2017**, *139*, 13628.

[89] J. Francos, F. Grande-carmona, H. Faustino, J. Iglesias-Sigüenza, E. Díez, I. Alonso, R. Fernández, J. M. Lassaletta, F. López, J. L. Mascareñas, *J. Am. Chem. Soc.* **2012**, *134*, 14322.

phosphoramidite-gold(I) complex. The process leads to enantioenriched cyclobutanes in very good yields and enantiomeric excesses (Scheme 49).[90,]
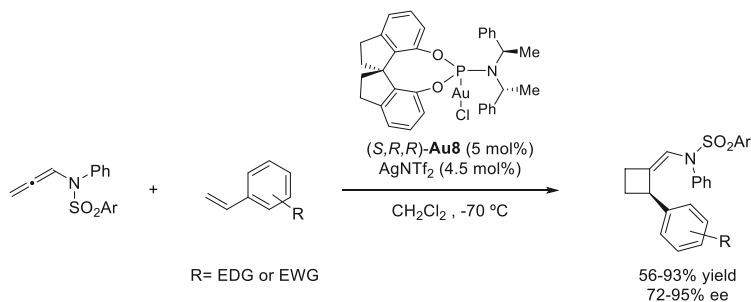
Scheme 49. Intermolecular gold(I)-catalyzed (2+2) enantioselective synthesis of cyclobutanes.

In 2015, J. Zhang reported an intermolecular gold(I)-catalyzed (2+2) and (4+2) enantioselective cycloadditions between 3-styrylindoles with *N*-allenamides. In this work, they can discriminate between the (2+2) or the (4+2) cycloaddition depending on the electronic nature of the *N*-substituent at the 3-styrylindole. Supported by theoretical and experimental data, they concluded that the presence of electron-withdrawing groups favors the (4+2) cycloaddition; whereas the (2+2) cycloaddition takes place with electron-donating groups (Scheme 50).[91]
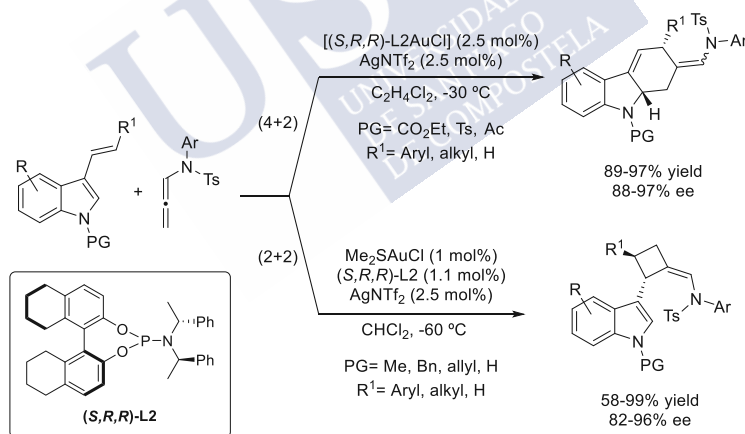

Scheme 50. Intermolecular gold(I)-catalyzed (2+2) *vs.* (4+2) enantioselective cycloaddition between 3-styrylindoles and allenamides.

More recently, in 2017, the same group developed a new chiral sulfonamide phosphine ligand for the intramolecular gold(I)-catalyzed enantioselective cyclization of *N*-allenamides, a process that provides tetrahydrocarbolines with excellent yields and enantioselectivities. For the induction of asymmetry, they proposed that the phosphine

---

[90] S. Suárez-Pantiga, C. Hernández-Díaz, E. Rubio, J. M. González, *Angew. Chemie - Int. Ed.* **2012**, *51*, 11552.

[91] Y. Wang, P. Zhang, Y. Liu, F. Xia, J. Zhang, *Chem. Sci.* **2015**, *6*, 5564.

of the ligand and the *N*-allenamide coordinate to the gold(I) atom. Meanwhile, the sulfonyl group of the allenamide would form a hydrogen bond with the sulfonamide moiety, shielding the *Si*-face of the allenamide. Thus, the indole attack takes place at the *Re*-face, yielding the product with excellent enantioselectivity (Scheme 51).[92]
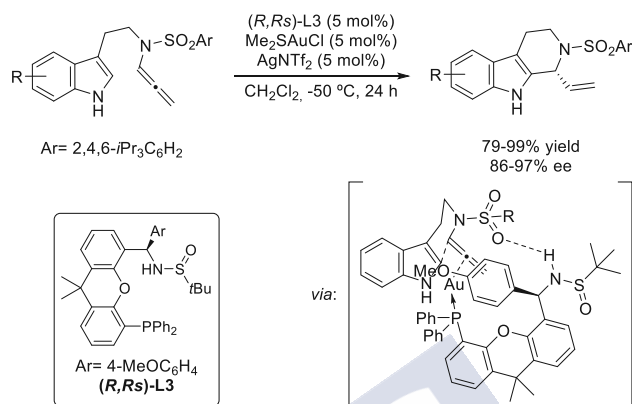
Scheme 51. Intramolecular gold(I)-catalyzed asymmetric cyclization of *N*-allenamides.

In almost all gold-catalyzed cycloadditions of *N*-allenamides, is the distal C=C bond of the *N*-allenamides the one that participates in the cycloaddition, in a reaction involving the formation of the zwitterionic intermediate **XI′**. However, in 2015 the group of J. Zhang reported a gold(I)-catalyzed (3+2) annulation of 2-(1-alkynyl)-2-alken-1-ones with participation of the proximal C=C bond of an *N*-allenamide. The reaction is believed to proceed through a key intermediate gold all-carbon 1,3-dipole **XIV**. It has been suggested that the formation of intermediate **XIV** is more favored than that of the gold zwitterionic intermediate **XI′**. Thus, the (3+2) annulation takes place at the proximal C=C bond of the *N*-allenamide via the intermediate **XV**, yielding the fused furans in good yields with high regio-, diastereo- and enantioselectivity (Scheme 52).[93]

[92] Y. Wang, P. Zhang, X. Di, Q. Dai, Z. M. Zhang, J. Zhang, *Angew. Chemie - Int. Ed.* **2017**, *56*, 15905.

[93] Y. Wang, P. Zhang, D. Qian, J. Zhang, *Angew. Chemie - Int. Ed.* **2015**, *54*, 14849.
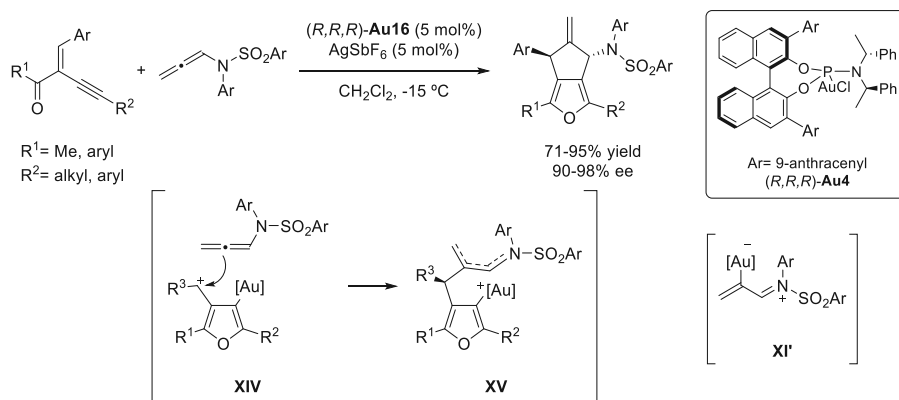
Scheme 52. Intermolecular gold(I)-catalyzed enantioselective annulations at the proximal C=C bond.

4. Organocatalysis

4.1. Introduction

Asymetric organocatalysis

Asymmetric organocatalysis is based on the use of small chiral organic molecules as catalysts for the stereocontrolled assembly of structurally diverse molecules. The origin of this chemistry can be tracked to the original work of Hajos-Parrish in 1974, reporting an intramolecular aldol cyclization of the triketone **12** to give the bicyclic diketone **13** in the presence of a catalytic amount of (*S*)-proline (Scheme 53).[94]
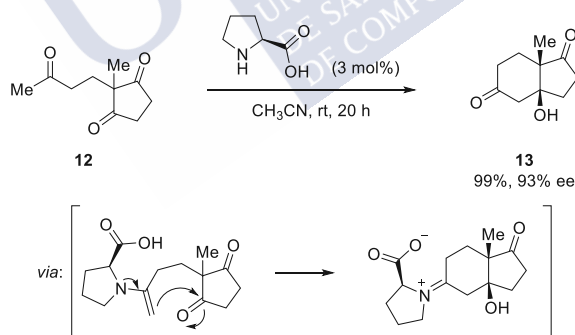
Scheme 53. Proline-catalyzed synthesis of the bicyclic diketone **18** by Hajos-Parrish.

The key development in organocatalysis was reported in the year 2000 when B. List and C. F. Barbas described a (*S*)-proline-catalyzed aldol reaction that takes place through an *in situ* generated enamine intermediate. In the proposed mechanism, a hydrogen-bond

---

[94] Z. G. Hajos, D. R. Parrish, *J. Org. Chem.* **1974**, *39*, 1615.

interaction between the carboxylate and the carbonyl group of the aldehyde determines a *re*-facial attack of the *in situ* generated enamine (Scheme 54).[95]

Scheme 54. Proline-catalyzed asymmetric aldol reaction through enamine catalysis.

In the same year, the group of MacMillan reported a Diels-Alder reaction based on iminium catalysis. In particular, condensation between an α,β-unsaturated aldehyde and the imidazolidinone organocatalyst led to the *in situ* generation of the dienophile, an (*E*)-iminium intermediate that is generated with precise stereoselectivity to avoid nonbonding interaction between the geminal methyl groups. Moreover, the benz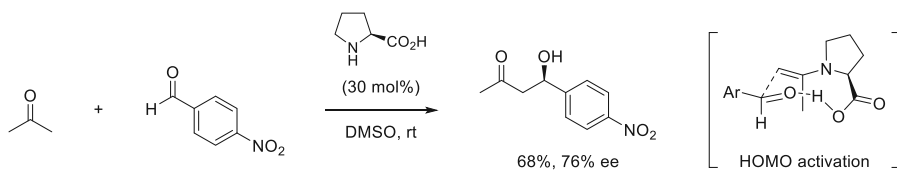yl group of the organocatalyst shields the top face of the dienophile, leaving the *Si*-face exposed to the diene, so that the cycloaddition is highly selective (Scheme 55).[96] Importantly, MacMillan coined the term *asymmetric organic catalysis* and *organocatalysis* to describe any type of asymmetric reaction that is catalyzed by a low molecular weight organic molecule.
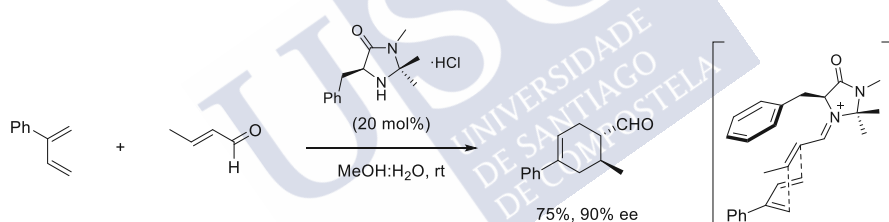
Scheme 55. Enantioselective organocatalytic Diels-Alder reaction through iminium catalysis.

These two works showed that the underlying mechanisms of these organocatalytic reactions (enamine and iminium activation modes) could be later extended and applied to other synthetic transformations, with a broader applicability.

In 2002, the group of Jacobsen defined a new activation mode based on hydrogen-bonding, promoted by chiral thioureas. They suggested that the activation of the substrate and the organization of the transition state could occur through well-defined hydrogen-bonding interactions between the organocatalyst and a carbonyl or imine group (Scheme 56).[97]

---

[95] (a) B. List, R. A. Lerner, C. F. Barbas III, *J. Am. Chem. Soc.* **2000**, *122*, 2395. (b) W. Notz, B. List, *J. Am. Chem. Soc.* **2000**, *122*, 7386.

[96] K. A. Ahrendt, C. J. Borths, D. W. C. MacMillan, *J. Am. Chem. Soc.* **2000**, *122*, 4243.

[97] A. G. Wenzel, E. N. Jacobsen, *J. Am. Chem. Soc.* **2002**, *124*, 12964.
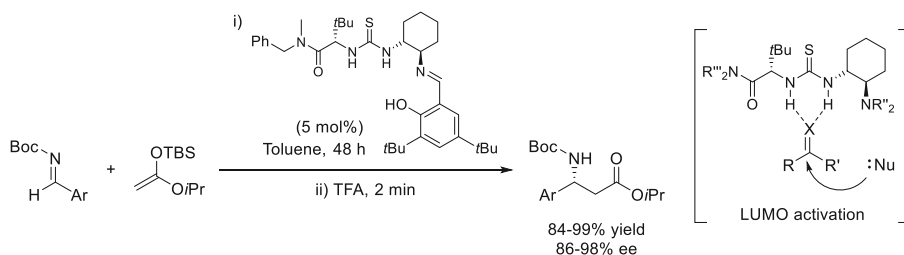
Scheme 56. Asymmetric catalytic Mannich reaction by Hydrogen-bonding catalysis reported by Jacobsen.

In 2004, Akiyama and Terada independently introduced a new non-covalent activation mode, based on the use of chiral Brønsted acids as organocatalysts. These catalysts lower the LUMO energy of an electrophile, via protonation, generating a chiral electrophilic species that undergoes nucleophilic attack (Scheme 57).[98]
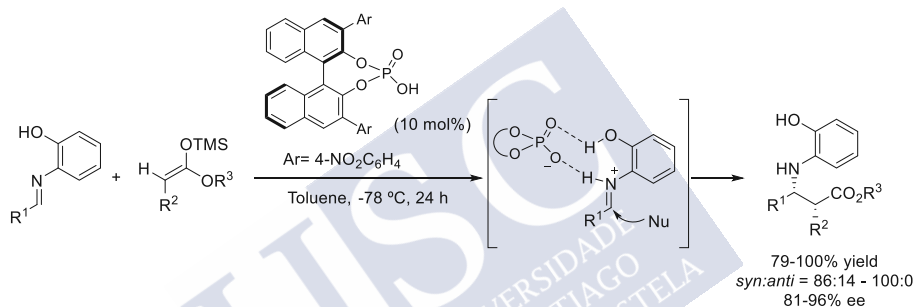
Scheme 57. Enantioselective Mannich reaction catalyzed by a chiral Brønsted acid reported by Akiyama.

In 2007, MacMillan introduced a new organocatalytic activation mode, the SOMO catalysis. This activation mode is founded upon the hypothesis that one-electron oxidation of an electron-rich enamine intermediate (derived from condensation between aldehydes and chiral amine catalysts) selectively generates a reactive radical cation with three π-electrons (SOMO). This intermediate can readily react with a variety of weakly nucleophilic "SOMOphiles" such as allylsilanes or silyl enol ethers, resulting in formal alkylation products (Scheme 58).[99]

---

[98] T. Akiyama, J. Itoh, K. Yokota, K. Fuchibe, *Angew. Chemie - Int. Ed.* **2004**, *43*, 1566.

[99] H.-Y. Jang, J.-B. Hong, D. W. C. MacMillan, *J. Am. Chem. Soc.* **2007**, *129*, 7004.
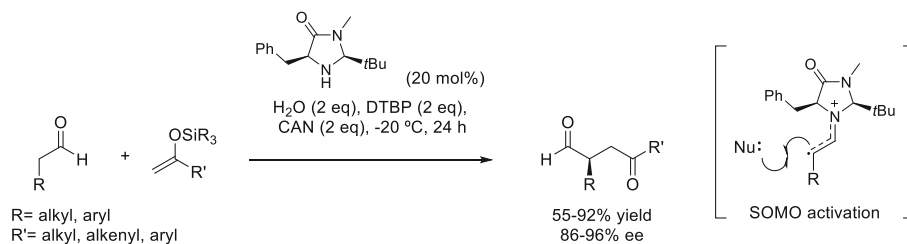
Scheme 58. Enantioselective organocatalytic SOMO catalysis for the α-enolation of aldehydes.

These pioneer developments, together with parallel achievements on phase-transfer asymmetric catalysis,[100] anion-binding activation,[101] chiral *N*-heterocyclic carbene catalysts,[102] as well as light induced organocatalysis,[103] have allowed organocatalysis to be widely accepted as one of the main branches of enantioselective synthesis, together with biocatalysis and metal catalysis.[104]

Overall, the use of organocatalytic processes in organic synthesis has several important advantages, such as the access to high stereoselectivities, mild and robust reaction conditions, adequate functional group tolerance as well as insensitivity towards air and moisture.[105] On the contrary, several limitations have still to be faced; in particular catalyst loadings are typically quite high, exceeding those commonly used in biocatalysis or in metal catalysis.

Enamine-based organocatalysis

Related to this thesis is the enamine-based organocatalysis, a type of activation mode that has been generally used to functionalize carbonyl compounds at their α-carbons. The general mechanism involves an acid-promoted condensation of the carbonyl with the amine to form an iminium ion **XVI**. One of the α-acidic protons of the iminium ion is then removed by the conjugate base of the acid, so that a key nucleophilic enamine is formed. Reaction of this intermediate with an electrophile (E) generates another iminium ion, whose hydrolysis liberates the product, the acid, and the amine catalyst, which can reenter the catalytic cycle (Scheme 59). The efficiency of this catalytic cycle relies on three important factors: (a) a fast and quantitative generation of the first iminium ion; (b) a regio- and stereoselective conversion of this iminium ion into the (*E*)-enamine

[100] (a) U. H. Dolling, P. Davis, E. J. J. Grabowski, *J. Am. Chem. Soc.* **1984**, *106*, 446. (b) S. Shirakawa, K. Maruoka, *Angew. Chemie - Int. Ed.* **2013**, *52*, 4312.

[101] S. E. Reisman, A. G. Doyle, E. N. Jacobsen, *J. Am. Chem. Soc.* **2008**, *130*, 7198.

[102] D. Enders, O. Niemeier, A. Henseler, *Chem. Rev.* **2007**, *107*, 5606.

[103] (a) M. Silvi, P. Melchiorre, *Nature* **2018**, *554*, 41. For a review on the use of photoredox catalysis in organic chemistry, see: (b) M. H. Shaw, J. Twilton, D. W. C. MacMillan, *J. Org. Chem.* **2016**, *81*, 6898. (c) N. A. Romero, D. A. Nicewicz, *Chem. Rev.* **2016**, *116*, 10075.

[104] (a) B. List, *Chem. Rev.* **2007**, *107*, 5413. (b) D. W. C. MacMillan, *Nature* **2008**, *455*, 304.

[105] For reviews on organocatalysis see: (a) S. Bertelsen, K. A. Jørgensen, *Chem. Soc. Rev.* **2009**, *38*, 2178. (b) A. Moyano, R. Rios, *Chem. Rev.* **2011**, *111*, 4703. (c) R. Rios, *Stereoselective Organocatalysis: Bond Formation Methodologies and Activation Modes*, Wiley, **2013**. (d) M. Bihani, J. C.-G. Zhao, *Adv. Synth. Catal.* **2017**, *359*, 534. (e) See reference 8: M. T. Reetz, B. List, S. Jaroch, H. Weinmann, *Organocatalysis*, Springer-Verlag, **2008**.

intermediate; and (c) a high stereochemical bias in the electrophilic attack. The nature of the carbonyl compound, chiral amine catalyst and of the Brønsted acid are crucial factors.
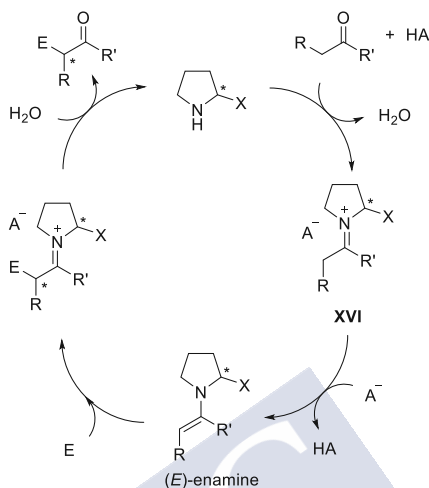
Scheme 59. General catalytic cycle for the activation mode based on enamine catalysis.

Since the publication of List and Barbas in 2000, several secondary amine-based catalysts have been developed, being proline analogs among the most common. In these cases, good hydrogen-bonding properties of the electrophile are important to achieve high asymmetric induction, since the carboxylic acid (or alternative hydrogen bond donor group) directs the attack of the electrophile through hydrogen-bonding in a highly ordered approach, via *Re*-face attack (Figure 6).[106]
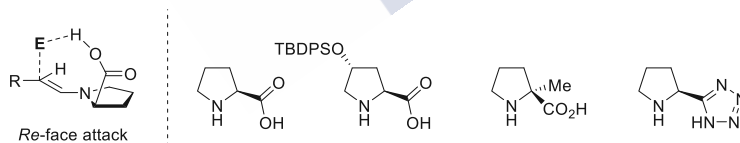
Figure 6. Working transition state and common organocatalysts with hydrogen-bond directing groups.

Hayashi and Jørgensen demonstrated independently that the introduction of bulky silyloxy groups at the proline structure leads to a very effective catalytic activity in the α-functionalization of aldehydes. In these cases, the bulky substituent of the amine directs the attack of the electrophile through the opposite *Si*-face, due to purely steric factors (Figure 7).[107]

---

[106] A. Moyano, in: *Stereoselective Organocatalysis: Bond Formation Methodologies and Activation Modes*. R. Rios (ed.), *Activation Modes in Asymmetric Organocatalysis*. Chapter 2, pages 11-80. Wiley, **2013**.

[107] (a) Y. Hayashi, H. Gotoh, T. Hayashi, M. Shoji, *Angew. Chemie - Int. Ed.* **2005**, *44*, 4212. (b) J. Franzén, M. Marigo, D. Fielenbach, T. C. Wabnitz, A. Kjærsgaard, K. A. Jørgensen, *J. Am. Chem. Soc.* **2005**, *127*, 18296. (c) K. L. Jensen, G. Dickmeiss, H. Jiang, Ł. Albrecht, K. A. Jørgensen, *Acc. Chem. Res.* **2012**, *45*, 248.
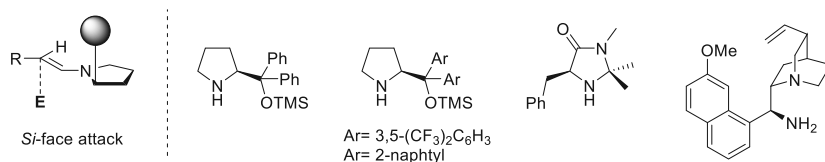
Figure 7. Working transition state and common organocatalysts with bulky substituents.

Thus, in 2005, Hayashi demonstrated that diphenylprolinol silyl ethers were suitable organocatalysts for the asymmetric Michael reaction of aldehydes and nitroalkenes.[107a] They proposed that the bulky substituent plays two important roles: to promote the selective formation of the *anti* enamine, and provide a selective shielding of the *Re*-face of the enamine double bond (Scheme 60, upper arrow). In the same year, Jørgensen reported an organocatalytic method for the enantioselective α-fluorination of aldehydes, followed by a subsequent reduction of the aldehyde to afford the corresponding alcohols with high enantioselectivity. The methodology was very effective for generating tertiary stereocenters (Scheme 60, lower arrow); however, α-branched aldehydes afforded the corresponding products featuring quaternary carbon centers with moderate enantioselectivity (48%ee).[107b, 108]
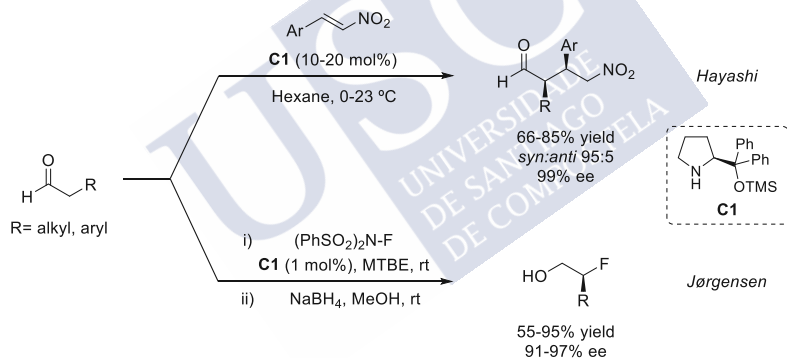
Scheme 60. Asymmetric organocatalytic reactions of aldehydes mediated by diphenylprolinol silyl ethers.

4.2. α-Alkylation of carbonyl compounds

During the last decade, enamine organocatalysis has proven to be particularly effective for the asymmetric synthesis of a wide range of α-heteroatom-substituted carbonyl compounds, as a result of transforming the C-H bond adjacent to the carbonyl moiety into a stereogenic C-X bond (X= C, N, O, P, F, Cl, Br, I, S, Se).[109]

---

[108] M. Marigo, D. Fielenbach, A. Braunton, A. Kjærsgaard, K. A. Jørgensen, *Angew. Chemie - Int. Ed.* **2005**, *44*, 3703.

[109] For reviews on asymmetric α-heteroatom functionalization of aldehydes and ketones see: (a) M. Marigo, K. A. Jørgensen, *Chem. Commun.* **2006**, 2001. (b) S. Mukherjee, J. W. Yang, S. Hoffmann, B. List, *Chem. Rev.* **2007**, *107*, 5471.

Despite this enormous versatility, the application of enamine catalysis to α-carbon-carbon bond forming processes usually requires the use of carbonyls, imines, or α,β-unsaturated derivatives as electrophilic partners; catalytic α-alkylations of aldehydes with carbon(sp³)-based electrophiles are extremely scarce.[110]

In 2004, List and coworkers reported an isolated example of the first intramolecular organocatalytic asymmetric α-alkylation of halo-aldehydes. They used a proline-based organocatalyst and carried out the reaction under mild conditions affording chiral substituted carbocycles, such as cyclopentanes and cyclopropanes in good yields and enantioselectivities (Scheme 61).[110a]
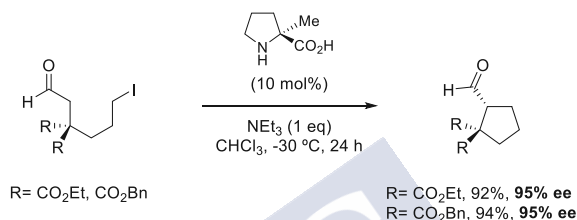
Scheme 61. Catalytic asymmetric intramolecular α-alkylation of aldehydes.

However, extension to the corresponding intermolecular reaction failed, mainly due to deactivation of the amine catalyst by *N*-alkylation with the alkyl halides. Thus, chemists developed alternative aminocatalytic strategies,[111] such as the enantioselective α-allylation of aldehydes using SOMO activation (Scheme 62).[111a] In the particular case shown in Scheme 62, the use of ceric ammonium nitrate (CAN) as stoichiometric oxidant, and allyltrimethylsilane as SOMO nucleophiles led to α-allylated aldehydes in very good yields and enantioselectivities.

[110] (a) N. Vignola, B. List, *J. Am. Chem. Soc.* **2004**, *126*, 450. (b) D. Enders, C. Wang, J. W. Bats, *Angew. Chemie - Int. Ed.* **2008**, *47*, 7539. (c) B. List, I. Čorić, O. O. Grygorenko, P. S. J. Kaib, I. Komarov, A. Lee, M. Leutzsch, S. Chandra Pan, A. V. Tymtsunik, M. Van Gemmeren, *Angew. Chemie - Int. Ed.* **2014**, *53*, 282.

[111] (a) T. D. Beeson, A. Mastracchio, J.-B. Hong, K. Ashton, D. W. C. MacMillan, *Science.* **2007**, *316*, 582. (b) R. R. Shaikh, A. Mazzanti, M. Petrini, G. Bartoli, P. Melchiorre, *Angew. Chemie - Int. Ed.* **2008**, *47*, 8707. (c) H.-W. Shih, M. N. Vander Wal, R. L. Grange, D. W. C. MacMillan, *J. Am. Chem. Soc.* **2010**, *132*, 13600. (d) A. R. Brown, W.-H. Kuo, E. N. Jacobsen, *J. Am. Chem. Soc.* **2010**, *132*, 9286. (e) E. R. Welin, A. A. Warkentin, J. C. Conrad, D. W. C. MacMillan, *Angew. Chemie - Int. Ed.* **2015**, *54*, 9668.
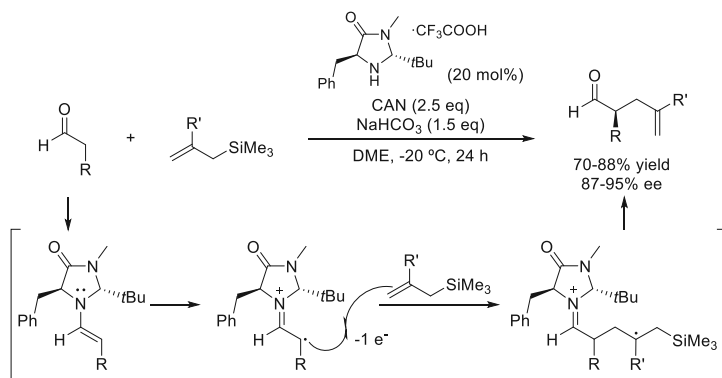
Scheme 62. Intermolecular enantioselective α-allylation of aldehydes by SOMO activation.

By the time I started my thesis, significant advances had been made in this area of organocatalytic asymmetric α-alkylation of carbonyl compounds, however, there were still many challenges to be explored in the intermolecular version such as, for instance, the generation of aldehydes bearing quaternary stereocenters at the carbonyl adjacent position. One way to face these challenges could be the use of electrophiles activated by transition metal complexes, which would expand the activation modes and the scope of the α-functionalization of carbonyl derivatives.

5. Dual catalysis: combining organocatalysis and transition metal catalysis

5.1. Introduction

Transition metal catalysis and organocatalysis individually have their own place in modern organic chemistry and can be considered two of the pillars of catalysis, along with biocatalysis, and the recently boosted photocatalysis. The combination of both catalytic strategies is a particularly attractive concept that can bring unique advantages, such as the development of new previously unattainable transformations, or the discovery of new types of reactivities not accessible with a single catalyst. On the other hand, it might allow to improve the enantioselectivity where stereochemical control was previously absent or challenging with a single catalyst; and improve the efficiency and broaden the substrate scope of existing transformations through the cooperative effect of two or more catalysts.[112,113]

However, the combination of organo- and transition metal catalysis is not trivial. The main challenge is to ensure compatibility of catalysts, substrates, intermediates and solvents throughout the whole reaction sequence.

---

[112] Z. Du, Z. Shao, *Chem. Soc. Rev.* **2013**, *42*, 1337.

[113] D.-F. Chen, Z.-Y. Han, X.-L. Zhou, L.-Z. Gong, *Acc. Chem. Res.* **2014**, *47*, 2365. For a recent review on the combination of aminocatalysts and metal catalysts see: S. Afewerki, A. Córdova, *Chem. Rev.* **2016**, *116*, 13512.

At the beginning of this thesis, the diverse types of multicatalytic systems have been defined and categorized as: cooperative catalysis, synergistic catalysis, and sequential or relay catalysis (see Scheme 1, page 18). Specifically, in Scheme 63 are again reproduced the systems that involve the combined use of organo- and metal catalysis.
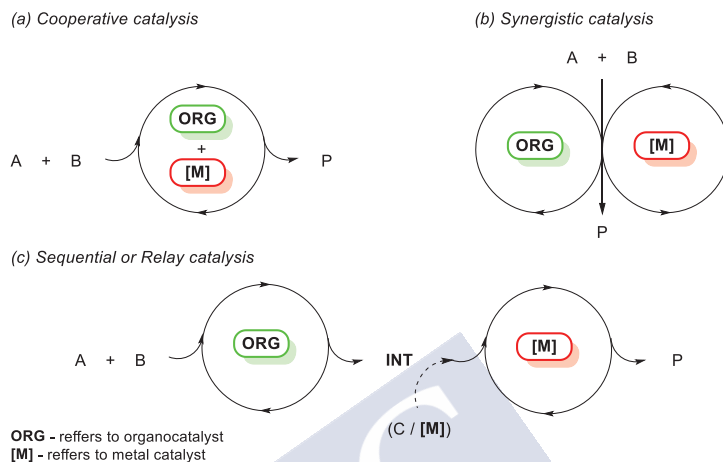
Scheme 63. Multicatalytic systems combining organo- and metal catalysis.

The most common types of organocatalysts employed in combination with metal catalysis are Brønsted acid catalysts (especially chiral phosphoric acids), although aminocatalysts (including secondary and primary amines), hydrogen-bonding catalysts, and *N*-heterocyclic carbene catalysts have also been studied. On the other hand, regarding transition metals, several metals have been investigated, being Pd, Ir or Cu the most commonly employed.[114] The use of carbophilic metals such as Pt or Au have clearly lagged behind.

In the following section, we describe some of the most representative examples involving metal catalysis and amine organocatalysis, which are the hub of this thesis.

The first example of the combination of amine and transition metal catalysis was reported by Córdova and coworkers in 2006. They described an intermolecular α-allylic alkylation of aldehydes and cyclic ketones with allylic acetates, mediated by the combination of a palladium catalyst and an enamine-based catalyst such as pyrrolidine.[115a] An asymmetric version of this reaction was also investigated using chiral pyrrolidine derivatives and, in 2012, high enantioselectivity and regiospecificity were

---

[114] For selected examples see: (a) J. M. Stevens, D. W. C. MacMillan, *J. Am. Chem. Soc.* **2013**, *135*, 11756. (b) M. Yoshida, T. Terumine, E. Masaki, S. Hara, *J. Org. Chem.* **2013**, *78*, 10853. (c) R. Shibuya, L. Lin, Y. Nakahara, K. Mashima, T. Ohshima, *Angew. Chemie - Int. Ed.* **2014**, *53*, 4377. (d) R. Manzano, S. Datta, R. S. Paton, D. J. Dixon, *Angew. Chemie - Int. Ed.* **2017**, *56*, 5834.

[115] (a) I. Ibrahem, A. Córdova, *Angew. Chemie - Int. Ed.* **2006**, *45*, 1952. (b) S. Afewerki, I. Ibrahem, J. Rydfjord, P. Breistein, A. Córdova, *Chem. Eur. J.* **2012**, *18*, 2972.

achieved using the Hayashi-Jørgensen chiral secondary amine (**C1**) as organocatalyst (Scheme 64).[115b]
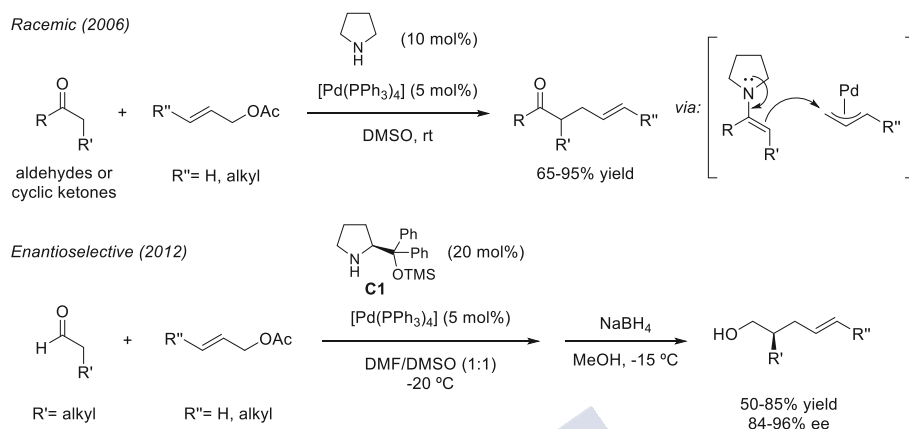
Scheme 64. Intermolecular α-allylic alkylation of aldehydes and cyclic ketones reported by Córdova.

This α-allylic alkylation reaction involves a good leaving group like an acetate to form the active Tsuji-Trost palladium π-allyl electrophile. In this regard, direct α-allyl alkylation using allylic alcohols as electrophiles seems an attractive protocol, since avoids the transformation of the hydroxyl group into a leaving group. In 2009, Breit and coworkers reported a dual Pd/proline-catalyzed α-allylation of aldehydes and ketones using allylic alcohols as reaction partners. Unfortunately, the development of the asymmetric version using optically pure organocatalysts failed, generally providing poor yields and low asymmetric inductions (Scheme 65).[116]
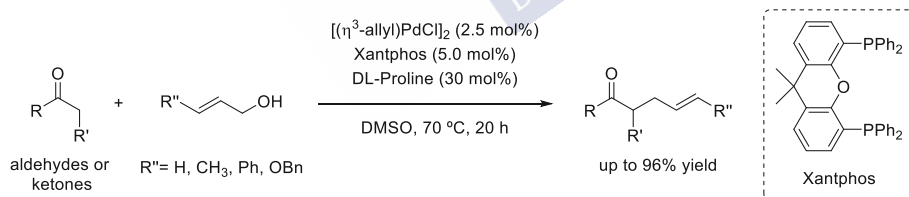
Scheme 65. Pd/proline-catalyzed α-allylation reaction with allylic alcohols.

In 2008, MacMillan and coworkers reported a new way to achieve intermolecular α-functionalization of aldehydes with α-bromocarbonyls, by merging the fields of organocatalysis and photoredox catalysis (dual photoredox/organocatalysis).[117] The reaction proceeds through condensation of the organocatalyst with the aldehyde, delivering a nucleophilic enamine that can react with an electrophilic radical, generated via single-electron reduction of an activated alkyl halide by a Ru(I) photocatalyst. The resulting α-amino radical **XVII** is oxidized by the *[Ru] excited state to produce the

---

[116] I. Usui, S. Schmidt, B. Breit, *Org. Lett.* **2009**, *11*, 1453.

[117] (a) D. A. Nicewicz, D. W. C. MacMillan, *Science.* **2008**, *322*, 77.

iminium ion that would deliver the enantioenriched α-alkyl aldehyde product (Scheme 66).
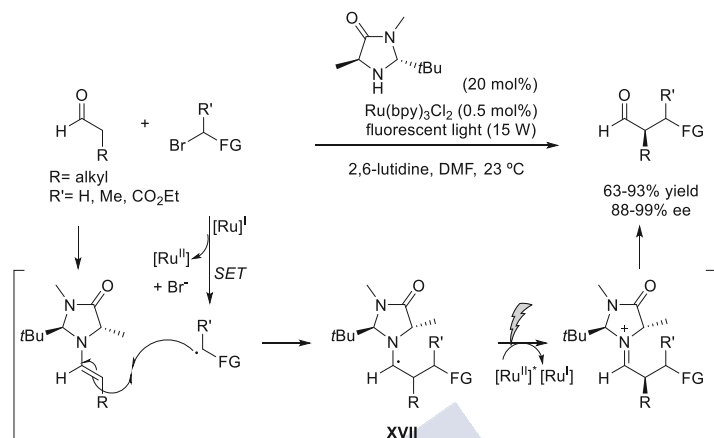
Scheme 66. Enantioselective α-functionalization of aldehydes via dual photoredox organocatalysis.

On the other hand, MacMillan also demonstrated the viability of combining in a synergistic fashion copper(II) and enamine catalysis for the enantioselective α-alkenylation of aldehydes with boronic acids, affording α-vinyl aldehydes in high yields and good enantioselectivities (Scheme 67). The authors proposed that the reaction proceeds through a key intermediate enamine-organocopper(III) complex, which after reductive elimination would furnish an α-alkenyl iminium and the corresponding copper(I) salt. Regeneration of each catalyst would be accomplished through hydrolysis of the iminium and single-electron oxidation of the copper(I) salt, delivering the enantioenriched products.[114a]
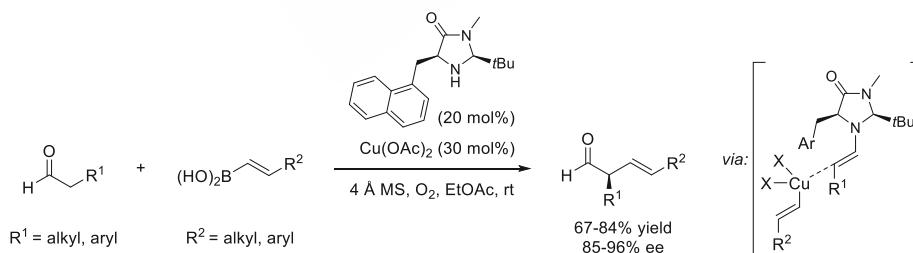
Scheme 67. Synergistic Cu(II)/amine catalyzed α-alkenylation with boronic acids.

In 2013, Carreira and coworkers developed an elegant enantioselective α-allylation of branched aldehydes by means of an iridium-catalyzed allylic substitution of allylic alcohols with *in situ* generated enamines. The process, which involves both chiral amine and chiral iridium catalysts, delivers in good yields and excellent selectivities γ,δ-unsaturated aldehydes bearing two vicinal stereocenters, including an α-quaternary

---

[114a] J. M. Stevens, D. W. C. MacMillan, *J. Am. Chem. Soc.* **2013**, *135*, 11756.

centers. This dual catalysis allowed the formation of all stereoisomers of the products just by appropriate selection of the enantiomers of the two catalysts (Scheme 68).[118]
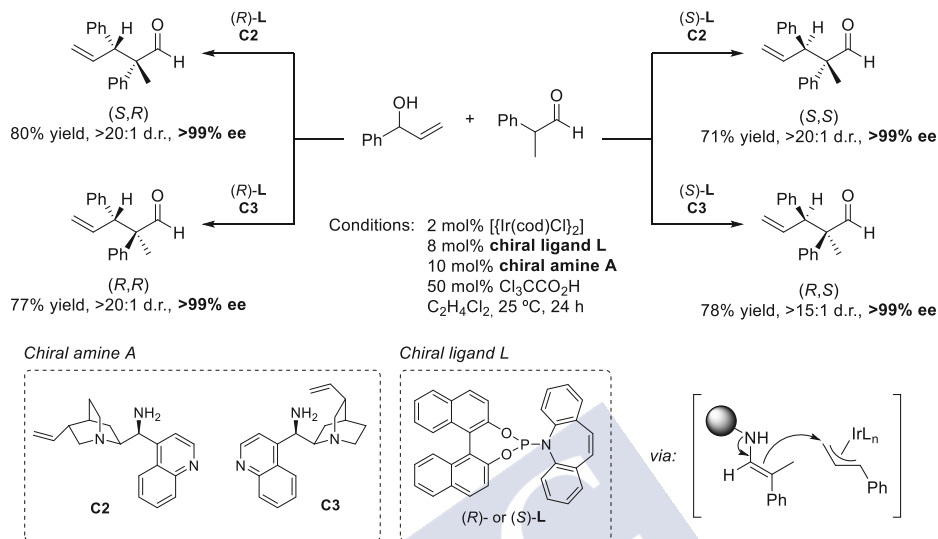
Scheme 68. Dual catalysis for the stereodivergent control of α-allylation of α-branched aldehydes.

Moreover, the same group further expanded the methodology to use linear, instead of α-branched, aldehydes. In this case, a similar protocol but employing the Hayashi-Jørgensen chiral secondary amine (**C1**) was reported.[119] Other groups have introduced related methods since then, essentially using rhodium and iridium as metal catalysts.[120]

5.2. Merging gold and organocatalysis

The combination of gold catalysts with amine-based organocatalysis is rare and most examples are limited to less challenging relay or sequential catalysis.

This paucity is related to the incompatibility of gold complexes (soft Lewis acids) with basic amines. Indeed, with a few exceptions[121,122] that require excessive heating (≥110 °C)[121a,b], favorable intramolecular scenarios,[121c,d,e] or redox processes on gold;[121f] reactions

---

[118] S. Krautwald, D. Sarlah, M. A. Schafroth, E. M. Carreira, *Science.* **2013**, *340*, 1065.

[119] S. Krautwald, M. A. Schafroth, D. Sarlah, Carre, *J. Am. Chem. Soc.* **2014**, *136*, 3020.

[120] (a) F. A. Cruz, V. M. Dong, *J. Am. Chem. Soc.* **2017**, *139*, 1029. (b) X. Jiang, J. J. Beiger, J. F. Hartwig, *J. Am. Chem. Soc.* **2017**, *139*, 87.

[121] (a) V. Lavallo, G. D. Frey, B. Donnadieu, M. Soleilhavoup, G. Bertrand, *Angew. Chemie - Int. Ed.* **2008**, *47*, 5224. (b) K. D. Hesp, M. Stradiotto, *J. Am. Chem. Soc.* **2010**, *132*, 18026. (c) J. T. Binder, B. Crone, T. T. Haug, H. Menz, S. F. Kirsch, *Org. Lett.* **2008**, *10*, 1025. (d) H. Wu, Y.-P. He, L.-Z. Gong, *Adv. Synth. Catal.* **2012**, *354*, 975. (e) A. Zhdanko, M. E. Maier, *Angew. Chemie Int. Ed.* **2014**, *53*, 7760. (f) J. Xie, S. Shi, T. Zhang, N. Mehrkens, M. Rudolph, A. S. K. Hashmi, *Angew. Chemie - Int. Ed.* **2015**, *54*, 6046.

[122] J. Li, M. Rudolph, F. Rominger, J. Xie, A. S. K. Hashmi, *Adv. Synth. Catal.* **2016**, *358*, 207.

catalyzed by cationic Au(I) are generally prohibited in the presence of basic aliphatic amine bases due to the formation of inactive Lewis adducts (LAu-NR$_3$).[123]

However, less-basic anilines can be tolerated and since are not completely detrimental to gold(I), albeit they affect its catalytic efficiency, as demonstrated by Lee and coworkers. These authors isolated and characterized gold(I)-aniline complexes of type [LAu-aniline][SbF$_6$], and investigated these species as catalysts for the addition of amines to cyclopropenes. Interestingly, significant lower conversions were obtained with these complexes, compared to those achieved with commercially available gold(I)-catalysts (Scheme 69).[124]
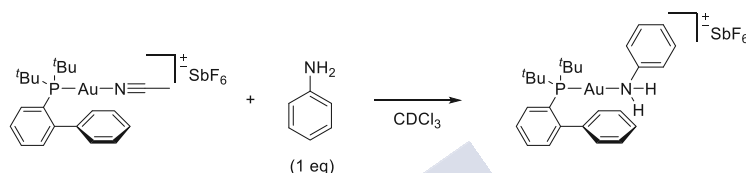
Scheme 69. Isolation of [JohnPhosAu-NH$_2$Ph][SbF$_6$].

Also, interestingly, Corma and coworkers reported in 2014 the deactivation of cationic gold(I) catalysts in the presence of pyrrolidine using CH$_2$Cl$_2$ as solvent. They demonstrated that condensation of CH$_2$Cl$_2$ and pyrrolidine leads to the release of hydrogen chloride, that can react with the cationic gold(I) catalyst generating cationic [(LAu)$_2$(μ-Cl)][SbF$_6$] as an intermediate complex, which evolves to gold chloride complexes of low catalytic activity. Furthermore, in the absence of the alkyne, they isolated a [LAu(pyrrolidine)][SbF$_6$] complex, before its transformation into the final gold chloride complex LAuCl (Scheme 70). [42]
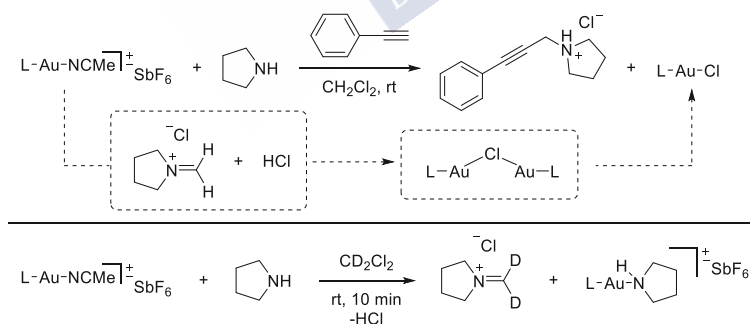
Scheme 70. Deactivation of cationic Au(I) catalysts in the presence of pyrrolidine.

---

[123] C. C. J. Loh, D. Enders, *Chem. - A Eur. J.* **2012**, *18*, 10212.

[124] (a) P. C. Young, S. L. J. Green, G. M. Rosair, A.-L. Lee, *Dalt. Trans.* **2013**, *42*, 9645. For gold(I)-enamine complexes, see: (b) M. Sriram, Y. Zhu, A. M. Camp, C. S. Day, A. C. Jones, *Organometallics* **2014**, *33*, 4157.

[42] (a) M. Kumar, G. B. Hammond, B. Xu, *Org. Lett.* **2014**, *16*, 3452. (b) A. Grirrane, E. Álvarez, H. García, A. Corma, *Angew. Chemie - Int. Ed.* **2014**, *53*, 7253.

Overcoming these deactivation processes in sequential or even relay processes, can be accomplished by the addition of Brønsted acid additives that protonate the tertiary amine facilitating the catalytic activity of the π-acidic Au(I) species. Thus, in 2009, Alexakis and coworkers developed a sequential organocatalytic Michael addition to nitroenynes which is followed by a subsequent gold(I)-catalyzed tandem acetalization/cyclization. In this work they observed a tremendous effect of the *p*-toluenesulfonic acid (*p*-TsOH), preventing deactivation of the gold catalyst by coordination of gold(I) to the nitrogen atom of the organocatalyst. When the loading of organocatalyst exceeded that of the *p*-TsOH, no reaction occurred. However, when equimolar amounts of additive and organocatalyst were used, they obtained the desired product (Scheme 71).[125]
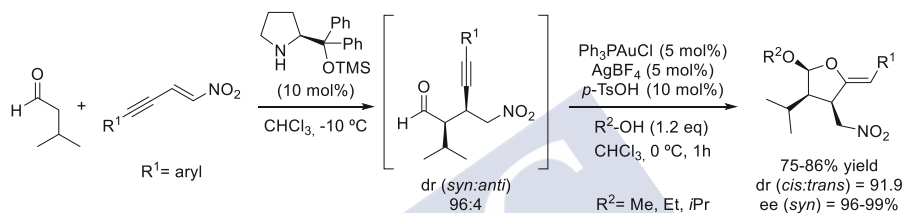
Scheme 71. Sequential organocatalytic/gold(I) catalyzed synthesis of tetrahydrofuranyl ethers.

In 2014, Enders reported an asymmetric synthesis of annulated pyrroles based on a sequential organocatalytic Friedel-Crafts Michael-type reaction and gold(I)-catalyzed 7-*endo*-dig cyclization, providing the products in high yields and enant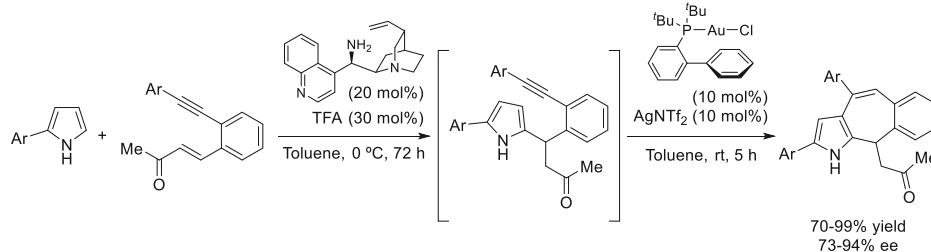ioselectivities. The authors described that in the absence of TFA the reaction does not proceed, demonstrating the need of an acidic additive to regenerate the active gold(I)-species (Scheme 72).[126]

Scheme 72. Sequential organocatalytic/gold(I) catalyzed synthesis of annulated pyrroles.

The first cooperative combination of amine and gold(I) catalysis was reported by Kirsch and coworkers in 2008 and consisted of an intramolecular 5-*exo*-dig cyclization of formyl

---

[125] S. Belot, K. A. Vogt, C. Besnard, N. Krause, A. Alexakis, *Angew. Chemie - Int. Ed.* **2009**, *48*, 8923. For a related work in which the addition of *p*-TsOH prevents coordination of the organocatalyst to the gold cation, see: T. Zweifel, D. Hollmann, B. Prüger, M. Nielsen, K. A. Jørgensen, *Tetrahedron Asymmetry* **2010**, *21*, 1624.

[126] D. Hack, C. C. J. Loh, J. M. Hartmann, G. Raabe, D. Enders, *Chem. - A Eur. J.* **2014**, *20*, 3917.

alkynes. The cooperative combination of a gold(I) catalyst and an achiral amine gave the products in good to excellent yields via intermediate **XVIII**. The main limitation of this protocol for the development of an enantioselective variant lies in the fact that if R is H, the gold(I)-catalyzed cyclization product isomerizes to the thermodynamically more stable achiral tetrasubstituted terminal alkyne **14**. This isomerization removes the new stereogenic center created during C-C bond formation step. However, when R is a methyl group, the formation of products bearing a quaternary stereocenter **15** takes place (Scheme 73).[121c]
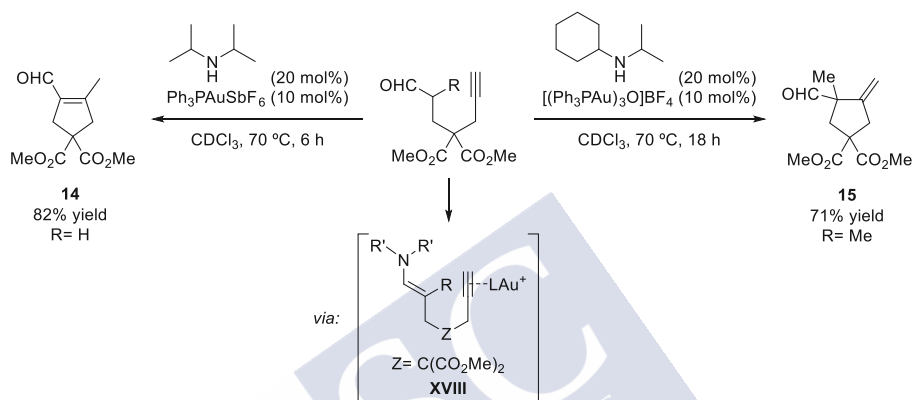
Scheme 73. First example of combining gold and amine catalysis for the direct carbocyclization of formyl alkynes reported by Kirsch.

In 2010, Jørgensen and coworkers reported an enantioselective inter-/intramolecular carbocyclization based on this concept developed by Kirsch.[121c] They envisioned a process where the sterically bulky TMS-protected diarylprolinol ether **C4** would induce the intermolecular attack of an alkyne-tethered malonate on an α,β-unsaturated aldehyde via iminium activation. Thus, the first Michael addition creates a Kirsch-type enamine intermediate **XVIII′** that undergoes intramolecular gold-promoted 5-*exo*-cyclization and a subsequent double bond isomerization to afford enantioenriched cyclopentane derivatives in good to excellent yields (Scheme 74).[127]

[121c] J. T. Binder, B. Crone, T. T. Haug, H. Menz, S. F. Kirsch, *Org. Lett.* **2008**, *10*, 1025.

[127] (a) K. L. Jensen, P. T. Franke, C. Arróniz, S. Kobbelgaard, K. A. Jørgensen, *Chem. - A Eur. J.* **2010**, *16*, 1750. Moreover, the same group also reported the same approach with cyclic α,β-unsaturated ketones: (b) T. Zweifel, D. Hollmann, B. Prüger, M. Nielsen, K. A. Jørgensen, *Tetrahedron Asymmetry* **2010**, *21*, 1624.
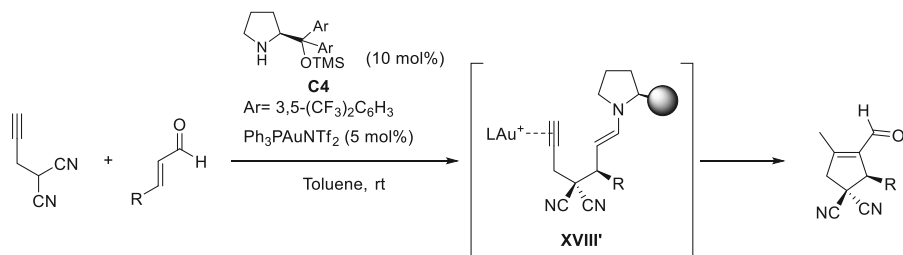
Scheme 74. Enantioselective iminium/enamine/gold(I) cascade reported by Jørgensen.

The group of Bandini reported in 2012 an intramolecular enantioselective α-allylic alkylation of aldehydes with allylic alcohols. The cooperative action of a gold(I) catalyst and MacMillan's organocatalyst provides the best selectivities. Condensation between chiral MacMillan's organocatalyst and the aldehyde provided an enamine intermediate that attacks the gold(I) activated allyl alcohol to afford the corresponding products in high yields and excellent enantioselectivities (Scheme 75).[128]
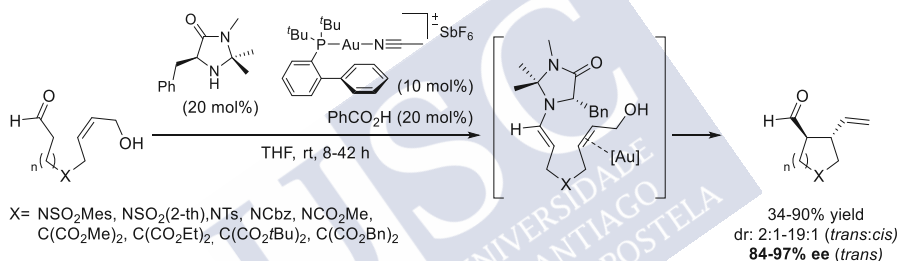
Scheme 75. Cooperative gold and enamine catalysis for the α-allylic alkylation of aldehydes.

Undoubtedly, the intramolecular character of these two reactions, as well as the steric hindrance of the chiral amine catalyst help to overcome the deactivation of gold catalysts.

Indeed, intermolecular variants of the above, or related, transformations are extremely scarce. Indeed, the first intermolecular example involving both gold and amine catalysts working synergistically was developed while our work was already ongoing. In particular, Huang and coworkers reported by the end of 2013, the direct α-vinylidenation of linear aldehydes using a silyl-EBX reagent, pyrrolidine as secondary amine catalyst and AuCl as gold catalyst, affording the corresponding allenyl aldehydes in high yields (Scheme 76).[129] The authors found that the use of a chelating nitrogen ligand, such as 4,5-diazafluorenone or 2,2′-bipyridine, improved significantly the performance of the reaction, although no mechanistic studies were carried out to elucidate the role of the additive. Importantly, despite the presence of chirality in the product, the method was exclusively developed in a racemic fashion.

---

[128] M. Chiarucci, M. di Lillo, A. Romaniello, P. G. Cozzi, G. Cera, M. Bandini, *Chem. Sci.* **2012**, *3*, 2859.

[129] Z. Wang, X. Li, Y. Huang, *Angew. Chemie - Int. Ed.* **2013**, *52*, 14219.
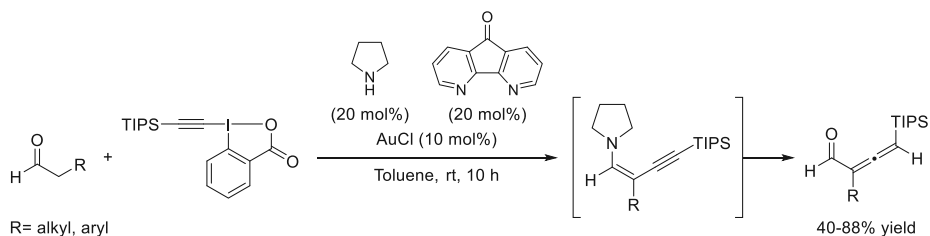
Scheme 76. Direct α-vinylidenation of aldehydes mediated by synergistic gold and amine catalysis.

In 2014, the same group extended the same methodology to the synthesis of ynones directly from aldehydes. The reaction proceeds through the aforementioned α-vinylidenation reaction by gold/pyrrolidine synergistic catalysis, followed by *in situ* aerobic cleavage of the C-C bond.[130]

Overall, the development of gold/amine **synergistic processes** is still scarcely developed but can be very powerful. However, it conveys several important challenges. Besides solving any deactivation issue, the reactions require a perfect synchronization between both catalytic cycles. This is particularly critical for those cases in which alternative racemic pathways might compete, or when the formation of competitive side-products derived from the separate action of one of the catalysts might occur.

Within the context of enantioselective addition and cycloaddition processes, and more particular of enantioselective gold(I) catalysis, including synergistic enamine-gold catalysis, this PhD thesis has been structured in the following chapters:

Chapter I: Synergistic gold(I) and enamine catalysis for the α-addition of aldehydes to allenamides

Chapter II: Asymmetric formal (2+2+2) cycloaddition between allenamides and alkenyl-oximes. Straightforward access to azabridged medium-sized carbocycles.

---

130 Z. Wang, L. Li, Y. Huang, *J. Am. Chem. Soc.* **2014**, *136*, 12233.
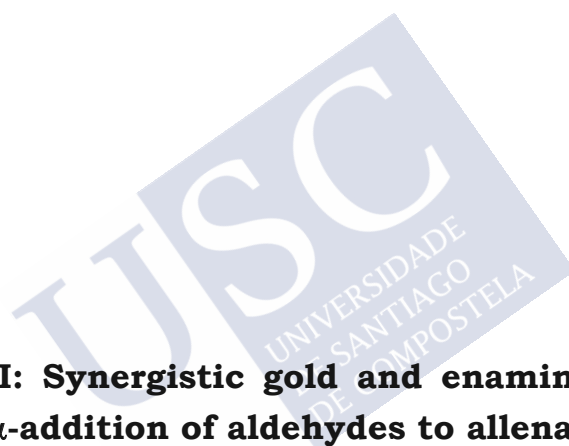
Chapter I: Synergistic gold and enamine catalysis for the α-addition of aldehydes to allenamides

1. Introduction

1.1. Relevance of building all-carbon quaternary stereocenters.

Life is three-dimensional and chirality plays a fundamental role. Therefore, the properties of organic molecules are closely related to their spatial configuration, which is dictated by the orientation of substituents at carbon stereocenters. Quaternary carbon stereocenters are found frequently in natural products, semisynthetic and synthetic pharmaceutical and agrochemical ingredients (Scheme 77).

cortisone
R. B. Woodward (1951)

morphine
M. Gates (1952)

Serotonin antagonist LY 426965
I. Marek (2007)

Scheme 77. Examples of molecules with biological activity containing quaternary stereocenters.

One of the major challenges in constructing quaternary stereocenters is to control the stereoselectivity of the four substituents. The emergence of enantioselective catalytic procedures brings new opportunities in this area by expanding the range of C-C bond-forming processes that can be created. Anyway, the asymmetric construction of acyclic quaternary carbon stereocenters represents a major challenge in current synthetic chemistry.[131]
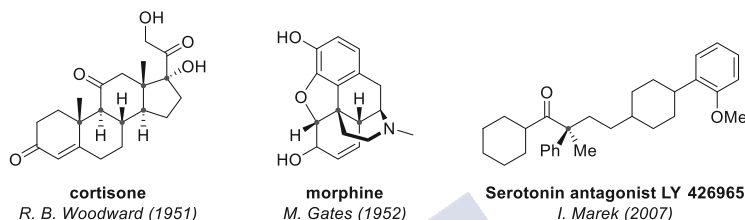
Enantioselective allylic substitution is one of the earliest methods that was proven effective for the construction of acyclic quaternary carbon stereocenters. In 2001, Hoveyda reported the enantioselective copper-catalyzed alkylation of γ,γ-disubstituted allylic phosphates with diethylzinc. Using a synthetic peptide-based ligand, they obtained good enantioselectivities (up to 78% ee).[132a] These results were further improved in 2005 when the same group reported a more effective copper-NHC system (up to 97% ee, Scheme 78).[132b]

---

[131] (a) K. W. Quasdorf, L. E. Overman, *Nature* **2014**, *516*, 181. (b) I. Marek, Y. Minko, M. Pasco, T. Mejuch, N. Gilboa, H. Chechik, J. P. Das, *J. Am. Chem. Soc.* **2014**, *136*, 2682. (c) E. V. Prusov, *Angew. Chemie - Int. Ed.* **2017**, *56*, 14356. (d) J. Feng, M. Holmes, M. J. Krische, *Chem. Rev.* **2017**, *117*, 12564.

[132] (a) C. A. Luchaco-Cullis, H. Mizutani, K. E. Murphy, A. H. Hoveyda, *Angew. Chem. Int. Ed. Engl.* **2001**, *40*, 1456. (b) J. J. Van Veldhuizen, J. E. Campbell, R. E. Giudici, A. H. Hoveyda, *J. Am. Chem. Soc.* **2005**, *127*, 6877.
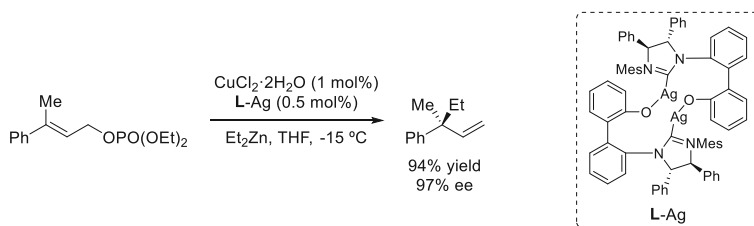
Scheme 78. Enantioselective copper-catalyzed alkylation of γ,γ-disubstituted allylic phosphates.

Nowadays, several other transition metal-catalyzed enantioselective organic transformations have been shown capable to provide products with carbon quaternary stereocenters with high enantioselectivities. These include conjugate additions, cycloadditions, allylic alkylations or cycloisomerizations, among others. Nevertheless, the overall scope of the methods is still limited in terms of scope and/or enantioselectivity, therefore the development of new complementary strategies for the construction of quaternary all-carbon stereocenters from simple and easily accessible starting materials is still urgent.

1.2. Generation of quaternary carbons by addition reactions to allene derivatives.

As already commented, allenes are very appealing and versatile functional groups for organic transformations, in particular as π-acceptor reactants.[69, 133] However, their participation in catalytic methods leading to quaternary stereocenters has been scarcely explored. B. Trost reported in 2011 a palladium-catalyzed asymmetric hydrocarbonation of allenes under mild conditions that provided products bearing quaternary carbon centers with high enantioselectivity. They applied this methodology to the construction of the pyrrolidinoindoline core of the gliocladin natural products (Scheme 79).[134]
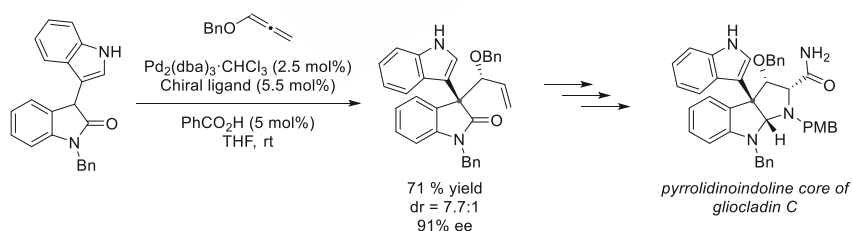
Scheme 79. Asymmetric addition of oxindoles to allenes for the construction of chiral indole alkaloids reported by Trost and coworkers.

---

[69] T. Lu, Z. Lu, Z. X. Ma, Y. Zhang, R. P. Hsung, *Chem. Rev.* **2013**, *113*, 4862.

[133] (a) N. Krause, A. S. K. Hashmi, *Modern Allene Chemistry*, Wiley-VCH, **2004**. See also: (b) L.-L. Wei, H. Xiong, R. P. Hsung, *Acc. Chem. Res.* **2003**, *36*, 773.

[134] B. M. Trost, J. Xie, J. D. Sieber, *J. Am. Chem. Soc.* **2011**, *133*, 20611.

With regard to the use of gold catalysis, Nelson and coworkers developed a gold(I)-catalyzed intramolecular cyclization of allene-pyrroles, demonstrating that the chirality of the allene can be transferred to the new generated quaternary stereocenter (Scheme 80). Although the reaction is stereospecific, the methodology lacks generality and scope.[135]
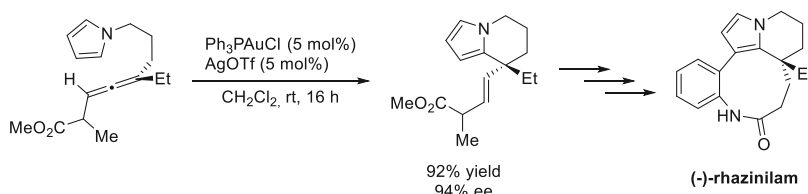
Scheme 80. Gold(I)-catalyzed annulation of allenes in the enantioselective total synthesis of (-)-rhazinilam.

Using allenamides instead of allenes, Kimber disclosed in 2010 an intermolecular gold-catalyzed hydroarylation. They found that $Ph_3PAuNTf_2$ is an excellent catalyst for the addition of electron-rich aromatics and heteroaromatics to allenamides in a regioselective manner and under mild conditions (Scheme 81).[136] The proposed mechanism involves the carbophilic activation of the allene that undergoes the addition of the nucleophile, followed by a subsequent protodeauration to yield the *E*-enamide product. However, this methodology does not generate a stereocenter (not even tertiary). Indeed, enantioselective intermolecular hydrofunctionalization reactions of these systems have been less developed and their use in synthetic methods that provide all-carbon quaternary stereocenters is extremely scarce.

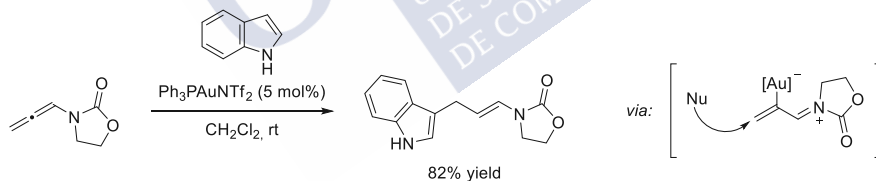**Scheme 81**. Gold-catalyzed intermolecular hydroarylation of allenamides reported by Kimber.

In this context, Chen reported in 2015 the enantioselective gold-catalyzed cascade construction of pyrroloindoline derivatives. The process starts through a nucleophilic attack of the double bond of the tryptamine to the cationic gold-allene complex, resulting in *C*3-dearomatization, which, followed by C2-cyclization, affording the desired annulation products that bear a carbon quaternary stereocenter (Scheme 82).[137]

---

[135] Z. Liu, A. S. Wasmuth, S. G. Nelson, *J. Am. Chem. Soc.* **2006**, *128*, 10352.

[136] M. C. Kimber, *Org. Lett.* **2010**, *12*, 1128.

[137] Z.-Q. Shen, X. Li, J.-W. Shi, B.-L. Chen, Z. Chen, *Tetrahedron Lett.* **2015**, *56*, 4080.
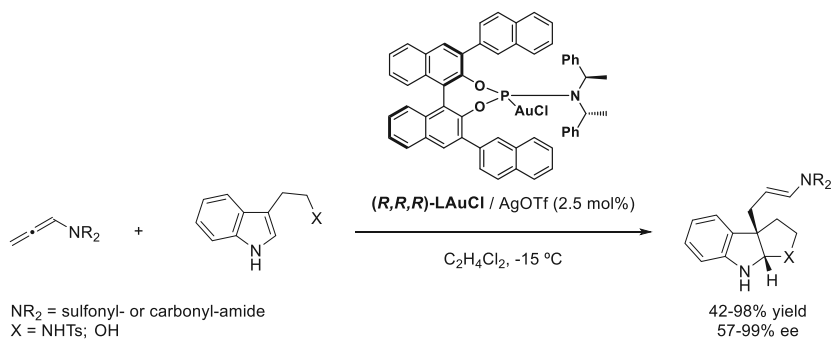
Scheme 82. Enantioselective gold catalyzed cascade construction of pyrroloindoline derivatives.

2. Objectives

Considering the challenges associated to the building of all-carbon quaternary stereocenters, especially in an enantioselective fashion, and the scarce precedents on synergistic amine/gold catalysis, particularly in intermolecular processes, the first goal of our research consisted of developing an efficient methodology for the stereoselective and enantioselective formation of carbon-carbon bonds, including quaternary stereocenters, from readily available precursors, by developing synergistic gold(I)/amine dual catalytic methods.

In particular, considering that the activation of *N*-allenamides with gold catalysts involve the formation of a gold-zwitterionic electrophilic intermediate **XI**, we envisioned that this gold(I)-intermediate could be trapped by an *in situ* generated enamine **XIX**, thus leading to α-alkyl substituted aldehydes. If α-branched aldehydes are involved in the condensation with a chiral amine organocatalyst, we could obtain γ,δ-unsaturated aldehydes bearing an all-carbon quaternary stereocenter.
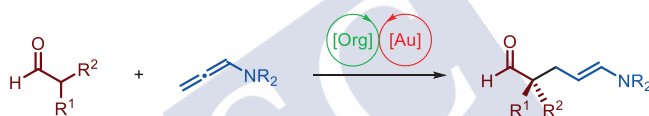
Scheme 83. General objective.
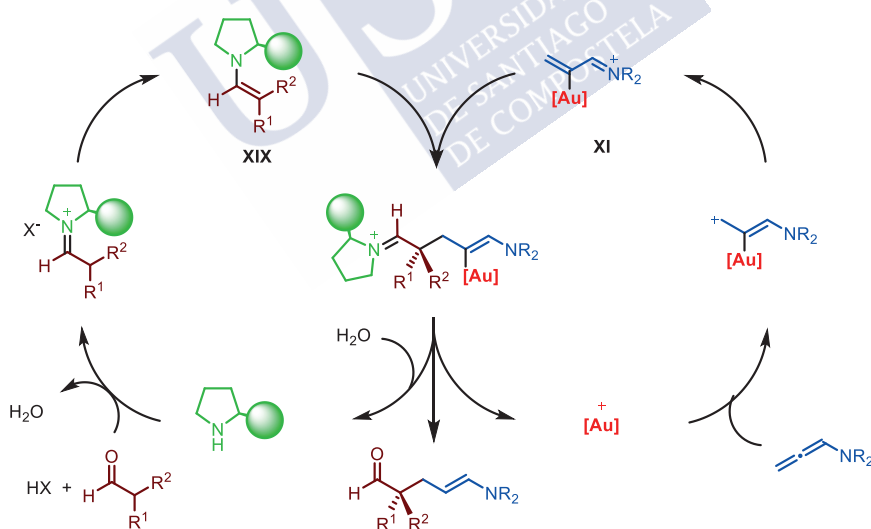
Scheme 84. Proposed synergistic combination of both catalytic cycles.

As previously mentioned, the development of such intermolecular synergistic process is almost unprecedented and entails several challenges:

- The requirement of an exquisite synchronization between both catalytic cycles.

- Solving the potential incompatibility between the gold complex and the amine or enamine.[42b, 124]

$$L-Au-X \quad + \quad \text{(pyrrolidine)} \quad \longrightarrow \quad L-Au-N\text{(pyrrolidine)}^{+} X^{-}$$
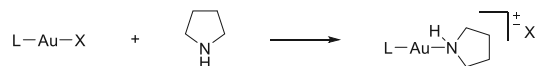
- Avoid the formation of side-products, such as self-aldol condensation products from the aldehydes, (2+2) cycloadducts resulting from a gold(I)-promoted homodimerization of the allenamide (see Scheme 39, page 39)[75b] or allenamide self-polymerization products.[138]

| Self-aldol condensation | (2+2) homodimerization | self-polymerization |
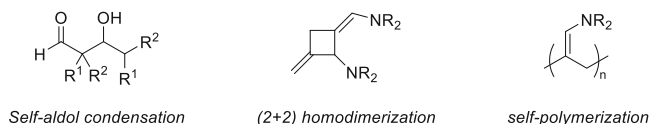
[42b] A. Grirrane, E. Álvarez, H. García, A. Corma, *Angew. Chemie - Int. Ed.* **2014**, *53*, 7253.

[124] (a) P. C. Young, S. L. J. Green, G. M. Rosair, A.-L. Lee, *Dalt. Trans.* **2013**, *42*, 9645. For gold(I)-enamine complexes, see: (b) M. Sriram, Y. Zhu, A. M. Camp, C. S. Day, A. C. Jones, *Organometallics* **2014**, *33*, 4157.

[75b] X. Li, L. Zhu, W. Zhou, Z. Chen, *Org. Lett.* **2012**, *14*, 436.

[138] K. Takagi, I. Tomita, T. Endo, *Macromolecules* **1998**, *31*, 6741.

3. Results and discussion

3.1. Discovery and optimization of reaction conditions

To study the viability of the reaction, we synthesized the model allenamide **17a**, by first making the *N*-propargyl-oxazolidinone **16a**, which can be isomerized to **17a** using *t*BuOK in anhydrous THF at ambient temperature.
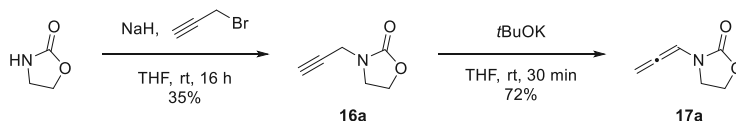
Scheme 85. Synthesis of model substrate **17a**.

With the model substrate in hand, we checked the viability of the synergistic process using a racemic protocol. Thus, allenamide **17a** was treated with 2-phenylpropanal **18a** in the presence of a gold(I) complex and a secondary amine that should work as an organocatalyst. As shown in table 1, the use of [L1AuNCPh]SbF$_6$ together with pyrrolidine (100 mol%) afforded traces of the desired product, while the conversion was very low even after several hours at rt (Table 1, entry 1). Running the reaction with 30% of pyrrolidine, in the presence of benzoic acid (BzOH, 20 mol%) as co-catalyst, brought only a marginal benefit (entry 2). However, an increase in the reaction temperature up to 60 °C led to a better 30% yield (entry 3). More excitingly, carrying the reaction in refluxing toluene led to a 90% yield after 15 minutes (entry 4).

Based on the precedent reported by Huang,[129a] in which the addition of chelating nitrogen ligands resulted in better yields, we added 2,2'-bipyridine (bpy, 20 mol%); however, we observed a drop in the yield (entry 5). A control experiment with Et$_3$N (30 mol%) instead of pyrrolidine, failed to give the desired product, and led to recovery of 60% of allenamide **17a**, thus confirming that the reaction is likely involving the formation of an enamine, rather than being promoted by a base (entry 6). Changing the counterion of the gold complex to bis(trifluoromethanesulfonyl)imidate (NTf$_2$) we observed an increase in reaction times and a significant decrease in the yield (25%, entry 4 *vs* 7). However, with L1AuNTf$_2$ as gold(I) catalyst, the combined use of bpy and BzOH led to a slightly increase in the yield from 25% up to 42% at 110 °C (entry 7 *vs* 8). Decreasing the temperature to 60 °C led to a very good 88% yield (entry 9 *vs* 8). The use of other counterion, such as hexafluoro antimonate (SbF$_6$), was prejudicial leading to a significant drop to 25% yield, and with only 50% conversion of allenamide **17a** after 3 hours (entry 10). Therefore, the addition of 2,2'-bipyridine allowed us to decrease the temperature to 60 °C, obtaining very good yields of the desired product using a gold(I) complex with NTf$_2$ as counterion.

[129a] Z. Wang, X. Li, Y. Huang, *Angew. Chemie - Int. Ed.* **2013**, *52*, 14219.

Table 1. Optimization of the reaction conditions for α-branched aldehydes.

Entry	[Au] (mol %)	Additive (mol %)	T (°C)	t (h)[b]	19aa[c] (%)
1[d]	[L1AuNCPh]SbF$_6$ (5)	BzOH (20)	rt	4	3[e]
2	[L1AuNCPh]SbF$_6$ (5)	BzOH (20)	rt	4	7[f]
3	[L1AuNCPh]SbF$_6$ (5)	BzOH (20)	60	1.2	30
4	[L1AuNCPh]SbF$_6$ (5)	BzOH (20)	110	0.2	90
5	[L1AuNCPh]SbF$_6$ (5)	bpy (20)/BzOH (20)	110	0.2	61
6[g]	[L1AuNCPh]SbF$_6$ (5)	bpy (20)	110	1.5	–[h]
7	L1AuNTf$_2$ (5)	BzOH (20)	110	3	25
8	L1AuNTf$_2$ (5)	bpy (20)/BzOH (20)	110	0.7	42
9	L1AuNTf$_2$ (10)	bpy (20)/BzOH (20)	60	3.5	88
10	L1AuCl/AgSbF$_6$ (10)	bpy (20)/BzOH (20)	60	3	25[e]

[a] *Reaction conditions*: **17a** (0.16 mmol), **18a** (2 equiv), [Au] (5-10 mol%), pyrrolidine (30 mol%), toluene [0.1 M]. [b] Full conversion of **17a** was observed at the specified time, unless otherwise noted [c] Yields determined by ^{1}H-NMR using 1,3,5-trimethoxybenzene as internal standard unless otherwise noted. [d] Carried out with pyrr (100 mol%). [e] 50% conversion. [f] 55% conversion. [g] Carried out with Et$_3$N (30 mol%) instead of pyrr. [h] 40% conversion.

We next explored the viability of using a more usual gold(I) complexes, such as Ph$_3$PAuNTf$_2$ instead of L1AuNTf$_2$. Gratifyingly, this gold(I) complex afforded the desired product in high yields, and with a significantly decrease in reaction time (from 3.5 hours to 30 minutes), although the use of 10 mol% of catalyst was required (Table 2, entry 3 *vs* entries 1 and 2). The presence of bpy as additive turned out to be important, since in its absence the yield dropped to 30% (entry 4). Likewise, the use of BzOH is also important (entry 5).

To prove the relevance of NTf$_2$ as counterion, the reaction was carried out with Ph$_3$PAuSbF$_6$, prepared *in situ* from Ph$_3$PAuCl by chloride "abstraction" with the corresponding silver salt AgSbF$_6$. Under otherwise identical reaction conditions, this gold(I) complex afforded the product in a low 23% yield (entry 6). On the other hand, the triazole-coordinated gold(I) complex Ph$_3$PAu(TA)OTf, described by Shi as an effective catalyst for some transformations,[40] was also tested, and we observed the desired product in a moderate 63% yield after 6 hours (entry 7).

A decrease in the organocatalyst loading to 20 mol% or an increase up to 40 mol% had not a remarkable effect on the efficiency of the reaction (entries 8 and 9). The use of other

---

[40] H. Duan, S. Sengupta, J. L. Petersen, N. G. Akhmedov, X. Shi, *J. Am. Chem. Soc.* **2009**, *131*, 12100.

additives such as 4,5-diazafluoren-9-one (fluorenone, 20 mol%) or acetonitrile (MeCN, 20 mol%), instead of bpy, did neither improve the reaction (entries 10 and 11). When the reaction catalyzed by Ph$_3$PAuNTf$_2$, bpy and BzOH was carried out at 110 ^{o}C instead of 60 ^{o}C, a faster conversion of the allenamide **17a** was observed, but the yield of the product dropped to 42% yield (entry 12). The same behavior was observed if the reaction is carried out in the absence of bpy at 110 ^{o}C, affording the product in 39% yield after 15 minutes (entry 13). As expected, a control experiment without gold(I) catalyst did not provide the product after 46 hours (entry 14). Another control experiment with HNTf$_2$ instead of the gold(I) catalyst, did not afford the desired aldehyde either (entry 15).

Table 2. Further optimization of reaction conditions.
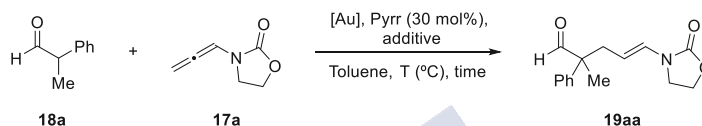
Entry	[Au] (mol %)	Additive (mol %)	T (^{o}C)	t (h)[b]	19aa[c] (%)
1	L1AuNTf$_2$ (5)	bpy (20)/BzOH (20)	60	3.5	88[d]
2	Ph$_3$PAuNTf$_2$ (5)	bpy (20)/BzOH (20)	60	1.5	43
3	Ph$_3$PAuNTf$_2$ (10)	bpy (20)/BzOH (20)	60	0.3	83
4	Ph$_3$PAuNTf$_2$ (10)	BzOH (20)	60	0.5	30
5	Ph$_3$PAuNTf$_2$ (10)	bpy (20)	60	0.5	25
6	Ph$_3$PAuCl/AgSbF$_6$ (10)	bpy (20)/BzOH (20)	60	18	23
7	Ph$_3$PAu(TA)OTf	bpy (20)/BzOH (20)	60	6	63
8[e]	Ph$_3$PAuNTf$_2$ (10)	bpy (20)/BzOH (20)	60	0.7	63
9[f]	Ph$_3$PAuNTf$_2$ (10)	bpy (20)/BzOH (20)	60	0.5	51[d]
10	Ph$_3$PAuNTf$_2$ (10)	fluorenone (20)/BzOH (20)	60	0.5	47
11	Ph$_3$PAuNTf$_2$ (10)	MeCN (20)/BzOH (20)	60	1.5	37[d,g]
12	Ph$_3$PAuNTf$_2$ (10)	bpy (20)/BzOH (20)	110	0.2	42[d]
13	Ph$_3$PAuNTf$_2$ (10)	BzOH (20)	110	0.2	39[d]
14	none	bpy (20)/BzOH (20)	60	46	0
15	HNTf$_2$ (20)	bpy (20)/BzOH (20)	60	17	0

[a] *Reaction conditions*: **17a** (0.16 mmol), **18a** (2 equiv), [Au] (5-10 mol%), amine (30 mol%), toluene [0.1 M], T (^{o}C). [b] Full conversion of **17a** was observed at the specified time, unless otherwise noted [c] Isolated yields, unless otherwise noted. [d] Yields determined by ^{1}H-NMR using 1,3,5-trimethoxybenzene as internal standard. [e] Carried out with pyrr (20 mol%). [f] Carried out with pyrr (40 mol%). [g] 75% conversion.
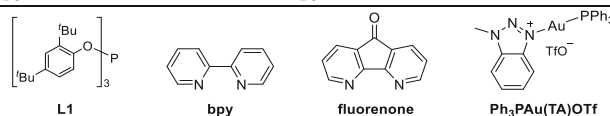
Therefore, three different conditions that enable the catalytic addition of aldehyde **18a** to allenamide **17a** were identified. The use of [L1AuNCPh]SbF$_6$ as gold catalyst requires heating at 110 ^{o}C but avoids the use of bpy as additive, whereas the use of L1AuNTf$_2$ and Ph$_3$PAuNTf$_2$ allows the reaction to occur at 60 ^{o}C, provided bpy (20 mol%) is used as

additive. In all cases, the use of BzOH to promote the formation of the enamine is required.

We next explored the performance of other solvents using $Ph_3PAuNTf_2$ as optimal catalyst at 60 °C. Although CH_2Cl_2 is a common solvent employed in gold(I)-catalyzed processes, we avoided its use due to the possible deactivation of the gold catalyst reported by Corma and coworkers (Scheme 70, page 59).[42b] As depicted in Table 3, the use of coordinating solvents such as tetrahydrofuran, dioxane or acetonitrile produced a significant drop in the yield, thus a non-coordinating solvent such as toluene is suitable for the reaction to proceed in high yields (entry 1 *vs* entries 2 to 4).

Table 3. Influence of different solvents in reaction conditions.

Entry	Solvent	t (h)[b]	19aa[c] (%)
1	Toluene	0.5	83
2	THF	0.5	10[d]
3	Dioxane	0.5	15[d]
4	Acetonitrile	0.3	39

[a] *Reaction conditions*: **17a** (0.16 mmol), **18a** (2 equiv), $Ph_3PAuNTf_2$ (10 mol%), pyrrolidine (30 mol%), bpy (20 mol%), BzOH (20 mol%), solvent [0.1 M], 60 °C. [b] Full conversion of **17a** was observed at the specified time, unless otherwise noted [c] Isolated yields, unless otherwise noted. [d] Yields determined by ^1H-NMR using 1,3,5-trimethoxybenzene as internal standard.

Different acids commonly used in organocatalysis were also tested, observing that neither diphenyl phosphoric acid (DPP), acetic acid, *para*-toluenesulfonic acid (*p*TsOH), or mandelic acid are able to improve the yield obtained with the BzOH (Table 4, entry 1 *vs* entries 2-5).

[42b] A. Grirrane, E. Álvarez, H. García, A. Corma, *Angew. Chemie - Int. Ed.* **2014**, *53*, 7253.

**Table 4**. Influence of different acids in reaction conditions.
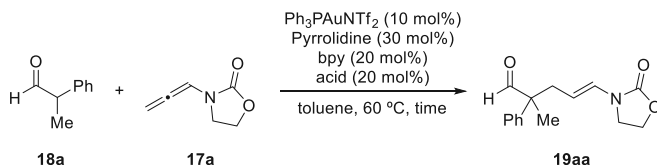
| Entry	Acid (20 mol%)	t (h)[b]	19aa[c] (%)
1	BzOH	0.5	83
2	DPP	0.5	39
3	Acetic acid	0.5	41
4	pTsOH	1	30
5	Mandelic acid	0.3	43

[a] *Reaction conditions*: **17a** (0.16 mmol), **18a** (2 equiv), Ph$_3$PAuNTf$_2$ (10 mol%), pyrrolidine (30 mol%), bpy (20 mol%), acid (20 mol%), toluene [0.1 M], 60 ºC. [b] Full conversion of **17a** was observed at the specified time, unless otherwise noted [c] Isolated yields, unless otherwise noted. [d] Yields determined by ^{1}H-NMR using 1,3,5-trimethoxybenzene as internal standard.
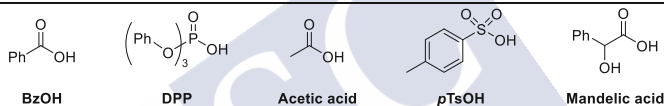

Using the optimal reaction conditions of Table 2, entry 3 (Ph$_3$PAuNTf$_2$ (10 mol%), bpy (20 mol%) anz BzOH (20 mol%) at 60 ºC), we next investigated the influence of the ancillary ligand. As depicted in Table 5, bulky diarylphophine gold(I) catalysts, such as JohnPhosAuNTf$_2$, were completely ineffective (entries 2-6), as well as bulky electron-rich phosphines like (tBu)$_3$PAuNTf$_2$ (entry 7). This is probably due to the fact that the synergistic process is less efficient with these gold(I) catalysts, so that the dimerization and polymerization of the allenamide becomes more competitive. On the other hand, an electron-deficient phosphine such as (pCF$_3$C$_6$H$_4$)$_3$PAuNTf$_2$, afforded comparable yields (entry 8 *vs* entry 1). Likewise, the use of a π-acceptor phosphite ligand like L1 (L1AuNTf$_2$), also provided a very good yield (88%, entry 9), as previously shown in Table 2, entry 1. On the other hand, σ-donor ligands like *N*-heterocyclic carbenes also proved to be suitable ligands, providing moderate to good yield of the product, although with variable reaction times (entries 10 and 11). Thus, with this results in hand, we selected Ph$_3$PAuNTf$_2$ (Table 5, entry 1) as the suitable catalyst for further investigations since it proceeds in shorter reaction times and with very good yields.

Table 5. Influence of the ancillary ligand of gold(I) catalysts.
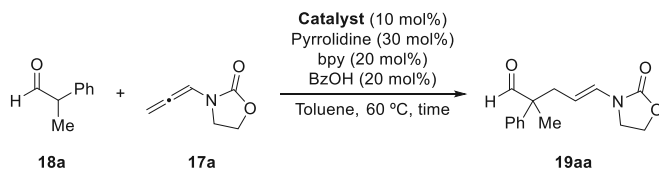
Entry	Catalyst (10 mol%)	t (h)[b]	19ba[c] (%)
1	$Ph_3PAuNTf_2$	0.5	83
2	JohnPhosAuNTf$_2$	0.5	6[d]
3	*t*BuXPhosAuNTf$_2$	0.5	3[d]
4	XPhosAuNTf$_2$	0.5	5[d]
5	RuPhosAuNTf$_2$	1	10[d]
6	SPhosAuNTf$_2$	0.7	12[d]
7	$(tBu)_3PAuNTf_2$	0.5	14[d]
8	$(pCF_3C_6H_4)_3PAuNTf_2$	0.7	73
9	L1AuNTf$_2$	3.5	88[d]
10	IMesAuNTf$_2$	0.5	63
11	IPrAuNTf$_2$	3	68

[a] *Reaction conditions*: **17a** (0.16 mmol), **18a** (2 equiv), [Au] (10 mol%), pyrrolidine (30 mol%), bpy (20 mol%), BzOH (20 mol%), toluene [0.1 M], 60 °C. [b] Full conversion of **17a** was observed at the specified time, unless otherwise noted [c] Isolated yields, unless otherwise noted. [d] Yields determined by ^{1}H-NMR using 1,3,5-trimethoxybenzene as internal standard.
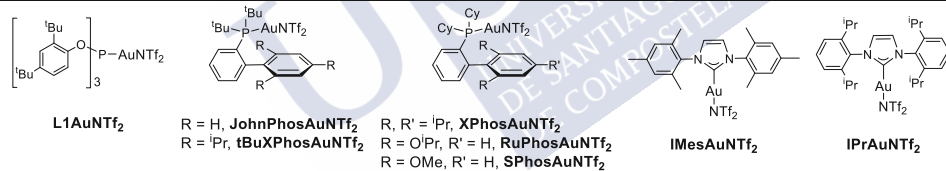
3.2. Scope of the reaction

With these optimal conditions in hand, we proceeded to study the scope of the reaction with different allenamides and α-branched aldehydes. [139] The synthesis of different non-commercially available allenamides was accomplished by initial formation of the *N*-propargyl-amines **16b-e**. The subsequent isomerization of **16b-e** using *t*BuOK in anhydrous THF at ambient temperature provided the corresponding *N*-allenamides **17b-e** (Scheme 86).

---

[139] In collaboration with Dr. Ronald Nelson.
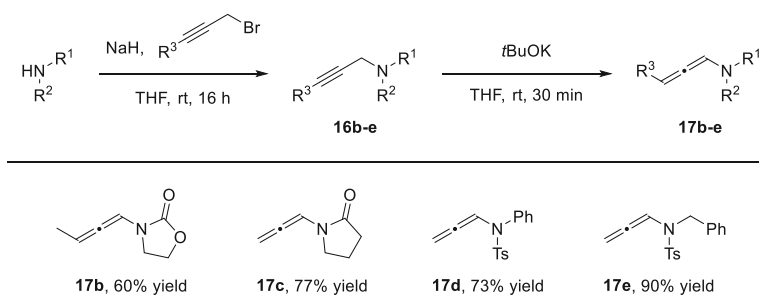
Scheme 86. Synthesis of different *N*-allenamides **17**.

The synthesis of α-branched aldehydes was achieved following a reported procedure,[140] by means of an initial Wittig reaction and a subsequent hydrolysis. This procedure led to the corresponding aldehydes **18**, that can be used in the catalytic reactions without further purification (Scheme 87).
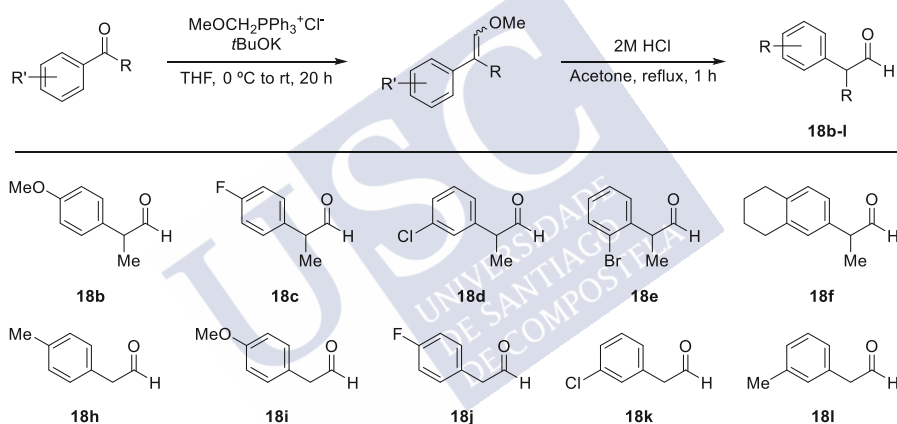

Scheme 87. Synthesis of different α-branched aldehydes **18**.

We then proceeded to study the scope of the reaction with regard to the aldehydes. In some cases, we found problems during the purification of the aldehyde products of type **19**. To avoid this, we carried out an *in situ* reduction of the aldehyde with NaBH$_4$ to afford the corresponding alcohol **20**, that can be easily purified without problems. The presence of an electron-rich substituent in the aryl group of the aldehyde did not affect the yield, so the corresponding aldehyde **19ab** could be isolated in a good 75% yield. On the other hand, electron-withdrawing substituents in the aryl group afforded the products in low yields, such as *p*-F (**20ac**, 40% yield) and *m*-Cl (**20ad**, 43% yield) or not reacted at all, like the *o*-Br (**19ae**). A bulkier substituent in the aryl group of the aldehyde,

---

[140] (a) S. Hoffmann, M. Nicoletti, B. List, *J. Am. Chem. Soc.* **2006**, *128*, 13074. (b) D. S. Ermolat'ev, J. B. Bariwal, H. P. L. Steenackers, S. C. J. De Keersmaecker, E. V. Van der Eycken, *Angew. Chemie Int. Ed.* **2010**, *49*, 9465. (c) P. S. Wang, H. C. Lin, Y. J. Zhai, Z. Y. Han, L. Z. Gong, *Angew. Chemie - Int. Ed.* **2014**, *53*, 12218. (d) P. Swamy, M. M. Reddy, M. Naresh, M. A. Kumar, K. Srujana, C. Durgaiah, N. Narender, *Adv. Synth. Catal.* **2015**, *357*, 1125.

such as 1,2,3,4-tetrahydronaphtalene, affected the efficiency of the reaction, leading to the product in a moderate 47% yield (**19af**).

Regarding the scope with other allenes, we found that a *N*-allenamide bearing a methyl group at its terminal position (**17b**) did not afford the desired product. On the other hand, other *N*-allenamides, such as the pyrrolidone analog (**17c**) or the *N*-tosyl allenamides (**17d** and **17e**), provided the desired products (**19ca**, **20da** and **20ea**) in moderate yields and full *E*-selectivity. However, other allenes with an *O*-heteroatoms, such as the allenol ether **17f**, or with all-carbon atoms, such as the 1,1-diphenylallene **17g**, did not provide the desired aldehyde products, with complete recovery of the allene (Scheme 88).
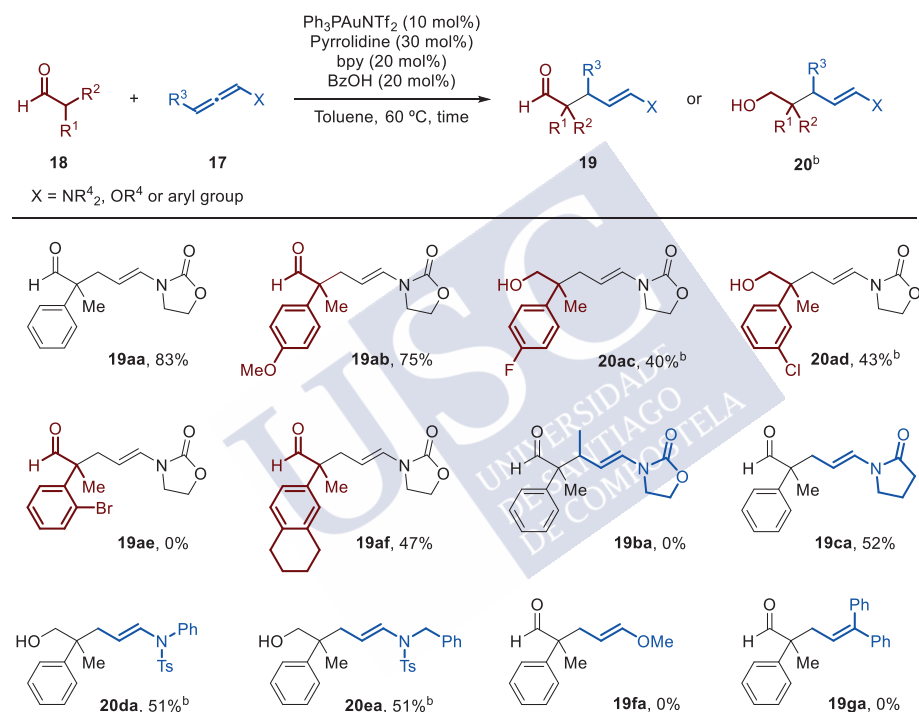
^a *Reaction conditions*: **17** (0.16 mmol), **18** (2 equiv), Ph₃PAuNTf₂ (10 mol%), Pyrrolidine (30 mol%), bpy (20 mol%), BzOH (20 mol%), Toluene [0.1 M], 60 °C. ^b Obtained after quenching with NaBH₄ to facilitate isolation.

Scheme 88. Scope of the reaction with α-branched aldehydes and allenes.

We then proceeded to study the scope of the reaction with α-monosubstituted aldehydes (2-arylpropanals), which would provide the products bearing a tertiary instead of a quaternary stereocenter. Remarkably, the use of 2-phenylacetaldehyde **18g** was tolerated providing the desired product **19ag** in almost quantitative yield in just 15 minutes, but as non-reproducible *E/Z* mixtures, which randomly varied from 1.2:1 up to 3:1 (Table 6, entries 1 and 2). Gratifyingly, quenching the reaction with NaBH₄ allowed us to obtain the corresponding alcohol **20ag** as a single *E* isomer (entry 4), thus confirming that the *E/Z* mixture results from an isomerization of the initially formed *E*-enamide. It is relevant to note that for this

particular aldehyde, the reaction can also be achieved without bpy, although the product **19ag** is obtained in slightly lower yields, 90% yield, and as a 9:1 *E/Z* mixture (entry 3).

Table 6. Reactivity of 2-phenylacetaldehyde and *in situ* reduction to avoid *E/Z* mixtures.

Entry	Additives (mol%)	Reductant (equiv)	t (h)[c]	*E/Z*	19ag / 20ag[d] (%)
1	bpy (20)/BzOH (20)	-	0.2	3:1	99 (**19ag**)
2	bpy (20)/BzOH (20)	-	0.2	1.2:1	98 (**19ag**)
3	BzA (20)	-	0.2	9:1	90[e] (**19ag**)
4	bpy (20)/BzA (20)	NaBH$_4$ (4)	0.2[e]	1:0	99 (**20ag**)

[a] *Reaction conditions*: **17a** (0.16 mmol), **18g** (2 equiv), Ph$_3$PAuNTf$_2$ (10 mol%), pyrrolidine (30 mol%), toluene [0.1 M], 60 ºC. [b] After full conversion of **17a** the reaction was quenched by the addition of a solution of NaBH$_4$ (4 equiv) in MeOH (2 ml) and stirred for 30 minutes, affording **20ag**. [c] Full conversion of **17a** was observed at the specified time, unless otherwise noted [d] Isolated yields, unless otherwise noted. [e] Yields determined by ^{1}H-NMR using 1,3,5-trimethoxybenzene as internal standard.

In order to avoid the formation of products with *E/Z* mixtures, we explored the reaction of α-monosubstituted aldehydes carrying out the *in situ* reduction of the aldehyde products after full conversion of the allenamide **17**. Remarkably, the presence of electron-rich or electron-withdrawing substituents in the aryl moiety of the 2-arylpropanal did not affect the reaction. Thus, the use of aldehydes bearing a methyl (**18h**) or a methoxy group (**18i**) at the *para* position, allowed us to obtain the desired addition/reduction products in quantitative yields (**20ah** and **20ai** respectively). Moreover, substrates with a fluorine at the *para* position (**18j**) or a chlorine in *meta* position (**18k**) of the benzene ring, also afforded the corresponding alcohols in quantitative yields (**20j** and **20ak** respectively). However, aldehyde **18l**, bearing a methyl group in *meta* position, did not provide the product.

Linear aliphatic aldehydes, such as hydrocinnamaldehyde (**18m**) and isovaleraldehyde (**18n**), were also tested, but in toluene we did not observe reaction (traces of self-aldol condensation products were detected by GC-MS analysis). However, in acetonitrile, we obtained the corresponding alcohols (**20am-20an**), albeit in low yields (no self-aldol condensation products were observed). Other allenamides, such as the *N*-tosyl allenamide **17e**, was also tested with 2-arylpropanals. Thus, the use of 2-phenylpropanal afforded the desired alcohol product in quantitative yield (**20eg**). Other 2-arylpropanals bearing electron-rich substituents like a *para*-Me (**18h**) or a *para*-OMe (**18i**) also afforded the alcohols in quantitative yields (**20eh-20ei**). Moreover, substrates with electron-withdrawing substituents like a *para*-F (**18j**) or a *meta*-Cl (**18k**) also afforded the alcohols in quantitative yields (**20ej-20ek**). (Scheme 89).

To sum up, although this methodology seems to be restricted to the use of aldehydes bearing an aryl group at the α-position, the intermolecular addition of *in situ* generated enamines to gold(I) activated allenamides can be achieved with moderate to excellent yields, generating tertiary or quaternary all-carbon stereocenters at the aldehyde α-position.
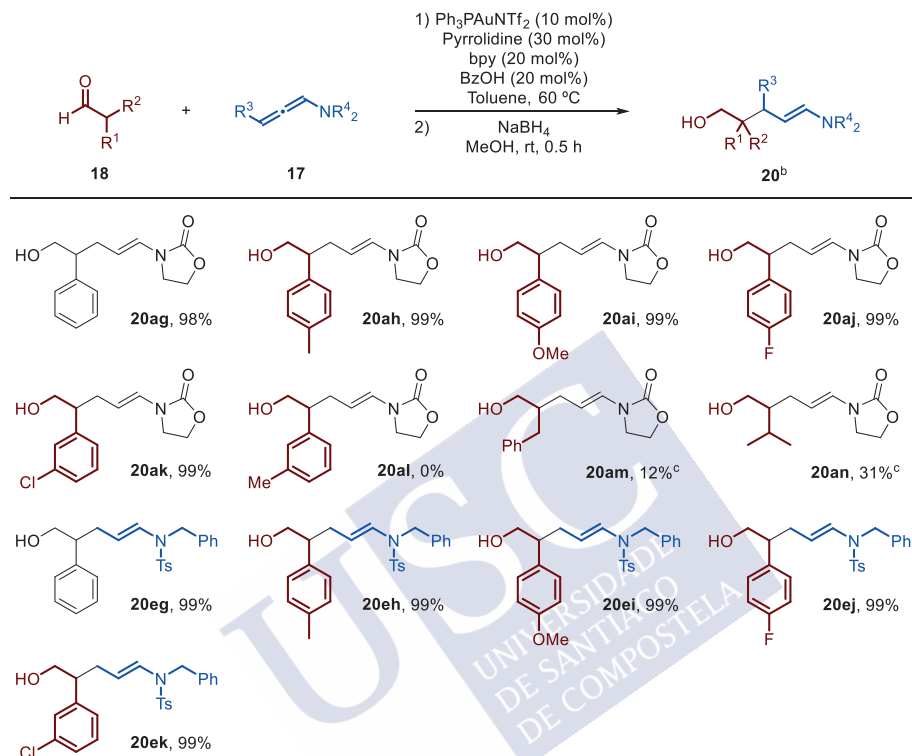
Scheme 89. Scope of the reaction with α-monosubstituted aldehydes and allenamides.

[a] *Reaction conditions*: **17** (0.16 mmol), **18** (2 equiv), Ph₃PAuNTf₂ (10 mol%), pyrrolidine (30 mol%), bpy (20 mol%), BzOH (20 mol%), Toluene [0.1 M], 60 °C. [b] Obtained after quenching with NaBH₄ to avoid the formation of enamide *E/Z* isomers. [c] Reaction carried out in acetonitrile under otherwise identical conditions.

3.3. Development of an enantioselective variant

Having in hand an optimal racemic reaction, we explored the viability of an enantioselective variant using chiral amines as asymmetric inducers.

In a preliminary screening we tested the most common chiral amines employed in organocatalysis. Among several MacMillan's imidazolidinones (**M1-M5**), only the **M1** provided the desired aldehyde **19aa**, although with a poor yield and a modest 38% ee (Table 7, entries 1-5). The MacMillan organocatalyst used by Bandini in his cooperative gold/enamine catalysis (see Scheme 75, page 62) did not work in our process, observing in all cases full conversion of the allenamide (entries 4-5). We also tested **L-Proline**, which afforded the product in a low 13% yield and a poor enantioselectivity of 12% (entry 6). The Hayashi-Jørgensen chiral secondary amine **C1** allowed us to decrease

reaction times providing a good 68% yield and a promising 60% ee (entry 7), whereas the analog prolinol with 3,5-bis(trifluoromethyl) groups at the phenyl rings (**C4**) afforded only traces of the desired product (entry 8). The cinchona alkaloid **C5** led to the same enantioselectivity as the Hayashi-Jørgensen organocatalyst **C1** (60% ee) but with lower yields (16%) and longer reaction times (entry 9).

Table 7. Preliminary screening of chiral organocatalysts.
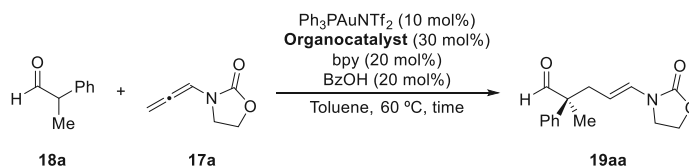
Entry	Organocatalyst (30 mol%)	t (h)[b]	19aa[c] (%)	ee (%)
1[d]	M1	1	13	38
2	M2	2	traces	-
3	M3	2	0	-
4[d]	M4	2	0	-
5[d]	M5	2	0	-
6	*L*-Proline	1	13	12
7	C1	0.5	68	60
8	C4	2	traces	-
9	C5	3	16	60

[a] *Reaction conditions*: **17a** (0.16 mmol), **18a** (2 equiv), Ph₃PAuNTf₂ (10 mol%), organocatalyst (30 mol%), toluene [0.1 M], 60 °C. [b] Full conversion of **17a** was observed at the specified time, unless otherwise noted [c] Isolated yields, unless otherwise noted. [d] Benzoic acid was not added to the reaction.
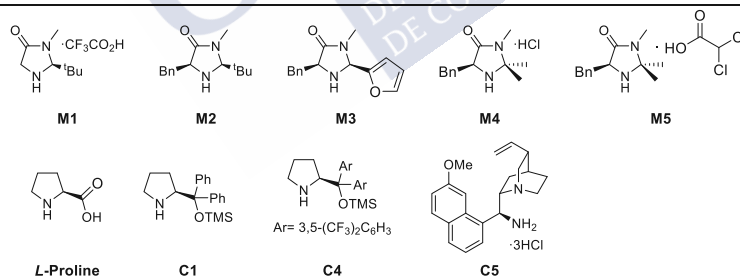
We next explored different gold(I) catalysts in combination with the organocatalysts that afforded the highest enantioselectivities (**C1** and **C5**) in order to see whether the enantiomeric excess could be tuned by using suitable racemic gold catalyst. First, the cinchona alkaloid **C5** was tested in the presence of the gold(I) complexes that performed well in the racemic version. As depicted in Table 8, all of them promoted the reaction with low yields (from 12% to 21%) and moderate enantioselectivities, which varied from 54% ee (with (*p*CF₃C₆H₄)₃PAuNTf₂, Ph₃PAu(TA)OTf and IPrAuNTf₂; entries 2, 3 and 5), to 66% (with IMesAuNTf₂, entry 5). On the other hand, the use of Hayashi-Jørgensen chiral amine **C1** in combination with a gold complex containing a more electron-deficient phosphine, such as (*p*CF₃C₆H₄)₃PAuNTf₂, afforded the product in a better 71% yield but

with a drop in enantioselectivity to 48% ee (entry 7), compared to Ph₃PAuNTf₂ (68% yield, 60% ee, entry 6). The use of the triazole complex developed by Shi (Ph₃PAu(TA)OTf) produced a rise in the enantiomeric excess up to 68% ee but negatively affecting the yield (44% yield, entry 8). Gold complexes bearing σ-donor NHC ligands, such as IMesAuNTf₂ and IPrAuNTf₂, promoted the reaction in low 20-44% yields respectively (entries 9-10) but, interestingly, IPrAuNTf₂ afforded the product with a promising 72% ee (entry 10). Gratifyingly, reducing the loading of the organocatalyst to 20 mol% allowed us to increase the yield up to 66% with this gold(I) catalyst, whereas the enantiomeric excess remained unaffected (72% ee, entry 11). The use of Ph₃PAuNTf₂ with lower organocatalyst loading also provided the product with a better yield of 77%, while maintaining the same 62% ee (entry 12).

Table 8. Screening of gold(I) catalysts combined with cinchona alkaloid **C5**.
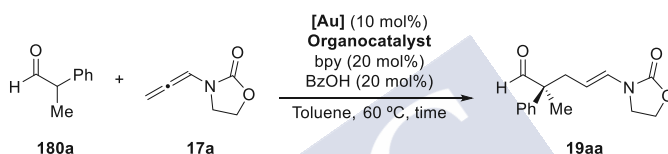
Entry	[Au]	Organocatalyst (mol%)	t (h)[b]	19aa (%)[c]	ee (%)
1[d]	Ph₃PAuNTf₂	C5 (30)	3	16	60
2[d]	(pCF₃C₆H₄)₃PAuNTf₂	C5 (30)	5.5	16[e]	54
3[d]	Ph₃PAu(TA)OTf	C5 (30)	5.5	14[e]	54
4[d]	IMesAuNTf₂	C5 (30)	3	12[e]	66
5[d]	IPrAuNTf₂	C5 (30)	5	21[e]	54
6	Ph₃PAuNTf₂	C1 (30)	0.5	68	60
7	(pCF₃C₆H₄)₃PAuNTf₂	C1 (30)	0.7	71[e]	48
8	Ph₃PAu(TA)OTf	C1 (30)	1	53	68
9	IMesAuNTf₂	C1 (30)	2.5	20[e]	58
10	IPrAuNTf₂	C1 (30)	0.5	44	72
11	IPrAuNTf₂	C1 (20)	0.5	66	72
12	Ph₃PAuNTf₂	C1 (20)	0.5	77	62

[a] *Reaction conditions*: **18a** (0.16 mmol), **19a** (2 equiv), [Au] (10 mol%), organocatalyst (20-30 mol%), bpy (20 mol%), BzOH (20 mol%), toluene [0.1 M], 60 °C. [b] Full conversion of **17a** was observed at the specified time, unless otherwise noted. [c] Isolated yields, unless otherwise noted. [d] Reaction carried out without benzoic acid. [e] Yields determined by ¹H-NMR using 1,3,5-trimethoxybenzene as internal standard.

As can be deduced from Table **9**, variations in the temperature led to a drop in the yield (entry 1 *vs* entries 2 and 3) while, unexpectedly, the enantiomeric excess remained almost constant either at 40 °C or 100 °C. Higher organocatalyst loadings afforded the product in a lower 44% yield (entry 4), but it can be recovered by matching the catalytic loadings of the organocatalyst and the acid (entries 4 *vs* 5). In entry 5, we observed an inversion in the enantiomeric ratio, which was due to the use of the other enantiomer of the organocatalyst **C1**. Therefore, as expected, both enantiomers of the desired aldehyde could be obtained just by switching the configuration of the organocatalyst. Checking

whether the increase of the organocatalyst/BzOH loadings could have an impact on the yield, we tested loadings up to 50 mol% of **C1** and acid, but we obtained the desired product in almost the same yield and with the same 70% enantiomeric excess (entry 6).

**Table 9**. Fine-tune of enantioselective conditions with **C1**.
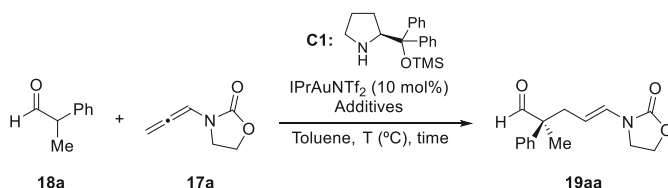
Entry	C1 (mol%)	Additives (mol%)	T (°C)	t (h)[b]	19aa (%)[c]	ee (%)
1	20	bpy (20)/BzA (20)	60	0.5	66[d]	72[e]
2	20	bpy (20)/BzA (20)	40	2.5	30	70
3	20	bpy (20)/BzA (20)	100	0.3	29	74
4	**30**	bpy (20)/BzA (**20**)	60	0.5	44	72
5	**30**	bpy (20)/BzA (**30**)	60	0.5	63[d]	70[f]
6	**50**	bpy (20)/BzA (**50**)	60	0.5	59	70

[a] *Reaction conditions*: **17a** (0.16 mmol), **18a** (2 equiv), IPrAuNTf$_2$ (10 mol%), C1 (mol%), toluene [0.1 M], 60 °C. [b] Full conversion of **17a** was observed at the specified time, unless otherwise noted. [c] Yields determined by ^{1}H-NMR using 1,3,5-trimethoxybenzene as internal standard, unless otherwise noted. [d] Isolated yield. [e] er = 85:15 [f] Reaction carried out with (**R**)-**C1**, er = 14:86.

We explored other non-coordinating solvents, such as trifluorotoluene and benzene, but we observed a significant drop in the yield (to 21% and 24% yield). Trifluorotoluene provided a 58% ee, while the use of benzene allowed a 74% ee to be obtained (Table 10, entries 2 and 3).

Table 10. Screening of solvents in the asymmetric reaction.
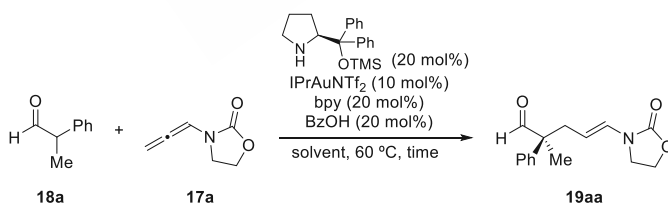
Entry	C1 (mol%)	Solvent (mol%)	T (°C)	t (h)[b]	19aa (%)[c]	ee (%)
1	20	toluene	60	0.5	66[d]	72
2	20	trifluorotoluene	60	1.2	24	58
3	20	benzene	60	0.7	21	74

[a] *Reaction conditions*: **17a** (0.16 mmol), **18a** (2 equiv), IPrAuNTf$_2$ (10 mol%), C1 (20 mol%), solvent [0.1 M], 60 °C. [b] Full conversion of **17a** was observed at the specified time, unless otherwise noted. [c] Yields determined by ^{1}H-NMR using 1,3,5-trimethoxybenzene as internal standard, unless otherwise noted. [d] Isolated yield.

We next investigated the influence of different additives that might stabilize the active gold(I) species. Therefore, the reaction without bpy provided a lower 49% yield with a slightly improvement in the ee (Table 11, entry 1), but the presence of bpy not only influenced the reaction yield, like in the racemic series, but also the ee, albeit in a minor extent (entry 2). Moreover, using 1,10-phenanthroline (phen) as additive we observed an increase in the ee up to 80%, but the yield diminished to 33% (entry 3). This result encouraged us to study other bidentate dimethyl-substituted bipyridines, even containing chiral motifs, in an attempt to increase both yield and enantiomeric excess; but they afforded the product in lower yields and without significant changes in ee (entries 4 to 6). We also explored monodentate pyridines, such as 2,6-lutidine or DMAP, obtaining similar results with 2,6-lutidine (66% yield, 70% ee) than with bpy (entry 7 *vs* 2); whereas DMAP afforded the desired product in 20% yield and 50% ee (entry 8).

Table 11. Screening of additives in the asymmetric reaction.
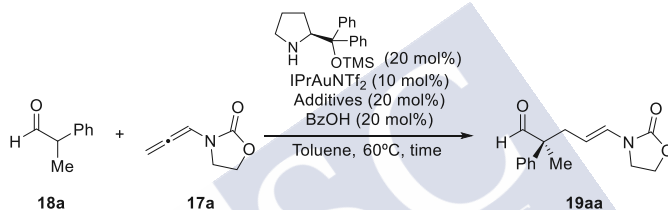
Entry	Additive (20 mol%)	t (h)[b]	19aa (%)[c]	ee (%)
1	-	0.3	49[d]	76
2	bpy	0.5	66[d]	72
3	phen	1	33[d]	80
4	5,5'-bpy	0.5	55	72
5	4,4'-bpy	0.5	50	74
6	(*R,R*)-bpy	3	26	64
7	2,6-lutidine	2.3	66	70
8	DMAP	2.3	20	50

[a] *Reaction conditions*: **17a** (0.16 mmol), **18a** (2 equiv), IPrAuNTf$_2$ (10 mol%), C1 (20 mol%), toluene [0.1 M], 60 ºC. [b] Full conversion of **17a** was observed at the specified time, unless otherwise noted. [c] Yields determined by ^{1}H-NMR using 1,3,5-trimethoxybenzene as internal standard, unless otherwise noted. [d] Isolated yield.
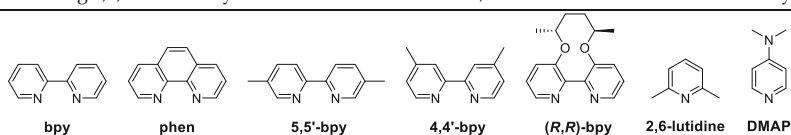
We also tested different acids commonly used as additives in organocatalysis. The 3,5-dinitro-substituted benzoic acid provided the desired product in the same 67% yield and a slightly worse enantiomeric excess (70%, Table 12, entry 2 *vs* entry 1), while 2,4-dinitro-substituted benzoic acid led to slightly better 76% ee but in a lower 42% yield. Other substituted benzoic acids did not provide significant improvements of the enantiomeric excess or yield (entries 4 and 5).

**Table 12**. Screening of acids in the asymmetric reaction.
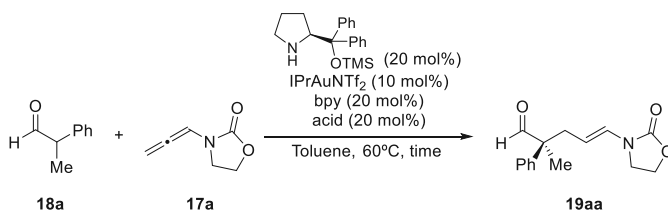
Entry	Acid (20 mol%)	t (h)[b]	19aa (%)[c]	ee (%)
1	BzOH	0.5	66[d]	72
2	3,5-(NO$_2$)$_2$-BzOH	0.7	67[d]	70
3	2,4-(NO$_2$)$_2$-BzOH	0.5	42	76
4	4-NO$_2$-BzOH	0.5	50	74
5	4-F-BzOH	0.3	53	74

[a] *Reaction conditions*: **17a** (0.16 mmol), **18a** (2 equiv), IPrAuNTf$_2$ (10 mol%), C1 (mol%), Toluene [0.1 M]. [b] Full conversion of **17a** was observed at the specified time, unless otherwise noted. [c] Yields determined by ^{1}H-NMR using 1,3,5-trimethoxybenzene as internal standard, unless otherwise noted. [d] Isolated yield.
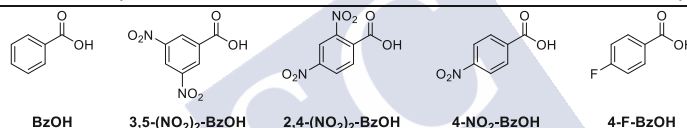

We next analyzed the performance of several prolinol silyl ethers with diverse steric requirements. As can be deduced from Scheme 90 (first row), by increasing the size of the silyl ether (from TMS to TBDPS), the ee of **19aa** becomes higher (up to 84% ee, with TBS and TPS derivatives **C6** and **C8** respectively). However, the efficiency of the process is eroded, and the product **19aa** was obtained in low yields (28% and 23% yield), or even not formed (with the TIPS derivative **C9**). This is probably due to the fact that the synergistic process is less efficient, so the dimerization and polymerization of the allenamide becomes competitive. To evaluate the importance of the silyl ether, we explored the organocatalyst bearing a hydrogen atom (**C10**) instead of the SiR$_3$ group. This led to a moderate 56% yield without inducing chirality in the desired product. The presence of a small atom like fluorine (**C11**) proved to be suitable for inducing enantioselectivity, although with low values (44% ee), and with poor yield (15%). Other aryl or alkyl groups in the prolinol also proved to be suitable for the transformation, but we did not observe an improvement in the yield or the ee (**C12** to **C15**). We also study if the presence of phenyl groups in the prolinol was necessary by substituting them by hydrogen atoms and also with different SiR$_3$ groups (with TBS, TIPS or TBDPS derivatives **C16** to **C18** respectively) and the reactions proceeded in low yields (28-32% yield) and enantioselectivities (34-48% ee). Other related organocatalysts such as **C19** and **C20** did not improve the previous results with **C1**.

To sum up, the TMS-prolinol **C1** proved to be a suitable organocatalyst for the synergistic process affording the desired product in moderate yield and with a good enantioselectivity of 72% ee.
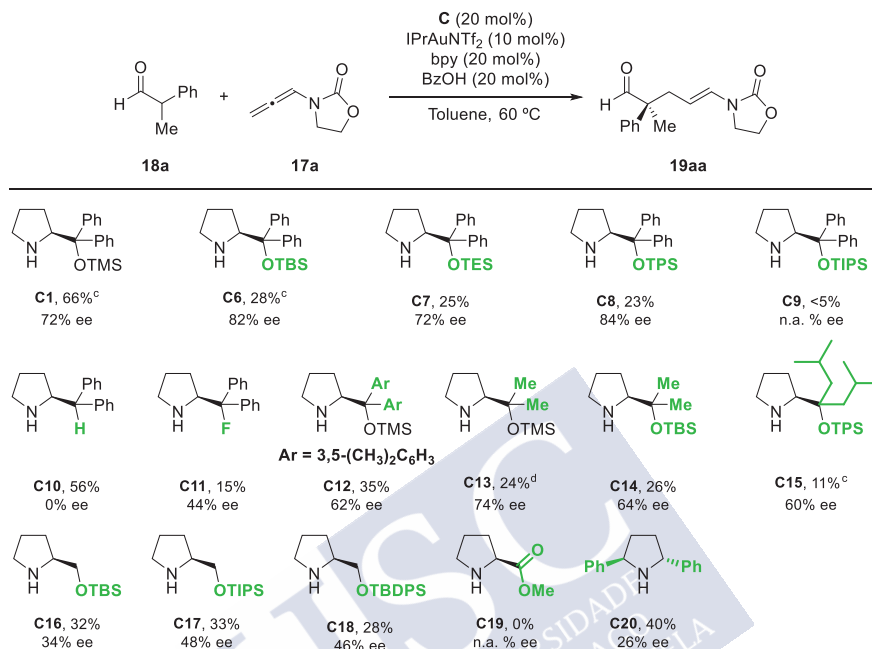
Scheme 90. Screening of different chiral organocatalysts.

[a] *Reaction conditions*: **17a** (0.16 mmol), **18a** (2 equiv), IPrAuNTf$_2$ (10 mol%), organocatalyst (mol%), bpy (20 mol%), BzOH (20 mol%), toluene [0.1 M], 60 °C. [b] Yields determined by ^{1}H-NMR using 1,3,5-trimethoxybenzene as internal standard, unless otherwise noted. [c] Isolated yield. [d] 50% conversion after 4 h.

3.4. Scope of the enantioselective variant with α-branched aldehydes

With the optimal conditions in hand, we explored the scope of the enantioselective variant of the reaction using IPrAuNTf$_2$ (10 mol%), the Hayashi-Jørgensen **C1** organocatalyst (20 mol%), 2,2'-bipyridine (20 mol%) and benzoic acid (20 mol%) in toluene at 60 °C (Scheme 91). In some cases, it was necessary to quench the reaction with NaBH$_4$ to avoid problems during the purification, therefore obtaining the corresponding alcohols **20**. The use of 2-arylpropanal with an electron-rich substituent afforded the corresponding product with a low 40% yield and a moderate 68% ee (**19ab**). The substrate with an electron-withdrawing substituent in the *para* position did not provide the product (**20ac**), whereas if the substituent is in the *meta* position the alcohol **20ad** could be obtained with poor yield and enantioselectivity.

Using a bulkier aldehyde like **18f** we observed a low yield, but the product was obtained with good ee (up to 70% ee). Using other allenamides, such as the pyrrolidone derivative **17c**, we obtained the desired product in moderate 50% yield and with a slightly better enantioselectivity of 82% (**19ca**). Curiously, *N*-tosylphenyl allenamide **17d**, which

provided the desired product in the racemic variant, did not afforded the desired product (**20da**). However, the analog *N*-tosylbenzyl derivative provided the product in 50% yield and 80% ee (isolated as the alcohol derivative **20ea**).
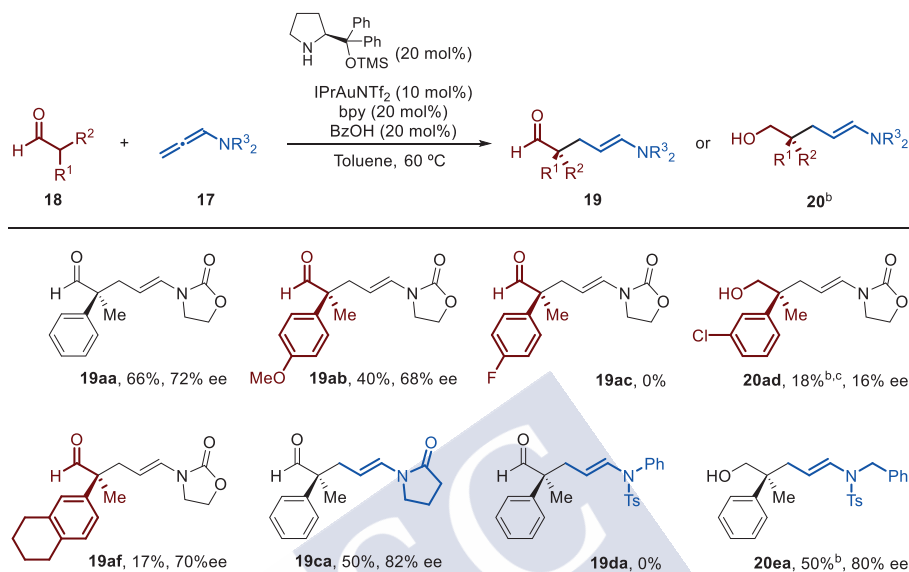
^a *Reaction conditions*: **17** (0.16 mmol), **18** (2 equiv), IPrAuNTf$_2$ (10 mol%), C1 (20 mol%), bpy (20 mol%), BzOH (20 mol%), toluene [0.1 M], 60 °C. ^b Obtained after quenching with NaBH$_4$ to facilitate isolation. ^c Carried out at 100 °C.

Scheme 91. Scope of the enantioselective variant of the reaction.

3.5. Optimization and scope of the reaction with α-monosubstituted aldehydes

We also evaluated the performance of 2-phenylacetaldehyde, which in the racemic version afforded the desired product in almost quantitative yield. We tested the reaction between oxazolidinone allenamide **17a** and 2-phenylacetaldehyde (**18g**), using the optimal reaction conditions of Table 9, entry 1 (IPrAuNTf$_2$ (10 mol%), Hayashi-Jørgensen organocatalyst **C1** (20 mol%), bpy (20 mol%) and BzOH (20 mol%) at 60 °C). As depicted in Table 13, with IPrAuNTf$_2$ as gold catalyst, we obtained almost quantitative yields, moderate *E/Z* mixtures, but a low 32 % enantioselectivity (entry 1). Thus, we explore different gold(I) catalysts in combination with the TMS-prolinol **C1** in order to see whether the ee could be improved. The use of Ph$_3$PAuNTf$_2$ allowed the reaction to proceed with a very good 88% yield, but again low enantioselectivity (36%, entry 2). The gold complex with an electron-withdrawing phosphite **L1** promoted the transformation in longer reaction times, providing excellent yields, but even lower ee (20% ee, entry 3). The use of the triazole complex developed by Shi slightly improved the enantiomeric excess (41% ee) but with a drop in the yield (79%, entry 4). We tested the reaction with AuCl and SMe$_2$AuCl and, curiously, both provided good yields with different diastereomeric ratios and enantioselectivities (from 36% to 56% ee, entries 5 and 6).

Therefore, we conclude that IPrAuNTf$_2$ was also the optimal gold(I) catalyst for the development of the enantioselective reaction with α-monosubstituted aldehydes since, although the enantiomeric excess is low, the desired products were obtained quantitatively.

Table 13. Screening of gold(I) catalysts combined with **C1** in the reaction with 2-phenylacetaldehyde.
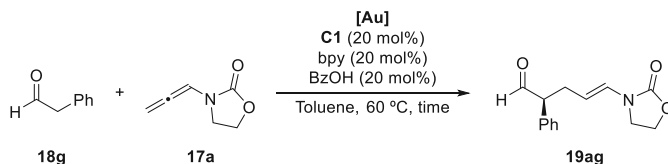
Entry	[Au] (mol%)	t (h)[b]	19ag (%)[c]	*E/Z*	ee (%)[d]
1	IPrAuNTf$_2$ (10)	0.3	99	6.4:1	32[e]
2	Ph$_3$PAuNTf$_2$ (10)	0.3	88	4.8:1	36
3	L1AuNTf$_2$ (5)	2.5	91	2.3:1	20
4	Ph$_3$PAu(TA)OTf (10)	0.5	79[f]	1.5:1	41
5	AuCl (10)	0.3	77	9.5:1	36
6	SMe$_2$AuCl (10)	0.5	77	3.7:1	56

[a] *Reaction conditions*: **17a** (0.16 mmol), **18b** (2 equiv), [Au] (10 mol%), **C1** (20 mol%), bpy (20 mol%), BzOH (20 mol%), toluene [0.1 M], 60 °C. [b] Full conversion of **17a** was observed at the specified time, unless otherwise noted. [c] Isolated yields, unless otherwise noted. [d] enantiomeric excess of the *E*-product. [e] Reaction carried out with **(R)-C1**. [f] Yields determined by ^{1}H-NMR using 1,3,5-trimethoxybenzene as internal standard.
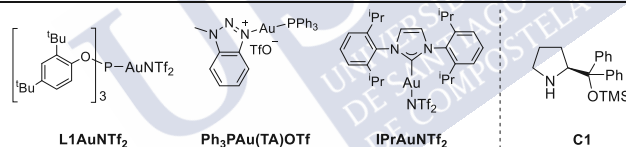
To further increase the ee, we evaluated some of the previous organocatalysts tested in the reaction of **18a** (Scheme 92).[141] The Hayashi-Jørgensen TBS-prolinol (**C6**), which provided very good ee (82% ee) but with low yields in the reaction of **18a**, afforded the desired aldehyde in almost quantitative yield, decent stereoselectivities (*E/Z* mixture 5.6/1) and poor enantioselectivity (10% ee). Our attempts to find a prolinol-derived organocatalyst that could promote the reaction in high enantioselectivities were unsuccessful (**C9**, **C10**, **C14**, **C15** and **C18**), although in some cases we were able to obtain excellent *E/Z* ratios.

---

[141] All the enantiomeric excesses are for the (*E*)-isomer of the products.

C (20 mol%)
IPrAuNTf₂ (10 mol%)
bpy (20 mol%)
BzOH (20 mol%)

Toluene, 60°C, time

18g   **17a**   **19ag**

C1, 99%ᶜ
E/Z: 6.4/1, 32% ee

C6, 98%ᶜ
E/Z: 5.6/1, 10% ee

C9, 46%ᶜ
E/Z: 20/1, 16% ee

C10, 99%
E/Z: 1/0, 10% ee

C14, 80%
E/Z: 19/1, 18% ee

C15, 99%ᶜ
E/Z: 13/1, 0% ee

C18, 99%
E/Z: 1/0, 34% ee
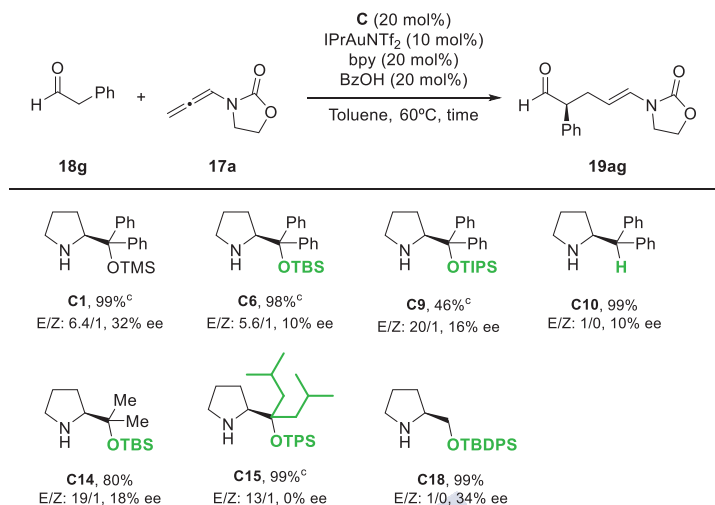
ᵃ *Reaction conditions*: **17a** (0.16 mmol), **18c** (2 equiv), IPrAuNTf₂ (10 mol%), Organocatalyst (mol%), bpy (20 mol%), BzOH (20 mol%), toluene [0.1 M], 60 °C. ᵇ Yields determined by ¹H-NMR using 1,3,5-trimethoxybenzene as internal standard, unless otherwise noted. ᶜ Isolated yield.

Scheme 92. Screening of different chiral organocatalysts with 2-phenylacetaldehyde.

Like in the case of the racemic optimization, 2-arylacetaldehydes can be transformed into the corresponding products in almost quantitative yields, but with non-reproducible *E/Z* mixtures. To avoid the formation of *E/Z* mixtures the reaction was quenched with NaBH₄, so the corresponding alcohol was obtained in quantitative yield as a single *E*-stereoisomer and maintaining the same 30% enantiomeric excess (Scheme 93).

1) **C1** (20 mol%)   IPrAuNTf₂ (10 mol%) bpy (20 mol%) BzOH (20 mol%) Toluene, 60 °C, 0.2 h

2) NaBH₄ (4 equiv), MeOH, rt, 0.5 h

**18g**   **17a**   **20ag**, 99% 30% ee
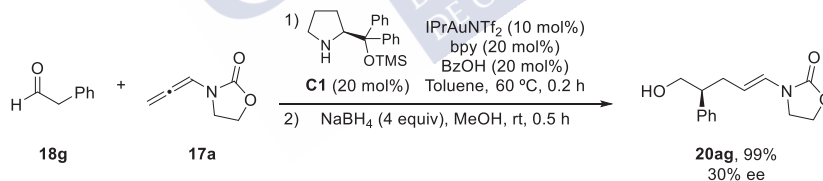
Scheme 93. Quenching with NaBH₄ affording **20ag** with the same yield and ee.

To check whether a racemic pathway via an enol intermediate was operative, and this could damage the enantioselectivity of the process, we prepared and tested the (*E*)-enamine intermediate **21**.[142] The product was obtained in a 42% yield and 41% enantiomeric excess (Scheme 94).

---

[142] The (*E*)-enamine intermediate was synthesized from (*R*)-C1, while (*S*)-C1 was the organocatalyst employed for the enantioselective optimization.
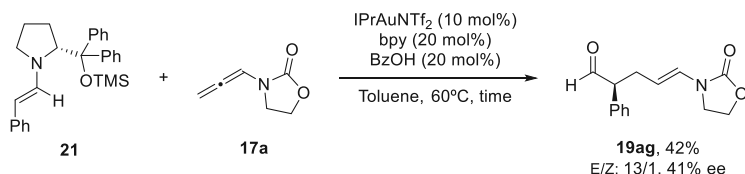
Scheme 94. Reactivity of the enamine intermediate **35** towards the activated allene **17a**.

We then check the influence of the allenamide structure on the enantiomeric excess. Gratifyingly, we found that using the *N*-tosyl allenamide **17e** the enantioselectivity increases up to 70% ee, affording the product in almost quantitative yield (Table 14, entry 1). A decrease in the temperature to 40 °C led to a drop in the yield and a slightly increase in the ee (74% ee, entry 2). Curiously, the absence of bpy did not affect the yield of the reaction (entry 3), while the use of 1,10-phenanthroline as additive led to a significant drop (67% yield) and also affected the enantiomeric excess (62% ee, entry 4). We next explored the organocatalysts that afforded the best enantioselectivities for the α-branched aldehydes (Scheme 90, page 88, C6 and C8). Interestingly, the use of TBS-prolinol (**C6**) and TPS-prolinol (**C8**) afforded the corresponding alcohol in almost quantitative yields and in short reaction times. Unfortunately, while in the previous screening they afforded enantioselectivities up to 84% ee, in this reaction the enantiomeric excesses obtained were slightly lower than with **C1**, between 64% and 68 ee (entries 5 and 6).

Table 14. Screening of conditions with allenamide **17e**.
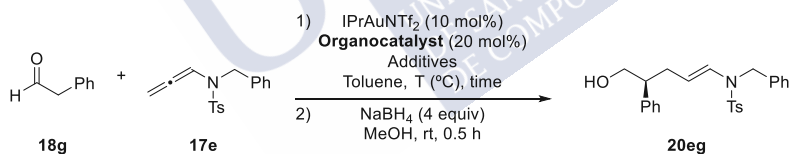
Entry	Organocatalyst (20 mol%)	Additives (mol%)	T (°C)	t (h)[b]	19eg (%)[c]	ee (%)
1	C1	bpy (20)/BzOH (20)	60	0.2	99	70
2	C1	bpy (20)/BzOH (20)	40	1	80	74
3	C1	BzOH (20)	60	0.5	99	70
4	C1	phen (20)/BzOH (20)	60	1.5	67	62
5	C6	bpy (20)/BzOH (20)	60	0.2	99	68
6	C8	bpy (20)/BzOH (20)	60	0.2	99	64

[a] *Reaction conditions*: **17e** (0.16 mmol), **18g** (2 equiv), IPrAuNTf$_2$ (10 mol%), organocatalyst (20 mol%), toluene [0.1 M], 60 °C. [b] Full conversion of **17a** was observed at the specified time, unless otherwise noted. [c] Isolated yield.
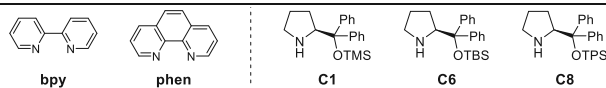
We next evaluate the evolution of the enantiomeric excess under the reaction conditions. We chose the reaction between allenamide **17e** and aldehyde **18g** as a model, since it

affords the product in almost quantitative yield and with good enantioselectivities. Before full conversion of **17e**, we observed enantiomeric excesses of **20eg** up to 76%, followed by a slight drop to 72% ee (Table 15, entries 1 to 4). After full conversion we obtained a 70% ee (entry 5). If the product (an aldehyde before treatment with NaBH₄) is maintained under reaction conditions for 90 minutes, we observed a lower ee of 64% (entry 6).

Table 15. Evolution of enantiomeric excess in reaction conditions.
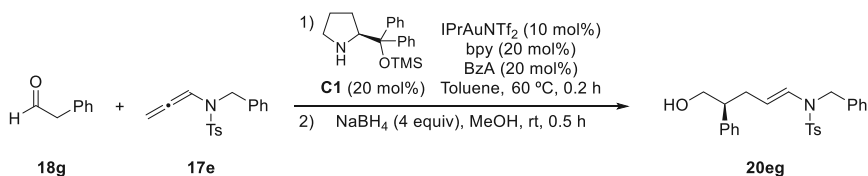
Entry	t (min)[b]	Conversion (%)[c]	ee (%)
1	0.5	0	-
2	2	40	70
3	5	56	76
4	10	82	72
5	15	100	70
6	90	100	64

[a] *Reaction conditions*: **17e** (0.16 mmol), **18g** (2 equiv), IPrAuNTf₂ (10 mol%), C1 (20 mol%), bpy (20 mol%), BzOH (20 mol%), Toluene [0.1 M], 60 °C. [b] Quenching with NaBH₄ carried out at the specified time. [c] Conversion of **29e** was determined by ¹H-NMR using 1,3,5-trimethoxybenzene as internal standard.

This drop in the enantiomeric excess could be explained by a racemization induced by the TMS-prolinol **C1**. The amine organocatalyst might react with **19eg** forming the iminium intermediate **XX**, that can be in slow equilibrium with the enamine intermediate **XXI** and, after protonation, a decrease in the enantiomeric excess could be observed. Nevertheless, the loss in enantiomeric excess is not significant (from 70% to 64% ee, Table 15, page 93, entries 5 and 6), so this process is not the main responsible for not achieving a high enantiomeric excess. (Scheme 95).
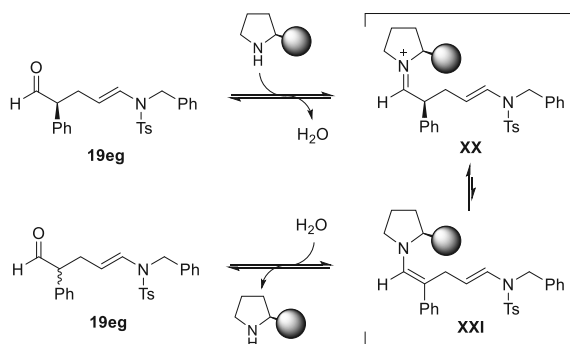
Scheme 95. Proposed equilibrium that might affect enantioselectivity of the process.

With these conditions in hand, we explored the scope of the enantioselective variant in the reactions using IPrAuNTf$_2$ (10 mol%), the Hayashi-Jørgensen **C1** organocatalyst (20 mol%), 2,2'-bipyridine (20 mol%), benzoic acid (20 mol%) in toluene at 60 °C (Scheme 96). We needed to quench the reaction with NaBH$_4$ to avoid non-reproducible *E/Z* mixtures at the enamide moiety. The reaction between oxazolidinone allenamide **17a** and 2-arylacetaldehydes afforded the corresponding alcohols in almost quantitative or very good yields regardless the electronic character of the substituents at the aryl group. Unfortunately, ee's were similar to that obtained with 2-phenylacetaldehyde, varying from 10% to 44% (**20ag-20ak**). The reaction with linear aliphatic aldehydes, such as hydrocinnamaldehyde and isovaleraldehyde, led to the corresponding alcohols (**20am** and **20an**), although in low yields (45% and 25% respectively) and enantioselectivities (34% and 32% respectively). Gratifyingly, the reaction between allenamide **17e** and 2-arylacetaldehydes also afforded the desired alcohols in almost quantitative yields. The ee's obtained were quite variable. While a *p*-Me or a *m*-Cl in the aryl group of the subtrates led to products with ee's closed to that obtained from phenylacetaldehyde (72% and 66% ee, **20eh** and **20ek**), *p*-OMe or *p*-F substituents significantly affected the enantioselectivity (22% and 48% ee, **20ei** and **20ej**), improving, in most cases, the enantioselectivities when compared to those resulting from the oxazolidinone allenamide **17a** (**20eg-20ek** *vs* **20ag-20ak**).
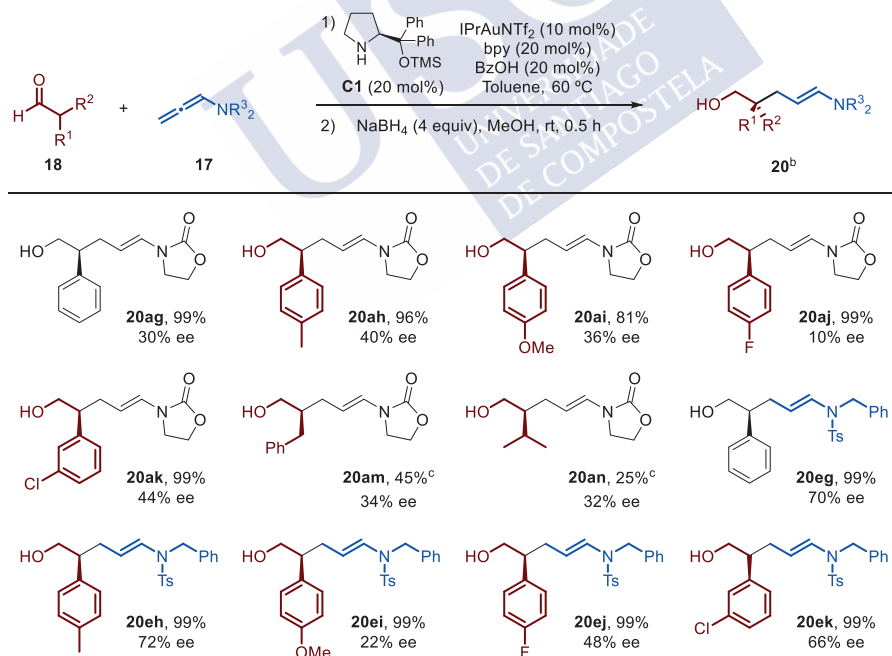
^{a} *Reaction conditions*: **29** (0.16 mmol), **30** (2 equiv), IPrAuNTf$_2$ (10 mol%), C1 (20 mol%), bpy (20 mol%), BzOH (20 mol%), toluene [0.1 M], 60 °C. ^{b} Obtained after quenching with NaBH$_4$ to avoid the formation of enamide *E/Z* isomers. ^{c} Carried out using acetonitrile as solvent.

Scheme 96. Scope of the enantioselective variant of the reaction with α-monosubstituted aldehydes.

3.6. Use of chiral gold catalysts

We have also evaluated the viability of affecting the enantioselectivity of the process by using gold(I) catalysts containing chiral ligands, that might produce match/mismatch effects with a chiral organocatalyst.

To evaluate the effects of chiral gold(I) complexes, we selected the reaction between *N*-tosylbenzyl allenamide **17e** and 2-phenylacetaldehyde **18g**, that afforded the desired product in almost quantitative yields and in short reaction times. To study the match/mismatch effects we set up two reactions for every chiral gold(I) complex. One reaction with **C1**, that is the (*S*) configuration of the TMS-prolinol, and another with **(R)-C1**. Thus, just by switching the configuration of the organocatalyst, we can evaluate the match/mismatch effect for any chiral gold(I) complex.

In a first approach, we decide to test some common chiral gold(I) complexes usually employed in enantioselective gold catalysis. Since the enantioselective reaction was carried out with a gold(I) catalyst bearing a NHC ligand (IPrAuNTf$_2$), we tested chiral NHC-gold(I) complexes. The BODE derivative **Au9** provided **20eg** in an excellent 92% yield with **(S)-C1** (Table 16, entry 2), while the use of **(R)-C1** yielded the product in a moderate 50% yield (entry 3). Both enantiomers of **C1** provided modest enantioselectivities (48-46% ee respectively). Other chiral NHC-gold(I) complex like **(R,R)-Au10** afforded the product with almost quantitative yields but lower enantiomeric excesses (62-56% ee) compared to those obtained with a racemic gold(I) catalyst (entries 4 and 5 *vs.* entry 1). The **(S,R,R)-Au12**, together with **(S)-C1**, afforded the product in almost quantitative yield and with slightly better enantioselectivities (72% ee) than the racemic gold(I) catalyst (70% ee), although in longer reaction times (entry 6 *vs.* entry 1).

However, if the organocatalyst is **(R)-C1**, the enantiomeric excess decreases to 42% (entry 7) but with the same yield and reaction times. A change in the configuration of the gold(I) catalyst, **(S,S,S)-Au12**, led to almost quantitative yields and a good 70% ee when amine **(S)-C1** is employed (entry 8). The **(R)-C1** organocatalysts yielded **20eg** with a lower 55% enantioselectivity (entry 9). The phosphoramidite gold(I) complex derived from SPINOL **(S,S,S)-Au8** afforded the desired product in almost quantitative yield and a moderate 60% ee (entry 10). The use of the bisphosphine digold(I) complex derived from DTBM-SEGPHOS **(S)-Au11** did not provide the desired product after 4 hours, although full conversion of the allenamide **17e** was observed. Then, we decide to evaluate different gold(I) complexes from VANOL derivatives. Other VANOL derivatives like **(S,R,R)-Au13** and **(S,R,R)-Au14** did not improve the enantioselectivities obtained with a racemic gold(I) catalyst (62-58% ee, entries 12 and 13 respectively).

Table 16. Screening of chiral gold(I) complexes with chiral organocatalysts.
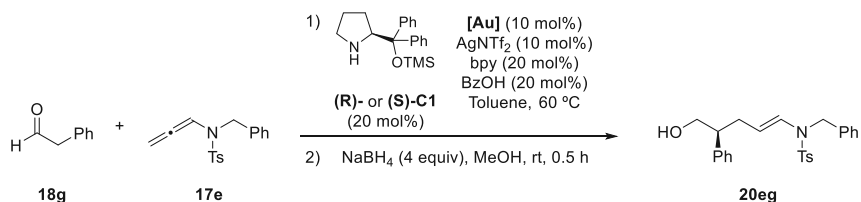
Entry	[Au] (10 mol%)	Organocatalyst (20 mol%)	t (h)[b]	20eg (%)[c]	ee (%)[d]
1	IPrAuNTf$_2$	(S)-C1	0.2	99	+70
2	Au9	(S)-C1	0.7	92	+48
3	Au9	(R)-C1	0.7	50	-46
4	(R,R)-Au10	(S)-C1	0.2	98	+62
5	(R,R)-Au10	(R)-C1	0.2	98	-56
6	(S,R,R)-Au12	(S)-C1	1.5	99	+72
7	(S,R,R)-Au12	(R)-C1	1.5	99	-42
8	(S,S,S)-Au12	(S)-C1	1.5	95	+70
9	(S,S,S)-Au12	(R)-C1	1.5	99	-55
10	(S,S,S)-Au8	(S)-C1	2	99	+60
11	(S)-Au11	(S)-C1	4	0	-
12	(S,R,R)-Au13	(S)-C1	1	99	+62
13	(S,R,R)-Au14	(S)-C1	2.5	99	+58

[a] *Reaction conditions*: **17e** (0.16 mmol), **18g** (2 equiv), IPrAuNTf$_2$ (10 mol%), amine (20 mol%), Toluene [0.1 M]. [b] Full conversion of **17e** was observed at the specified time, unless otherwise noted. [c] Isolated yield. [d] +/- refers to the major peak detected by chiral HPLC analysis.
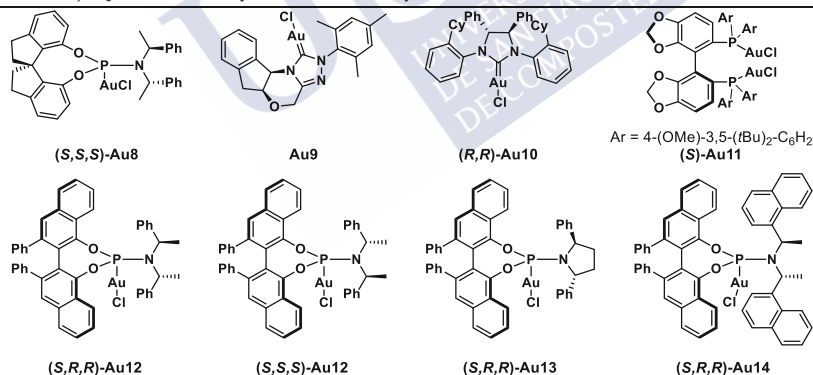
As depicted in Table 16, it looks like there is match effect with amine **(S)-C1** and a mismatch effect with **(R)-C1**. However, the use of chiral gold(I) complexes did not produce any significant improvement of the enantiomeric excess with regard to that obtained with a racemic catalyst such as IPrAuNTf$_2$. In this context, further studies will be carried out concerning the structure of the chiral gold(I) catalyst and the chiral amine attached to the VANOL core in an attempt to find steric interactions between both catalysts to improve the enantioselectivity of the reaction.

3.7. Role of 2,2'-bipyridine, interactions between catalysts

As mentioned before, during the optimization of both, the racemic and enantioselective variants of the reaction; the presence of bpy as additive is necessary to improve the performance of the reaction, especially with α-branched aldehydes (Table 2, entry 3 *vs* 4, page 75). Moreover, the presence of bpy in the reaction media has shown some influence also in the enantiomeric excess (Table 11, entry 2, page 86). Thus, we envisioned that bpy might be acting as a ligand,[143] coordinated to the gold atom and avoiding coordination of the gold catalyst with the amine organocatalyst.

A major issue in this type of synergistic enamine/gold catalysis is related to compatibility between the amine reactants and an active gold catalyst. Therefore, we performed ^{31}P-NMR and ESI-MS experiments to detect gold complexes that could be present in the reaction media (see experimental part). First, we identified the active gold(I) species doing a ^{31}P-NMR of $Ph_3PAuNTf_2$ (Figure 8; Table 17, entry 1). Mixing $Ph_3PAuNTf_2$ with bpy (1:1 ratio) in d_8-toluene at 60 °C immediately led to the quantitative formation of the complex $Ph_3PAu(bpy)NTf_2$ (Figure 8; Table 17, entry 2). Similarly, mixing $Ph_3PAuNTf_2$ with organocatalyst **C1** led to the immediate formation of the gold-amine complex $Ph_3PAu(\mathbf{C1})NTf_2$ (Figure 8; Table 17, entry 3).
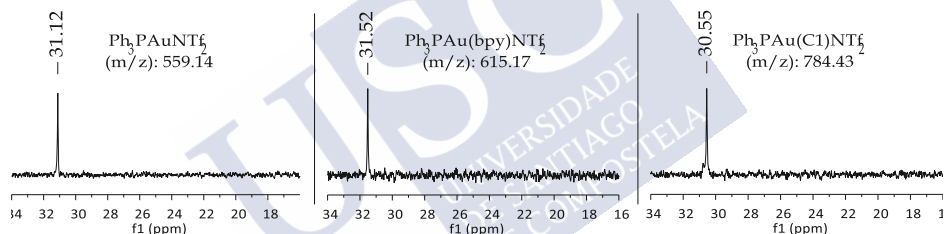
Figure 8. ^{31}P-NMR experiments of gold(I) complexes.

Moreover, by adding **C1** to $Ph_3PAu(bpy)NTf_2$ (1:1 ratio), the formation of $Ph_3PAu(C1)NTf_2$ was cleanly observed by ^{31}P-NMR and by ESI-MS (entry 4). The reverse process, the addition of bpy to $Ph_3PAu(\mathbf{C1})NTf_2$ again allowed to detect by ESI-MS traces of $Ph_3PAu(bpy)NTf_2$, although it was only possible with the addition of more than 1 equivalent of bpy (entries 5 to 7).

The ^{31}P-NMR signal assigned to $Ph_3PAu(\mathbf{C1})NTf_2$ showed a slightly shift towards that of $Ph_3PAu(bpy)NTf_2$ which, together with the ESI-MS result, could indicate that these two Au-species are in equilibrium. As mentioned before, the complex $Ph_3PAu(bpy)NTf_2$ in the presence of **C1** is transformed immediately into $Ph_3PAu(\mathbf{C1})NTf_2$ (entry4). Interestingly, a subsequent addition of 4 equivalents of 2-phenylacetaldehyde (**30c**) to this mixture showed a larger ^{31}P-NMR shift (0.2 ppm), indicative of the formation of $Ph_3PAu(bpy)NTf_2$, detected by ESI-MS along with $Ph_3PAu(\mathbf{C1})NTf_2$, and also with what

---

143 For a related complex, $Ph_3PAu(bpy)PF_6$, see: (a) W. Clegg, *Acta Crystallogr., Sect. B Struct. Crystallogr. Cryst. Chem.* **1976**, *32*, 2712. See also: (b) R. Cai, M. Lu, E. Y. Aguilera, Y. Xi, N. G. Akhmedov, J. L. Petersen, H. Chen, X. Shi, *Angew. Chemie - Int. Ed.* **2015**, *54*, 8772.

it seemed to be the enamine intermediate coordinated to the gold catalyst (entry 8). We assumed that the amine **C1** prefers to react mostly with the aldehyde rather than coordinate the gold species, hence favoring the formation of the active complex Ph$_3$PAu(bpy)NTf$_2$.

Table 17. ^{31}P-NMR and ESI-MS experiments of gold(I) complexes.

Entry	[Au] complex	Additives (equiv)	δ ^{31}P-NMR (ppm)[b]	ESI-MS M$^+$ (m/z)
1	Ph$_3$PAuNTf$_2$	-	31.12	559.14
2	Ph$_3$PAu(bpy)NTf$_2$	-	31.52	615.17
3	Ph$_3$PAu(C1)NTf$_2$	-	30.55	784.43
4	Ph$_3$PAu(bpy)NTf$_2$	C1 (1)	30.57	784.35
5	Ph$_3$PAu(C1)NTf$_2$	bpy (1)	30.58	784.40
6	Ph$_3$PAu(C1)NTf$_2$	bpy (2)	30.60	615.23; 784.40
7	Ph$_3$PAu(C1)NTf$_2$	bpy (4)	30.65	615.22; 784.42
8	Ph$_3$PAu(bpy)NTf$_2$	C1 (1) + **18g** (4 eq)	30.77	615.17; 784.25; 886.27

[a] *Reaction conditions*: Ph$_3$PAuNTf$_2$:toluene adduct (2:1) (0.016 mmol) were dissolved in 0.6 ml d$_8$-toluene and placed in a NMR tube. [b] All the ^{31}P-NMR experiments were carried out using H$_3$PO$_4$ as reference.

Overall, these data suggest that the organocatalyst **C1** stablishes a stronger interaction than bpy with [Ph$_3$PAu]$^+$, but when bpy is present, the complex Ph$_3$PAu(bpy)NTf$_2$ becomes available, at least to some extent. Most probably, bpy facilitates the decomplexation of the secondary amine **C1** from Ph$_3$PAu(**C1**)NTf$_2$, and thereby the activation of the allenamide by the gold species. In consonance with this hypothesis, the (2+2) homodimerization of allenamide **17a** provided very different outcomes with these three gold complexes (Table 18). Whereas the reaction catalyzed by Ph$_3$PAuNTf$_2$ was completed in 0.5 h, providing **11aa** in 61% yield (entry1), Ph$_3$PAu(**C1**)NTf$_2$ did not afford this adduct even after 24 h (entry 3). Meanwhile, Ph$_3$PAu(bpy)NTf$_2$ showed a moderate activity, leading to full conversion after 20 h at rt with 21% yield (entry 2).

Table 18. Homodimerization experiments of **29a** with relevant gold-complexes.
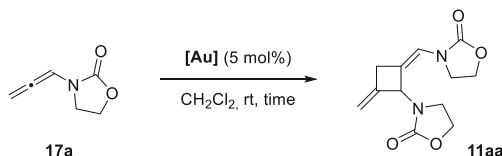
Entry	[Au] (5 mol%)	t (h)[b]	11aa (%)[c]
1	Ph$_3$PAuNTf$_2$	0.5	61
2	Ph$_3$PAu(bpy)NTf$_2$	20	21
3	Ph$_3$PAu(C1)NTf$_2$	>24	0

[a] *Reaction conditions*: **17a** (0.16 mmol), **[Au]** (5 mol%), CH$_2$Cl$_2$ [0.1 M]. [b] Full conversion of **17a** was observed at the specified time. [c] Conversion of **17a** was determined by ^{1}H-NMR using 1,3,5-trimethoxybenzene as internal standard.

4. Simultaneous and posterior work by other groups

While this research was ongoing, we became aware that the group of J. M. González was also working in a quite similar synergistic catalysis for the intermolecular α-addition reaction of aldehydes to allenamides. Despite the similarities, the scope of this method is complementary to ours, and for this reason both papers were published as "back to back" articles.[144] Although many of the examples described by J. M. González overlapped with ours, the use of a different organocatalyst for the racemic version like **L-Proline**; and different solvents, allowed them to achieve α-alkylations of aliphatic aldehydes in moderate yields at low temperatures (Scheme 97).
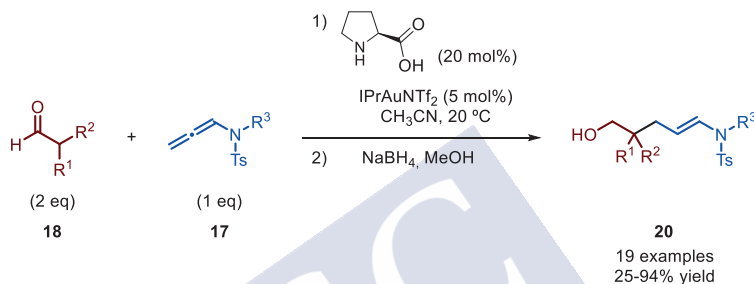
Scheme 97. Racemic synergistic gold-enamine catalysis developed by J. M. González.

They also developed an enantioselective variant in an attempt of generate asymmetric all-carbon quaternary stereocenters. They found conditions for the enantioselective variant using TBS-prolinol **C6** as organocatalyst and 2-F-BzA as additive, obtaining the desired product with good yields and enantioselectivities (up to 76% ee), but with a limited scope. They reported that the use of other silyl ether, like TIPS-prolinol **C9**, provided the product in better enantioselectivities (up to 86% ee) but with a significant drop in the yield to 25% (Scheme 98).
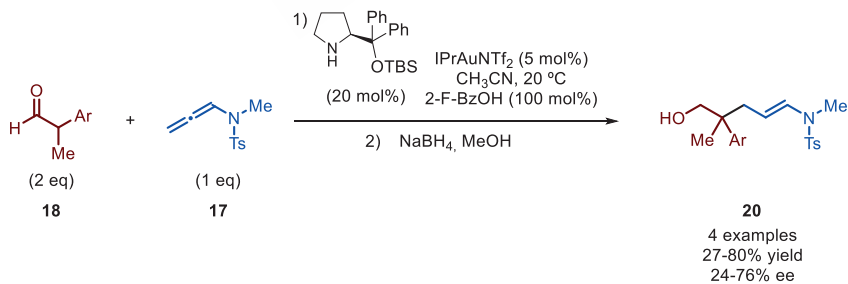
Scheme 98. Enantioselective synergistic gold-enamine catalysis developed by J. M. González.

The same year, albeit not using a dual catalytic process, Toste reported the asymmetric addition of unactivated α-branched cyclic ketones to allenamides catalyzed by a chiral phosphoric acid catalyst. The reaction proceeds at 40 ºC and generates a chiral

---

[144] A. Ballesteros, P. Morán-Poladura, J. M. González, *Chem. Commun.* **2016**, *52*, 2905.

quaternary stereocenter with broad substrate scope, including various aryl, alkenyl, alkynyl and alkyl substitution (Scheme 99).[145]
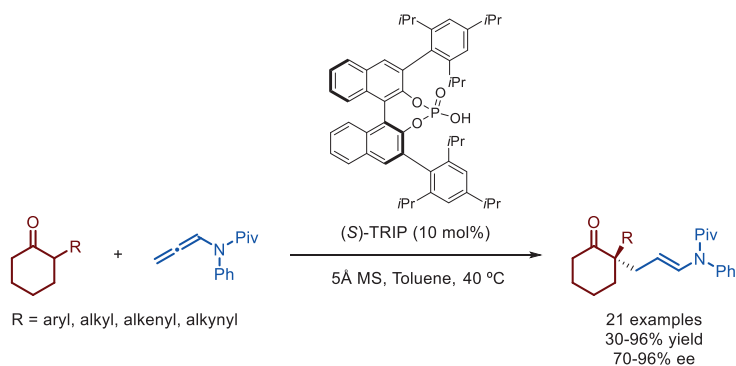
Scheme 99. Asymmetric addition of α-branched cyclic ketones to allenamides reported by Toste.

More recently, S. Luo described a synergistic enamine-palladium catalyzed enantioselective terminal addition to allenes with α-branched β-ketocarbonyls and aldehydes. The reaction could be generally applied to α-branched aldehydes and ketones to afford γ,δ-unsaturated adducts bearing acyclic all-carbon quaternary stereocenters.[146] The protocol proceeds at 50 °C and encompasses allenes including aryl, aliphatic and 1,1'-disubstituted ones. To promote the formation of the π-allylic palladium intermediate they used an electron-rich bidentate phosphine ligand that, together with a bulky chiral primary amine, afforded the desired products in very good yields and enantioselectivities, up to 91% (Scheme 100).
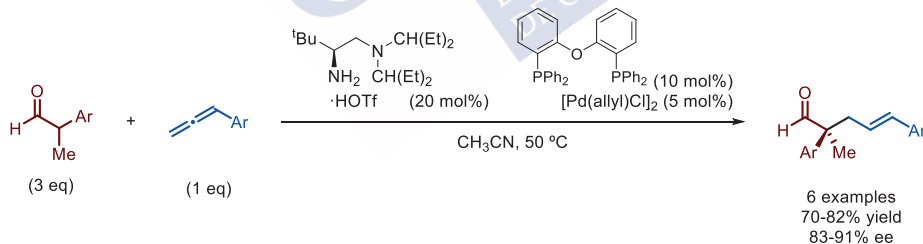
Scheme 100. Enantioselective dual enamine-palladium catalysis developed by S. Luo.

[145] X. Yang, F. D. Toste, *Chem. Sci.* **2016**, *7*, 2653.

[146] H. Zhou, Y. Wang, L. Zhang, M. Cai, S. Luo, *J. Am. Chem. Soc.* **2017**, *139*, 3631.

5. Conclusions

In conclusion, we have developed an intermolecular reaction involving a synergistic combination of enamine-mediated organocatalysis and gold(I) catalysis.[147] The process, which consists of the addition of the α-carbon of an aldehyde to an allenamide, affords very interesting aldehydes or alcohols incorporating tertiary and even quaternary α-stereocenters (Scheme 101).
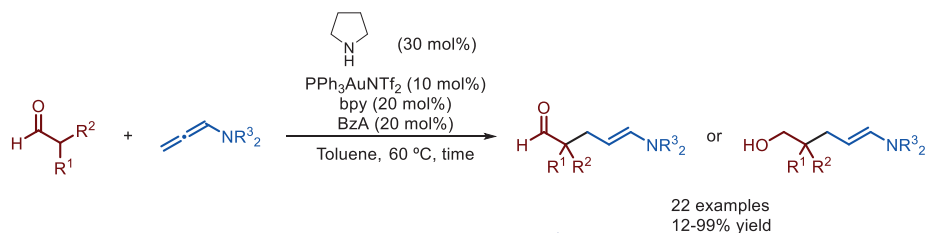
Scheme 101. Racemic synergistic gold and enamine catalysis.

Moreover, we have developed an enantioselective version of the reaction by using the Hayashi-Jørgensen TMS-prolinol as organocatalyst. While the reaction outcome is influenced by several parameters, we have found conditions that provide the products bearing tertiary or event quaternary all-carbon stereocenters with moderate to good levels of enantioselectivity (Scheme 102).
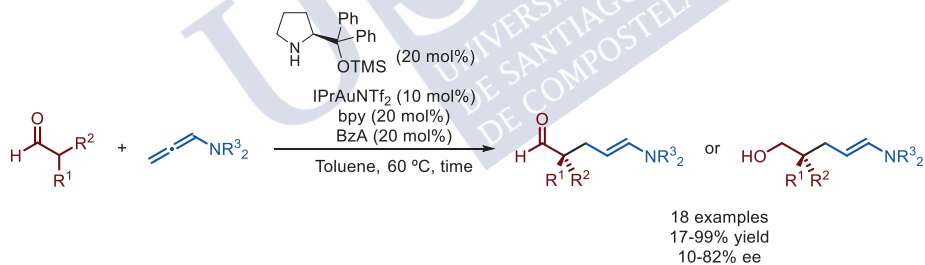
Scheme 102. Enantioselective synergistic gold and enamine catalysis.

---

[147] These results were published in: J. Fernández-Casado, R. Nelson, J. L. Mascareñas, F. López, *Chem. Commun.* **2016**, *52*, 2909.
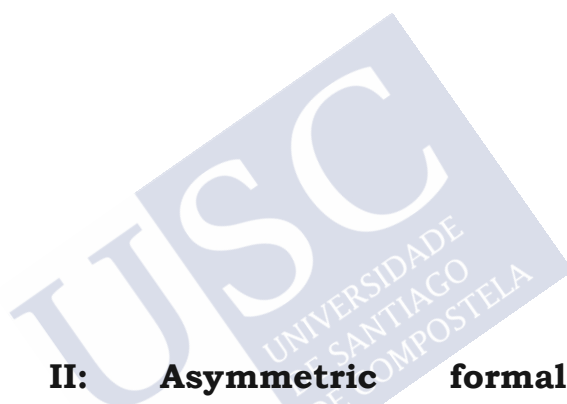
Chapter II: Asymmetric formal (2+2+2) cycloaddition between allenamides and alkenyl-oximes. Straightforward access to azabridged medium-sized carbocycles

Resumen de la tesis doctoral

En esta memoria de investigación se recogen los resultados obtenidos en los estudios sobre el desarrollo de nuevas reacciones de adición y cicloadición de alenos catalizadas por complejos de oro. Concretamente, en las reacciones de adición se estudió el desarrollo de un sistema de catálisis dual combinando catálisis mediada por complejos de oro y organocatálisis. Inicialmente se discute la importancia de desarrollar metodologías que permitan acceder a moléculas con esqueletos o estructuras complejas en el menor número de etapas posibles, en dónde los procesos catalíticos emergen como una herramienta muy útil y versátil; destacando los procesos catalizados por metales (catálisis metálica) y aquellos catalizados por moléculas orgánicas (organocatálisis). Se explica además, como el uso combinado de dos o más catalizadores (procesos catalíticos duales o multicatalíticos) pueden ser beneficiosos para promover procesos químicos que no tendrían lugar en presencia de un único catalizador.

Dentro del campo de la catálisis metálica, esta memoria de investigación se centra en el uso de catalizadores de oro, haciendo un breve análisis de las características más destacadas de este metal. Se hace hincapié en la reactividad de los complejos de oro en presencia de enlaces múltiples (triples y dobles enlaces carbono-carbono) para dar lugar a reacciones de cicloisomerización, cicloadición y adición. En este sentido, los alenos y, concretamente, las alenamidas emergen como un bloque estructural muy versátil que pueden participar como componentes de dos o tres átomos de carbono, ya sea en procesos de cicloadición como de adición tanto intra- como intermoleculares.

Se discute también la posibilidad de usar catálisis mediada por complejos de oro para desarrollar procesos enantioselectivos. Durante los últimos años ha habido un gran interés en aumentar la utilidad sintética de dichos procesos añadiendo un componente de quiralidad, a pesar de que la naturaleza lineal de los complejos de oro hace muy difícil el diseño de ligandos que puedan transmitir la información de quiralidad a los procesos catalíticos. En esta memoria de investigación se analizaron los diferentes ligandos empleados en las últimas décadas en el desarrollo de variantes enantioselectivas de los procesos catalizados por complejos de oro, destacando el uso de bisfosfinas y de los fosforamiditos, una familia de ligandos empleados por primera vez en catálisis asimétrica por nuestro grupo de investigación y el grupo del profesor D. Toste. Además, se inicia el estudio y diseño de ligandos que puedan orientar y dirigir a los sustratos de partida mediante otro tipo de interacciones como los puentes de hidrógeno.

Se analiza también el uso de moléculas orgánicas como catalizadores (organocatálisis) para la construcción de diversas moléculas de manera estereocontrolada. A pesar de que este tipo de transformaciones se conocen desde hace más de un siglo, los artículos en los que se describe el uso de moléculas orgánicas como catalizadores son escasos hasta el año 2000, dónde destacan los trabajos realizados simultáneamente por los grupos de B. List y D. W. C. MacMillan, que le dieron un impulso al campo de la organocatálisis

permitiendo que se llevasen a cabo estudios para descifrar los mecanismos en los que se basan este tipo de transformaciones, con el fin de extrapolarlos y aplicarlos a otro tipo de transformaciones sintéticas. En la memoria de investigación se describen brevemente los distintos modos de activación que pueden presentar los procesos organocatalíticos, siendo los más destacados los de modos de activación mediante enaminas o mediante iones iminio.
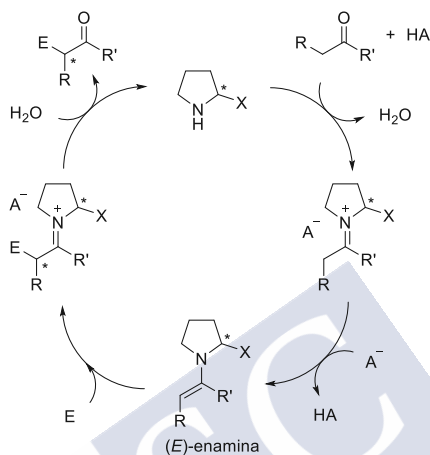
Relacionado con el contenido recogido en esta memoria de investigación se encuentra el modo de activación mediante enaminas, que se usa generalmente para funcionalizar compuestos carbonílicos en su posición α. Se discute que la eficiencia de estos procesos mediante enaminas recae sobre la formación rápida y cuantitativa del primer intermedio iminio, que seguidamente formará el intermedio (*E*)-enamina, el cual atacará al electrófilo induciendo en esta etapa la asimetría al producto final. Se hace hincapié también en el tipo de organocatalizadores usados para inducir quiralidad, que se elegirán dependiendo del tipo de electrófilo sobre el que se quiere llevar a cabo el ataque del intermedio (*E*)-enamina. La información de quiralidad se puede transmitir mediante interacciones de tipo puente de hidrógeno en las que el ataque al electrófilo tiene lugar por la cara *re*; o bien mediante interacciones puramente estéricas en las que el ataque de la enamina al electrófilo tendría lugar por la cara *si*.

Ataque cara *re*   Ataque cara *si*
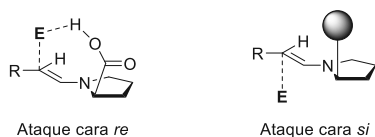
Dentro de los organocatalizadores que transmiten la información de quiralidad mediante interacciones estéricas destacan los desarrollados por los grupos de Y. Hayashi y K. A. Jørgensen, que presentan grupos voluminosos derivados de éteres de silicio. Este tipo de organocatalizadores demostraron ser muy versátiles para llevar a cabo reacciones de alquilación en α a carbonilos, aunque los ejemplos con electrófilos basados en carbonos

sp³ son escasos y generalmente requieren, o bien la presencia de un grupo saliente como un haluro, o bien que el proceso sea intramolecular.

En esta memoria de investigación se discute además la posibilidad de desarrollar procesos catalíticos duales (que requieren el uso de dos catalizadores) combinando las ventajas de la catálisis mediada por metales de transición junto con las ventajas de la organocatálisis, lo que permitiría el descubrimiento de nuevas reactividades que serían inaccesibles con un solo catalizador. Además, también se podría mejorar la enantioselectividad en procesos dónde antes resultaba un gran reto, incrementando la eficiencia de las reacciones y ampliando el alcance de las mismas a través del efecto cooperativo de dos o más catalizadores. Se hace hincapié también en las posibles maneras en la que los distintos catalizadores podrían interactuar, dando lugar a diferentes ciclos catalíticos. Podría parecer que esta combinación es algo trivial, pero el reto principal que se debe superar es asegurar la compatibilidad de los catalizadores, sustratos, intermedios y disolventes a lo largo de todo el proceso. Se describen también brevemente los tipos de sistemas multicatalíticos, que generalmente se categorizan en tres: a) catálisis cooperativa (en la que ambos catalizadores están envueltos en el mismo ciclo catalítico); b) catálisis sinérgica (en la que los catalizadores, cada uno por separado, activan diferentes sustratos, cuyos intermedios reactivos reaccionan entre sí, integrando los dos ciclos catalíticos hacia la formación del producto final); y c) catálisis secuencial (en la que primero actuaría un catalizador formando un intermedio que sería activado por el siguiente catalizador para dar lugar al producto final).
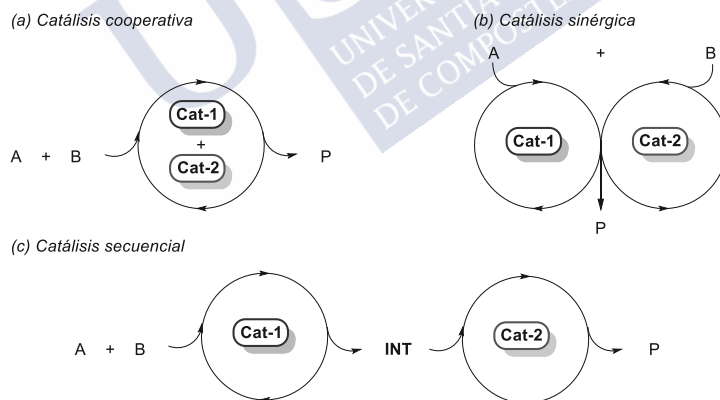
Los tipos de organocatalizadores más usados en combinación con metales de transición son: ácidos de Brønsted (especialmente ácidos fosfóricos quirales), aminocatalizadores (incluyendo aminas secundarias y primarias), catalizadores con interacciones de enlace de hidrógeno y carbenos *N*-heterocíclicos. Mientras que los metales más comúnmente empleados son el paladio, iridio o cobre, siendo el oro menos usado. Se hace hincapié en los procesos que combinan catalizadores metálicos con aminas secundarias o terciarias como organocatalizadores, dando lugar a reacciones muy eficientes que permiten acceder a productos lineales con muy buenos rendimientos y una transferencia de la

quiralidad muy alta. Además, se describen algunos trabajos en los que se obtienen todos los estereoisómeros posibles de los productos finales mediante la elección adecuada de los enantiómeros de los catalizadores.

Se discuten especialmente los ejemplos en los que se combina la organocatálisis con la catálisis de oro. Este tipo de combinación presenta unos retos importantes, siendo el principal y más importante la potencial incompatibilidad de los catalizadores de oro con las aminas, que darían lugar al envenenamiento de los catalizadores de oro y su correspondiente desactivación. Aquí destaca el trabajo de A. Corma, que aisló complejos de oro que presentan una amina coordinada, demostrando la desactivación del catalizador. Se discuten brevemente las maneras de evitar estos procesos de desactivación, aunque generalmente requieren del aumento de temperatura o de la presencia de otros aditivos en el medio de reacción. Se explican también los diferentes procesos descritos que combinan catálisis de oro con organocatálisis, siendo principalmente sistemas de catálisis dual cooperativa o secuencial, quedando relegados a un segundo plano aquellos procesos que requieren la acción sinérgica de los dos ciclos catalíticos.

Una vez enmarcada la tesis doctoral dentro de los trabajos publicados en los campos tanto de la catálisis con oro como de la catálisis dual con oro y organocatalizadores, se procede a la exposición de los resultados obtenidos durante la etapa de investigación.

Catálisis sinérgica de oro y enaminas para la alquilación en α de aldehídos y alenamidas.

En el primer capítulo se describe la primera reacción de alquilación en α de aldehídos con alenamidas, la cual se lleva a cabo gracias a la acción sinérgica de un catalizador de oro con un organocatalizador. El catalizador de oro activará la alenamida, formando un intermedio zwitteriónico susceptible de sufrir ataques de nucleófilos, que en este caso concreto son enaminas generadas *in situ* a través de la condensación de un aldehído con una amina secundaria (organocatalizador). La combinación de ambos procesos nos permitiría generar centros terciarios y cuaternarios que, en el caso de usar un organocatalizador quiral, serían generados de manera enantioselectiva.

Un análisis exhaustivo de los mejores catalizadores para llevar a cabo la reacción racémica entre la alenamida-oxazolidinona y aldehídos α-disustituidos permitió detectar que el uso combinado de $Ph_3PAuNTf_2$ con pirrolidina como organocatalizador, es el adecuado para obtener los aldehídos funcionalizados en su posición α con rendimientos superiores al ochenta por ciento. En esta parte también se evalúan distintos disolventes, ácidos, aditivos, temperaturas y contraiones, dejando entrever que cualquier variación en las condiciones de reacción tiene un impacto significativo en la formación del producto deseado.

También se describe cómo la reacción funciona con otras alenamidas como las sulfonil-alenamidas, y además cómo tolera diversas funcionalidades en el aldehído como grupos

atractores o dadores de carga, ya sea en la posición *meta* o *para* del anillo aromático, generando los productos deseados con centros cuaternarios.
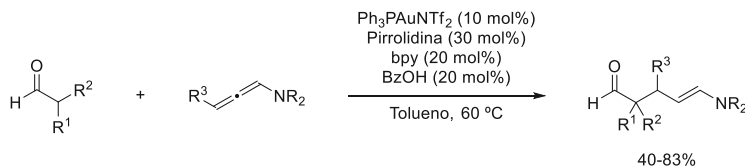
Además, se estudió la viabilidad de usar aldehídos α-monosustituidos, concretamente, el fenilacetaldehído y sus derivados con diferentes sustituyentes dadores o atractores en las posiciones tanto *meta* como *para* del anillo aromático. En el caso del fenilacetaldehído, se encontró que reaccionaba con las diferentes alenamidas generando el producto deseado con un rendimiento cuantitativo, aunque con una mezcla de isómeros *cis:trans* no reproducible en la enamida. Para evitar esta mezcla, se encontró que la reducción *in situ* del aldehído generado daba lugar, también de manera cuantitativa, a los correspondientes alcoholes como un único isómero en su configuración *trans* en la enamida.
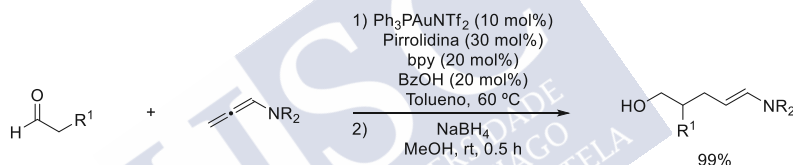
Una vez estudiado el alcance de la versión racémica, se procedió a desarrollar una variante enantioselectiva del proceso sinérgico, siendo un organocatalizador quiral el componente encargado de transmitir la información quiral.

Para llevar a cabo este objetivo, se comenzó probando diferentes organocatalizadores quirales de uso común, entre los que se encuentran, entre otros, los desarrollados por los grupos de D. W. C. MacMillan, Y. Hayashi y K. A. Jørgensen. Se encontró que el organocatalizador de Hayashi-Jørgensen (prolinol trimetilsilil éter) llevaba a cabo la formación del producto deseado en un sesenta y ocho por ciento de rendimiento y con un exceso enantiomérico del sesenta por ciento. Además, se llevó a cabo un análisis de diferentes catalizadores de oro en presencia del organocatalizador de Hayashi-Jørgensen para evaluar cómo afectaba a la enantioselectividad. Se encontró que la naturaleza del ligando racémico coordinado al átomo de oro también ejercía cierta influencia en el exceso enantiomérico, resultando el complejo con un ligando carbeno *N*-heterocíclico IPrAuNTf$_2$ el catalizador de oro que producía el mejor resultado de enantioselectividad (hasta un setenta y dos por ciento de exceso enantiomérico) en presencia de un organocatalizador quiral. En esta parte también se evalúa cómo afecta a la eficiencia del proceso el uso de diferentes disolventes, ácidos, aditivos, temperaturas y cargas catalíticas.

Además, se intentó optimizar el valor de los excesos enantioméricos obtenidos mediante diferentes organocatalizadores derivados del Hayashi-Jørgensen. Para ello se probaron derivados con diferentes éteres de silicio, diferentes grupos aromáticos, diferentes grupos alquilo e incluso con la sustitución de los grupos alquilo por átomos de hidrógeno. Desafortunadamente, ninguno de estos derivados del organocatalizador de Hayashi-Jørgensen consiguió mejorar la relación de rendimiento-exceso enantiomérico obtenida con el organocatalizador de Hayashi-Jørgensen (prolinol trimetilsilil éter).

Una vez optimizadas las condiciones para la variante enantioselectiva, se analizó el alcance de la reacción con los mismos aldehídos usados previamente en la versión racémica. En la reacción asimétrica entre la alenamida-oxazolidinona y aldehídos α-disustituidos se encontró que los sustituyentes atractores en el anillo aromático afectaban a la eficacia del proceso, mientras que los sustituyentes dadores de carga afectaban ligeramente al rendimiento, no así al exceso enantiomérico (en torno al setenta por ciento de enantioselectividad). Además, también se evaluaron otras sulfonil-alenamidas, que mejoraron ligeramente los excesos enantioméricos obtenidos, logrando generar centros cuaternarios con hasta un ochenta por ciento de exceso enantiomérico.
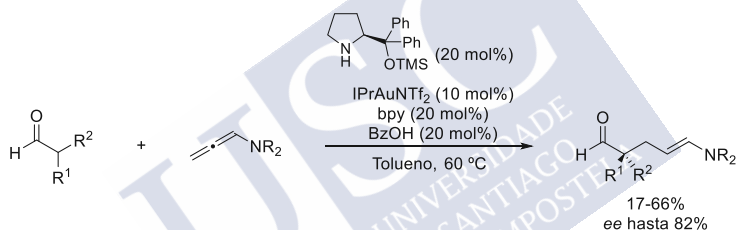
Además, también se evaluaron diferentes aldehídos α-monosustituidos derivados del fenilacetaldehído. En la versión asimétrica también se obtuvieron los aldehídos como mezclas *cis*:*trans* no reproducibles, por lo que fue necesario llevar a cabo la reducción *in situ* del producto al correspondiente alcohol, obteniéndose así un único isómero *trans* en la enamida. Para este tipo de aldehídos, se obtuvieron los correspondientes alcoholes con rendimientos entre el ochenta y uno por ciento y cuantitativos, independientemente del tipo de alenamida empleada. En cuanto a los excesos enantioméricos, cuando se usa la alenamida-oxazolidinona, se obtienen valores entre el diez y el cuarenta y cuatro por ciento. No obstante, se encontró que el uso de sulfonil-alenamidas genera los correspondientes alcoholes (en dónde se generó un centro terciario) con excesos enantioméricos de hasta el setenta y dos por ciento.
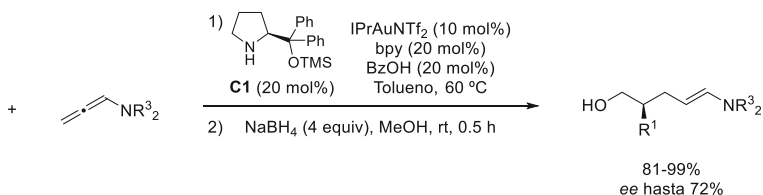
Por otro lado, se evaluó la posibilidad de usar un ligando quiral en el complejo de oro, que podría producir efectos de "match/mismatch" con el organocatalizador quiral, bien aumentando el exceso enantiomérico o bien disminuyéndolo. Para ello se probaron diferentes ligandos quirales del tipo carbeno *N*-heterocíclico, bisfosfinas y fosforamiditos de uso común en procesos asimétricos catalizados por oro. Para evaluar un posible efecto "match/mismatch" con el organocatalizador se probaron todos los ligandos con los dos enantiómeros del organocatalizador de Hayashi-Jørgensen. Se encontró que los mejores resultados de exceso enantiomérico fueron obtenidos con el uso de un ligando fosforamidito quiral derivado del VANOL con el enantiómero (*S*) del organocatalizador. Aún así, la eficiencia de este ligando quiral derivado del VANOL era la misma que cuando se empleaba un ligando racémico en el complejo de oro.

Además, durante la optimización de las condiciones racémicas, se observó que era necesaria la presencia de aditivos en el medio de reacción. Concretamente, el uso de 2,2'-bipiridina (bpy) resultó fundamental para obtener buenos resultados en la obtención de los productos. Se cree que el papel que juega la 2,2'-bipiridina es el de actuar como ligando, coordinándose al átomo de oro y evitando así una posible desactivación por parte de la amina secundaria (organocatalizador). Para ello se llevaron a cabo unas pruebas control de dimerización de la alenamida-oxazolidinona, además de experimentos de ESI-MS y experimentos de RMN de ^{31}P.

Se encontró que tanto la 2,2'-bipiridina como la amina secundaria, por separado, se coordinaban al catalizador Ph$_3$PAuNTf$_2$, formando sus correspondientes complejos de oro. Estos complejos fueron determinados por ESI-MS y RMN de ^{31}P y fueron probados en la dimerización catalizada por oro de la alenamida-oxazolidinona, en dónde se observó que el complejo formado por la amina secundaria no presentaba actividad catalítica, mientras que el complejo formado por la 2,2'-bipiridina mostraba una ligera actividad.

Además, cuando la amina secundaria está coordinada al átomo de oro, se encontró que ésta se puede desplazar en presencia de la 2,2'-bipiridina, recuperando así una especie activa de oro y evitando la desactivación en presencia de la amina secundaria.
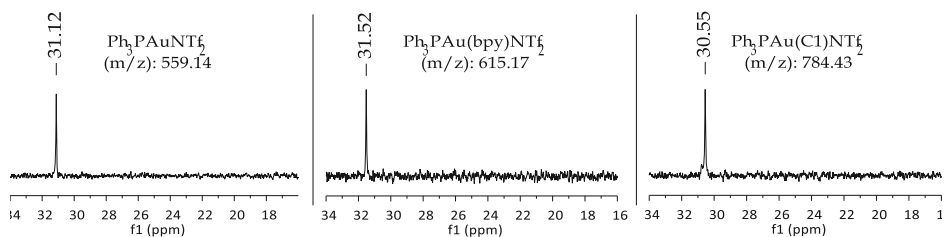
Cicloadiciones asimétricas intermoleculares (2+2+2) entre alenamidas y alquenil-oximas.

Experimental part

General procedures

Dry solvents were freshly distilled under argon from an appropriate drying agent according to Perrin[194] indications before its use. Toluene and dioxane were dried over Na; THF over Na/benzophenone; CH_2Cl_2, pyrrolidine, diisopropylamine and Et_3N over CaH_2. Other solvents such as CH_3CN, C_6H_6 and $C_6H_5CF_3$ were obtained commercially dry.

Reagents employed in the synthesis of starting materials were purchased from Aldrich, Alfa Aesar, TCI or Acros and used without further purification. Gold complexes were prepared according to previously reported methods[40, 75b, 195] or purchased from Aldrich. Chiral gold complexes (*R,R,R*)-Au4,[65] (*S,S,S*)-Au8,[61b] (*S,R,R*)-Au12,[165] (*S,S,S*)-Au12, [61b] (*S,R,R*)-Au13,[168] (*S,R,R*)-Au14,[168] (*R,R,R*)-Au14,[168] (*S,R,R*)-Au20,[65] (*R,R*)-Au21,[65] (*R,R,R*)-Au22,[61b] (*S,S,S*)-Au23,[65] (*R,R,R*)-Au24,[196] (*S,R,R*)-Au25,[197] (*S,S,S*)-Au25,[197] are known compounds and were synthesized from the corresponding phosphoramidite ligands following reported procedures. (*R*)-Au6,[85] Au9,[89] (*R,R*)-Au10,[89] (*S*)-Au11,[198] (*S*)-Au15,[198] (*S*)-Au16,[199] (*S*)-Au17,[200] (*R,R*)-Au18,[200] (*R,R,S,S*)-Au19[201] are known compounds and were prepared according well-established procedures.

The glassware used in the reactions was dried in an oven heating at 150 °C for 4 h, followed by cooling under argon atmosphere. Reactions were conducted in dry solvents under argon atmosphere unless otherwise stated. The abbreviation "rt" refers to reactions carried out approximately at 23 °C. Reaction mixtures were stirred using Teflon-coated magnetic stirring bars. For reactions at high temperatures, Thermowatch-

[194] D. Perrin, W. L. F. Armarego, *Purification of Laboratory Chemicals*, Butterworth-Heinemann, **2003**.

[40] H. Duan, S. Sengupta, J. L. Petersen, N. G. Akhmedov, X. Shi, *J. Am. Chem. Soc.* **2009**, *131*, 12100.

[75b] S. Suárez-Pantiga, C. Hernández-Díaz, M. Piedrafita, E. Rubio, J. M. González, *Adv. Synth. Catal.* **2012**, *354*, 1651.

[195] (a) P. de Frémont, N. Marion, S. P. Nolan, *J. Organomet. Chem.* **2009**, *694*, 551. (b) A. Leyva-Pérez, J. R. Cabrero-Antonino, Á. Cantín, A. Corma, *J. Org. Chem.* **2010**, *75*, 7769.

[65] I. Alonso, B. Trillo, F. López, S. Montserrat, G. Ujaque, L. Castedo, A. Lledós, J. L. Mascareñas, *J. Am. Chem. Soc.* **2009**, *131*, 13020.

[61b] A. Z. González, D. Benitez, E. Tkatchouk, W. A. Goddard, III, F. D. Toste, *J. Am. Chem. Soc.* **2011**, *133*, 5500.

[165] H. Faustino, I. Alonso, J. L. Mascareñas, F. López, *Angew. Chemie - Int. Ed.* **2013**, *52*, 6526.

[168] I. Varela, H. Faustino, E. Díez, J. Iglesias-Sigüenza, F. Grande-Carmona, R. Fernández, J. M. Lassaletta, J. L. Mascareñas, F. López, *ACS Catal.* **2017**, *7*, 2397.

[196] D. Qian, H. Hu, F. Liu, B. Tang, W. Ye, Y. Wang, J. Zhang, *Angew. Chemie - Int. Ed.* **2014**, *53*, 13751.

[197] G.-H. Li, W. Zhou, X.-X. Li, Q.-W. Bi, Z. Wang, Z.-G. Zhao, W.-X. Hu, Z. Chen, *Chem. Commun.* **2013**, *49*, 4770.

[85] A. Z. González, F. D. Toste, *Org. Lett.* **2010**, *12*, 200.

[89] J. Francos, F. Grande-carmona, H. Faustino, J. Iglesias-Sigüenza, E. Díez, I. Alonso, R. Fernández, J. M. Lassaletta, F. López, J. L. Mascareñas, *J. Am. Chem. Soc.* **2012**, *134*, 14322.

[198] A. D. Melhado, M. Luparia, F. D. Toste, *J. Am. Chem. Soc.* **2007**, *129*, 12638.

[199] S. Du Lee, J. C. Timmerman, R. A. Widenhoefer, *Adv. Synth. Catal.* **2014**, *356*, 3187.

[200] A. Pradal, C. Chao, M. R. Vitale, P. Y. Toullec, V. Michelet, *Tetrahedron* **2011**, *67*, 4371.

[201] M. Z. Wang, C. Y. Zhou, Z. Guo, E. L. M. Wong, M. K. Wong, C. M. Che, *Chem. - An Asian J.* **2011**, *6*, 812.

controlled silicone oil baths or aluminum heating plates were used. For reaction at low temperatures, ice baths (0 ºC) and ice/NaCl (-15 ºC) were used. The additions of solutions were carried out via syringe or cannula. The syringes used were plastic (Braun©) and Teflon (Hamilton©), with Sterican® (Braun ©) needles. Thin-layer chromatography (TLC) was performed on silica gel plates F_{254} Merck and components were visualized by observation under UV light (254 nm), and then by treating the plates with *p*-anisaldehyde or cerium nitrate solutions, followed by heating. Flash chromatography was carried out on silica gel 60 (40-63 µm) unless otherwise noted, and as eleunt a mixture of hexane/EtOAc (or diethyl ether) in varying proportion depending on the need. The solutions resulting from the elaboration of the different reactions were dried with anhydrous Na_2SO_4 or $MgSO_4$. Concentration refers to the removal of volatile solvents via distillation using a Büchi rotary evaporator followed by residual solvent removal under high vacuum.

NMR spectra were recorded in $CDCl_3$ unless otherwise noted, at spectrometers VARIAN Mercury-300 (300.13 MHz for ^1H and 75.47 MHz for ^{13}C), VARIAN innova-400 (399.97 MHz for ^1H and 100.58 MHz for ^{13}C) and VARIAN innova-500 or BRUKER DRX-500 (500.13 MHz for ^1H, 125.76 MHz for ^{13}C and 202 MHz for ^{31}P). Chemical shifts are expressed in δ (ppm) and coupling constants in Hz. Carbon types and structure assignments were determined from ^{13}C-DEPT-135. The following abbreviations are used to indicate signal multiplicity: s, singlet; d, doublet; t, triplet; q, quartet; dd, double doublet; ddd, doublet of doublet of doublets; td, triple doublet; dt, doublet of triplets; dq, doublet of quartet; m, multiplet; br, broad. NMR spectra were analyzed using MestreNova© NMR data processing software (www.mestrelab.com). Low Resolution Mass Spectra (LRMS) were recorded using the chemical ionization technique by a gas chromatography using an Agilent Technologies 6896N, Network GC System, equipped with the HP 190915-433 column and the Agilent 5976 Network Mass Selective Detector in the chemical ionization mode. For electrospray ionization (ESI), an UHPLC-Mass with Bruker AmaZon SL IT-MS detector was used. High Resolution Mass Spectra (HRMS) were carried out at the CACTUS facility of the University of Santiago de Compostela using a Bruker ESI-TOF BIOTOF II. For HPLC analysis, the samples were filtered through Whatman™ syringe filters (13 mm diameter nylon filter membrane, pore size 0.45 µm). Enantioselectivities were determined in an Agilent HPLC 1100 Series with Chiralpak® IA, IB, IC, IE, IF, IA3, OZ-H and AY-H analytical chiral columns.
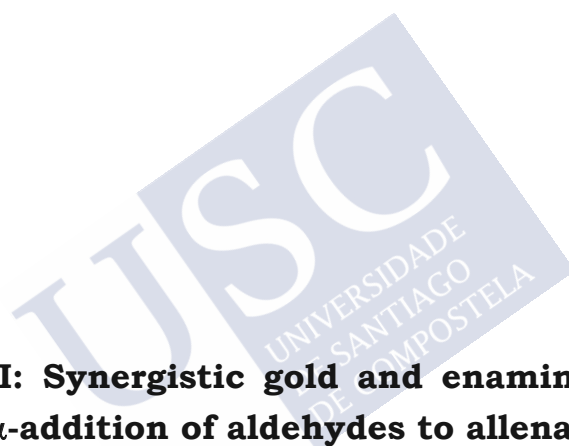
Chapter I: Synergistic gold and enamine catalysis for the α-addition of aldehydes to allenamides

1. General considerations

N-allenamides and allenes 3-(propa-1,2-dien-1-yl)oxazolidin-2-one (**17a**),[202] 3-(buta-1,2-dien-1-yl)oxazolidin-2-one (**17b**),[203] 1-(propa-1,2-dien-1-yl)pyrrolidin-2-one (**17c**),[202] 4-methyl-N-phenyl-N-(propa-1,2-dien-1-yl)benzenesulfonamide (**17d**),[75b] N-benzyl-4-methyl-N-(propa-1,2-dien-1-yl)benzenesulfonamide (**17e**),[75b] propa-1,2-diene-1,1-diyldibenzene (**17g**),[204] are known compounds and were synthesized following reported procedures. Allene 1-methoxypropa-1,2-diene (**17f**) is commercially available.

All aldehydes are known compounds and are commercially available or synthesized according to the reported procedures.[140]

Chiral organocatalysts **M1**, **M2**, **M3**, **M4**, **M5**, *L*-**Proline**, **C1**, **C4**, **C5**, **C10**, **C11**, **C12**, **C19**, **C20**, are commercially available. **C6**,[107a] **C7**,[107a] **C8**,[205], **C9**,[206] **C13**,[207] **C14**,[207] **C15**,[206] **C16**,[208] **C17**,[208] **C18**,[208] are known compounds and were synthesized according to the reported procedures.

Enamine **21**, derived from condensation of Hayashi-Jørgensen TMS-prolinol **(R)-C1** and 2-phenylacetaldehyde **18g**, was prepared according to a reported procedure.[209]

Chiral additive **(R,R)-bpy**[210] is a known compound and was synthesized according to a reported procedure. All other reagents used were purchased from Aldrich, Alfa Aesar, TCI or Acros and used without further purification.

[202] L.-L. Wei, J. A. Mulder, H. Xiong, C. A. Zificsak, C. J. Douglas, R. P. Hsung, *Tetrahedron* **2001**, *57*, 459.

[203] L. Shen, R. P. Hsung, Y. Zhang, J. E. Antoline, X. Zhang, *Org. Lett.* **2005**, *7*, 3081.

[75b] S. Suárez-Pantiga, C. Hernández-Díaz, M. Piedrafita, E. Rubio, J. M. González, *Adv. Synth. Catal.* **2012**, *354*, 1651.

[204] Z. Liu, P. Liao, X. Bi, *Chem. - A Eur. J.* **2014**, *20*, 17277.

[140] (a) S. Hoffmann, M. Nicoletti, B. List, *J. Am. Chem. Soc.* **2006**, *128*, 13074. (b) D. S. Ermolat'ev, J. B. Bariwal, H. P. L. Steenackers, S. C. J. De Keersmaecker, E. V. Van der Eycken, *Angew. Chemie Int. Ed.* **2010**, *49*, 9465. (c) P. S. Wang, H. C. Lin, Y. J. Zhai, Z. Y. Han, L. Z. Gong, *Angew. Chemie - Int. Ed.* **2014**, *53*, 12218. (d) P. Swamy, M. M. Reddy, M. Naresh, M. A. Kumar, K. Srujana, C. Durgaiah, N. Narender, *Adv. Synth. Catal.* **2015**, *357*, 1125.

[107a] Y. Hayashi, H. Gotoh, T. Hayashi, M. Shoji, *Angew. Chemie - Int. Ed.* **2005**, *44*, 4212.

[205] E. Gómez-Bengoa, A. Landa, A. Lizarraga, A. Mielgo, M. Oiarbide, C. Palomo, *Chem. Sci.* **2011**, *2*, 353.

[206] E. Gómez-Bengoa, J. Jiménez, I. Lapuerta, A. Mielgo, M. Oiarbide, I. Otazo, I. Velilla, S. Vera, C. Palomo, *Chem. Sci.* **2012**, *3*, 2949.

[207] C. Palomo, A. Landa, A. Mielgo, M. Oiarbide, Á. Puente, S. Vera, *Angew. Chemie - Int. Ed.* **2007**, *46*, 8431.

[208] D. Sánchez, D. Bastida, J. Burés, C. Isart, O. Pineda, J. Vilarrasa, *Org. Lett.* **2012**, *14*, 536.

[209] U. Grošelj, D. Seebach, D. M. Badine, W. B. Schweizer, A. K. Beck, I. Krossing, P. Klose, Y. Hayashi, T. Uchimaru, *Helv. Chim. Acta* **2009**, *92*, 1225.

[210] X. Gao, B. Wu, W. X. Huang, M. W. Chen, Y. G. Zhou, *Angew. Chemie - Int. Ed.* **2015**, *54*, 11956.

2. Representative procedure for the racemic α-alkylation of aldehydes with allenamides

*Procedure A: exemplified for the reaction between **17a** and **18a**.*

To a solution of Ph₃PAuNTf₂ (2:1) toluene adduct (12.55 mg, 0.008 mmol), 2,2′-bipyridine (4.99 mg, 0.032 mmol) and benzoic acid (3.90 mg, 0.032 mmol) in Toluene (0.5 ml), was sequentially added a solution of 2-phenylpropanal (**18a**, 42.8 µl, 0.320 mmol) and pyrrolidine (3.97 µl, 0.048 mmol) in Toluene (0.5 ml), followed by addition of a solution of 3-(propa-1,2-dien-1-yl)oxazolidin-2-one (**17a**, 20 mg, 0.160 mmol) in Toluene (0.5 ml; dropwise addition), under Argon atmosphere, in a dried Schlenk tube at 60 °C. The mixture was stirred at that temperature until the allenamide was consumed (the progress of the reaction was easily monitored by tlc) and filtered through a short pad of Florisil®, eluting with EtOAc. The solvent was removed, and the crude residue was dissolved in 0.6 ml of a 1,3,5-trimethoxybenzene 0.0887 M solution in CDCl₃ for ¹H-NMR analysis. The crude mixture was then purified on column chromatography (hexanes/EtOAc 10-40%), affording 34.4 mg of **19aa** (83% yield).

*Procedure B: exemplified for the reaction between **17a** and **18g**.*

To a solution of Ph₃PAuNTf₂ (2:1) toluene adduct (12.55 mg, 0.008 mmol), 2,2′-bipyridine (4.99 mg, 0.032 mmol) and benzoic acid (3.90 mg, 0.032 mmol) in Toluene (0.5 ml), was sequentially added a solution of 2-phenylacetaldehyde (**18g**, 37.4 µl, 0.320 mmol) and pyrrolidine (3.97 µl, 0.048 mmol) in Toluene (0.5 ml), followed by addition of a solution of 3-(propa-1,2-dien-1-yl)oxazolidin-2-one (**17a**, 20 mg, 0.160 mmol) in Toluene (0.5 ml; dropwise addition), under Argon atmosphere, in a dried Schlenk tube at 60 °C. The mixture was stirred at that temperature until the allenamide was consumed (the progress of the reaction was easily monitored by tlc). The reaction is quenched by the addition of a solution of NaBH₄ (24.21 mg, 0.64 mmol) in MeOH (2 ml), stirred for 0.5 hours and filtered through a short pad of Florisil®, eluting with EtOAc. The solvent was

removed, and the crude residue was dissolved in 0.6 ml of a 1,3,5-trimethoxybenzene 0.0887 M solution in CDCl$_3$ for ^{1}H-NMR analysis. The crude mixture was then purified on column chromatography (hexanes/EtOAc 10-40%), affording 39.2 mg of **20ag** (>99% yield).

(*E*)-2-methyl-5-(2-oxooxazolidin-3-yl)-2-phenylpent-4-enal (19aa)
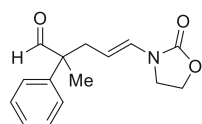
Procedure A: colorless oil, 83% yield. **^{1}H-NMR** (300 MHz, CDCl$_3$) δ (ppm): 9.51 (s, 1H), 7.46 – 7.20 (m, 5H), 6.64 (d, J = 14.3 Hz, 1H), 4.50 (dt, J = 14.3, 7.6 Hz, 1H), 4.42 – 4.30 (m, 2H), 3.63 – 3.47 (m, 2H), 2.64 (d, J = 7.6 Hz, 1H), 1.43 (s, 3H). **^{13}C-NMR** (75 MHz, CDCl$_3$) δ (ppm): 201.97 (CH), 155.33 (C), 139.37 (C), 129.03 (CH), 127.55 (CH), 127.12 (CH), 126.67 (CH), 105.19 (CH), 62.18 (CH$_2$), 54.13 (C), 42.58 (CH$_2$), 36.99 (CH$_2$), 18.90 (CH$_3$). **LRMS** (*m/z*, ESI): 282.11 [M+Na]$^+$, 258.11, 201.04, 126.05. **HRMS** Calculated for C$_{15}$H$_{17}$NNaO$_3$: 282.1101, found 282.1103.

(*E*)-2-(4-methoxyphenyl)-2-methyl-5-(2-oxooxazolidin-3-yl)pent-4-enal (19ab)
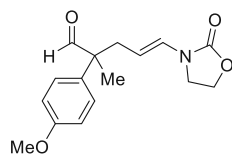
Procedure A: colorless oil, 75% yield. **^{1}H-NMR** (300 MHz, CDCl$_3$) δ (ppm): 9.46 (s, 1H), 7.15 (d, J = 8.9 Hz, 2H), 6.91 (d, J = 8.9 Hz, 2H), 6.65 (d, J = 14.3 Hz, 1H), 4.59 – 4.42 (m, 1H), 4.45 – 4.29 (m, 2H), 3.81 (s, 3H), 3.64 – 3.50 (m, 2H), 2.62 (d, J = 6.7 Hz, 2H), 1.41 (s, 3H). **^{13}C-NMR** (75 MHz, CDCl$_3$) δ (ppm): 201.93 (CH), 159.01 (C), 155.39 (C), 131.15 (C), 128.35 (CH), 126.66 (CH), 114.50 (CH), 105.44 (CH), 62.21 (CH$_2$), 55.42 (CH$_3$), 53.48 (C), 42.67 (CH$_2$), 37.03 (CH$_2$), 19.02 (CH$_3$). **LRMS** (*m/z*, ESI): 312.12 [M+Na]$^+$, 185.09, 175.10, 159.08, 144.05, 126.05. **HRMS** Calculated for C$_{16}$H$_{19}$NNaO$_4$: 312.1206, found 312.1210.

### (*E*)-3-(4-(4-fluorophenyl)-5-hydroxy-4-methylpent-1-en-1-yl)oxazolidin-2-one (20ac)
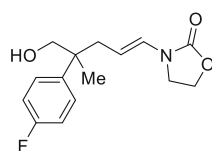
Procedure B: colorless oil, 40% yield. **^{1}H-NMR** (300 MHz, CDCl$_3$) δ (ppm): 7.37 – 7.27 (m, 2H), 7.03 (t, J = 8.8 Hz, 2H), 6.65 (d, J = 14.3 Hz, 1H), 4.48 (ddd, J = 14.3, 8.1, 6.9 Hz, 1H), 4.42 – 4.30 (m, 2H), 3.72 (d, J = 10.9 Hz, 1H), 3.63 – 3.47 (m, 3H), 2.61 – 2.47 (m, 1H), 2.34 (ddd, J = 14.1, 8.2, 1.1 Hz, 1H), 1.59 (br, 1H), 1.31 (s, 3H). **^{13}C-NMR** (75 MHz, CDCl$_3$) δ (ppm): 161.49 (d, J = 245.6 Hz, C), 155.43 (C), 140.25 (C), 128.39 (d, J = 7.8 Hz, CH), 126.20 (CH), 115.39 (d, J = 20.8 Hz, CH), 106.12 (CH), 71.69 (CH$_2$), 62.19 (CH$_2$), 43.34 (C), 42.69 (CH$_2$), 39.16 (CH$_2$), 22.17 (CH$_3$). **LRMS** (*m/z*, ESI): 302.11 [M+Na]$^+$, 193.10, 175.09, 149.08. **HRMS** Calculated for C$_{15}$H$_{18}$FNNaO$_3$: 302.1163, found 302.1169.

(*E*)-3-(4-(3-chlorophenyl)-5-hydroxy-4-methylpent-1-en-1-yl)oxazolidin-2-one (20ad)
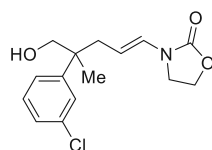
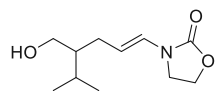Procedure B: colorless oil, 43% yield. **^{1}H-NMR** (300 MHz, CDCl$_3$) δ (ppm): 7.36 – 7.28 (m, 1H), 7.30 – 7.19 (m, 3H), 6.66 (d, J = 14.2 Hz, 1H), 4.47 (ddd, J = 14.2, 8.3, 7.0 Hz, 1H), 4.44 – 4.32 (m, 2H), 3.77 –

3.70 (m, 1H), 3.65 – 3.52 (m, 3H), 2.54 (ddd, *J* = 14.1, 6.9, 1.3 Hz, 1H), 2.34 (ddd, *J* = 14.1, 8.3, 1.1 Hz, 1H), 1.31 (s, 3H). **^{13}C-NMR** (75 MHz, CDCl$_3$) δ (ppm): 155.43 (C), 147.02 (C), 129.89 (CH), 127.25 (CH), 126.75 (CH), 126.37 (CH), 125.01 (CH), 105.86 (CH), 71.42 (CH$_2$), 62.21 (CH$_2$), 43.84 (C), 42.70 (CH$_2$), 38.99 (CH$_2$), 21.97 (CH$_3$). **LRMS** (*m/z*, ESI): 320.08, 318.08 [M+Na]$^+$, 209.07, 191.06, 165.04, 125.02 **HRMS** Calculated for C$_{15}$H$_{18}$ClNNaO$_3$: 318.0867, found 318.0867.

(*E*)-2-methyl-5-(2-oxooxazolidin-3-yl)-2-(5,6,7,8-tetrahydronaphthalen-2-yl)pent-4-enal (19af)
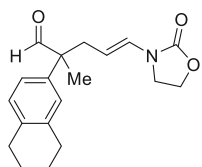
Procedure A: colorless oil, 47% yield. **^{1}H-NMR** (300 MHz, CDCl$_3$) δ (ppm): 9.47 (s, 1H), 7.08 (d, *J* = 8.0 Hz, 1H), 6.95 (dd, *J* = 8.0, 2.1 Hz, 1H), 6.90 (s, 1H), 6.66 (d, *J* = 14.3 Hz, 1H), 4.56 (dt, *J* = 14.3, 7.6 Hz, 1H), 4.44 – 4.32 (m, 2H), 3.66 – 3.49 (m, 2H), 2.80 – 2.70 (m, 4H), 2.63 (ddd, *J* = 7.3, 6.0, 1.2 Hz, 2H), 1.85 – 1.74 (m, 4H), 1.40 (s, 3H). **^{13}C-NMR** (75 MHz, CDCl$_3$) δ (ppm): 202.13 (CH), 155.39 (C), 137.89 (C), 136.67 (C), 136.40 (C), 129.83 (CH), 127.87 (CH), 126.60 (CH), 124.17 (CH), 105.62 (CH), 62.22 (CH$_2$), 53.78 (CH), 42.71 (CH$_2$), 36.92 (CH$_2$), 30.46 (C), 29.70 (CH$_2$), 29.09 (CH$_2$), 23.22 (CH$_2$), 18.99 (CH$_3$). **LRMS** (*m/z*, ESI): 336.15 [M+Na]$^+$, 209.13, 199.12, 149.05, 141.07. **HRMS** Calculated for C$_{19}$H$_{23}$NNaO$_3$: 336.1570, found 336.1575.

(*E*)-3-(5-hydroxy-4-phenylpent-1-en-1-yl)oxazolidin-2-one (20ag)
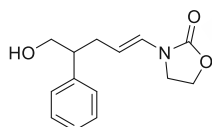
Procedure B: colorless oil, 98% yield. **^{1}H-NMR** (300 MHz, CDCl$_3$) δ (ppm): 7.36 – 7.16 (m, 5H), 6.64 (d, *J* = 14.3 Hz, 1H), 4.66 (dt, *J* = 14.8, 7.4 Hz, 1H), 4.36 (t, *J* = 8.3 Hz, 2H), 3.86 – 3.67 (m, 2H), 3.56 (t, *J* = 8.7 Hz, 2H), 2.83 (dt, *J* = 13.2, 6.8 Hz, 1H), 2.51 (ddd, *J* = 14.3, 7.8, 6.5 Hz, 1H), 2.47 – 2.30 (m, 1H), 1.58 (br s, 1H). **^{13}C-NMR** (75 MHz, CDCl$_3$) δ (ppm): 155.47 (C), 141.72 (C), 128.81 (CH), 128.09 (CH), 127.01 (CH), 125.24 (CH), 108.57 (CH), 66.83 (CH$_2$), 62.21 (CH$_2$), 49.24 (CH), 42.64 (CH$_2$), 32.70 (CH$_2$). **LRMS** (*m/z*, ESI): 270.10 [M+Na]$^+$, 236.14, 230.11, 143.08. **HRMS** Calculated for C$_{14}$H$_{17}$NNaO$_3$: 270.1101, found 270.1100.

(*E*)-3-(5-hydroxy-4-(p-tolyl)pent-1-en-1-yl)oxazolidin-2-one (20ah)
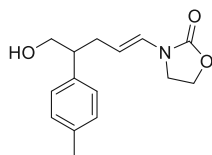
Procedure B: colorless oil, 99% yield. **^{1}H NMR** (300 MHz, CDCl$_3$) δ (ppm): 7.13 (d, *J* = 8.5 Hz, 2H), 7.07 (d, *J* = 8.2 Hz, 2H), 6.63 (d, *J* = 14.3 Hz, 1H), 4.74 – 4.58 (m, 1H), 4.36 (t, *J* = 8.3 Hz, 2H), 3.81 – 3.64 (m, 2H), 3.57 (td, *J* = 7.8, 1.9 Hz, 2H), 2.88 – 2.70 (m, 1H), 2.59 – 2.40 (m, 1H), 2.44 – 2.32 (m, 1H), 2.32 (s, 3H), 1.62 (br, 1H). **^{13}C NMR** (75 MHz, CDCl$_3$) δ (ppm): 155.48 (C), 138.54 (C), 136.51 (C), 129.50 (CH), 127.93 (CH), 125.12 (CH), 108.73 (CH), 66.89 (CH$_2$), 62.20 (CH$_2$), 48.79 (CH), 42.65 (CH$_2$), 32.74 (CH$_2$), 21.12 (CH$_3$). **LRMS** (m/z, ESI): 284.12 [M+Na]$^+$, 175.11, 157.10, 142.07, 131.08. **HRMS** Calculated for C$_{15}$H$_{19}$NNaO$_3$: 284.1257, found 284.1257.

(*E*)-3-(5-hydroxy-4-(4-methoxyphenyl)pent-1-en-1-yl)oxazolidin-2-one (20ai)
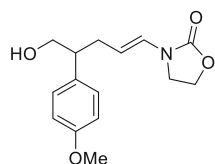
Procedure B: colorless oil, 99% yield. **¹H-NMR** (300 MHz, CDCl₃) δ (ppm): 7.11 (d, *J* = 8.6 Hz, 2H), 6.87 (d, *J* = 8.8 Hz, 2H), 6.64 (d, *J* = 14.3 Hz, 1H), 4.65 (dt, *J* = 14.4, 7.4 Hz, 1H), 4.37 (t, *J* = 8.2 Hz, 2H), 3.79 (s, 3H), 3.81 – 3.63 (m, 2H), 3.64 – 3.41 (m, 2H), 2.79 (p, *J* = 6.8 Hz, 1H), 2.56 – 2.39 (m, 1H), 2.43 – 2.26 (m, 1H), 1.45 (br s, 1H). **¹³C-NMR** (75 MHz, CDCl₃) δ (ppm): 158.64 (C), 155.45 (C), 133.52 (C), 129.03 (CH), 125.23 (CH), 114.29 (CH), 108.63 (CH), 67.05 (CH₂), 62.19 (CH₂), 55.38 (CH₃), 48.45 (CH), 42.67 (CH₂), 32.88 (CH₂). **LRMS** (*m/z*, ESI): 300.12 [M+Na]⁺, 173.09, 158.08, 147.08, 121.06. **HRMS** Calculated for C₁₅H₁₉NNaO₄: 300.1206, found 300.1206.

(*E*)-3-(4-(4-fluorophenyl)-5-hydroxypent-1-en-1-yl)oxazolidin-2-one (20aj)
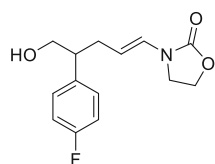
Procedure B: colorless oil, 99% yield. **¹H-NMR** (300 MHz, CDCl₃) δ (ppm): 7.19 – 7.10 (m, 2H), 7.05 – 6.96 (m, 2H), 6.63 (d, *J* = 14.3 Hz, 1H), 4.62 (ddd, *J* = 14.5, 7.8, 6.9 Hz, 1H), 4.37 (t, *J* = 8.2 Hz, 2H), 3.85 – 3.66 (m, 2H), 3.66 – 3.47 (m, 2H), 2.81 (dq, *J* = 8.4, 6.4 Hz, 1H), 2.50 (dddd, *J* = 14.2, 7.7, 6.3, 1.2 Hz, 1H), 2.34 (dddd, *J* = 14.3, 8.4, 6.9, 1.4 Hz, 1H), 1.68 (br, 1H). **¹³C-NMR** (75 MHz, CDCl₃) δ (ppm): 161.70 (d, *J* = 244.6 Hz, C), 155.33 (C), 137.34 (d, *J* = 3.5 Hz, C), 129.35 (d, *J* = 7.9 Hz, CH), 125.25 (CH), 115.45 (d, *J* = 21.1 Hz, CH), 108.15 (CH), 66.62 (CH₂), 62.09 (CH₂), 48.35 (CH), 42.50 (CH₂), 32.66 (CH₂). **¹⁹F-NMR** (282 MHz, CDCl₃) δ (ppm): -116.14. **LRMS** (*m/z*, ESI): 288.10 [M+Na]⁺, 279.09, 135.06, 109.04 **HRMS** Calculated for C₁₄H₁₆FNNaO₃: 288.1006, found 288.1008.

(*E*)-3-(4-(3-chlorophenyl)-5-hydroxypent-1-en-1-yl)oxazolidin-2-one (20ak)
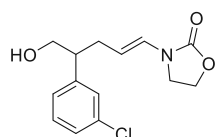
Procedure B: colorless oil, 99% yield. **¹H-NMR** (300 MHz, CDCl₃) δ (ppm): 7.29 – 7.14 (m, 3H), 7.13 – 7.03 (m, 1H), 6.63 (d, *J* = 14.3 Hz, 1H), 4.62 (dt, *J* = 14.5, 7.3 Hz, 1H), 4.37 (t, *J* = 8.4 Hz, 2H), 3.84 – 3.65 (m, 2H), 3.63 – 3.50 (m, 2H), 2.88 – 2.71 (m, 1H), 2.58 – 2.41 (m, 1H), 2.43 – 2.26 (m, 1H), 1.87 (br, 1H). **¹³C-NMR** (75 MHz, CDCl₃) δ (ppm): 155.39 (C), 144.04 (C), 134.38 (C), 129.89 (CH), 128.15 (CH), 126.99 (CH), 126.16 (CH), 125.34 (CH), 108.00 (CH), 66.26 (CH₂), 62.15 (CH₂), 48.85 (CH), 42.52 (CH₂), 32.43 (CH₂). **LRMS** (*m/z*, ESI): 306.06, 304.07 [M+Na]⁺, 151.03, 125.01. **HRMS** Calculated for C₁₄H₁₆ClNNaO₃: 304.0711, found 304.0712.

(*E*)-3-(4-benzyl-5-hydroxypent-1-en-1-yl)oxazolidin-2-one (20am)
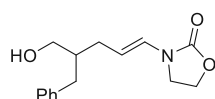
Procedure B: colorless oil, 12% yield. **¹H-NMR** (300 MHz, CDCl₃) δ (ppm): 7.36 – 7.12 (m, 5H), 6.67 (d, J = 14.3 Hz, 1H), 4.84 – 4.67 (m, 1H), 4.42 (dd, J = 8.5, 7.7 Hz, 2H), 3.64 (td, J = 7.7, 1.7 Hz, 2H), 3.59 – 3.52 (m, 2H), 2.64 (qd, J = 13.7, 7.2 Hz, 2H), 2.27 – 2.01 (m, 2H), 1.99 – 1.79 (m, 1H), 1.25 (s, 1H). **¹³C-NMR** (75 MHz, CDCl₃) δ (ppm): 155.48 (C), 140.55 (C), 129.28 (CH), 128.54 (CH), 126.16 (CH), 125.42 (CH), 108.85 (CH), 64.75 (CH₂), 62.25 (CH₂), 43.39 (CH),

42.74 (CH$_2$), 37.54 (CH$_2$), 31.53 (CH$_2$). **LRMS** (*m/z*, ESI): 284.12 [M+Na]$^+$, 273.08, 236.14. **HRMS** Calculated for C$_{15}$H$_{19}$NNaO$_3$: 284.1257, found 284.1258.

(*E*)-3-(4-(hydroxymethyl)-5-methylhex-1-en-1-yl)oxazolidin-2-one (20an)

Procedure B: colorless oil, 31% yield. **^{1}H-NMR** (300 MHz, CDCl$_3$) δ (ppm): 6.68 (d, *J* = 14.4 Hz, 1H), 4.81 (dt, *J* = 14.5, 7.5 Hz, 1H), 4.52 – 4.36 (m, 2H), 3.80 – 3.48 (m, 4H), 2.26 – 1.93 (m, 2H), 1.86 – 1.72 (m, 1H), 1.61 (br, 1H), 1.46 – 1.33 (m, 1H), 0.92 (d, *J* = 6.9 Hz, 6H). **^{13}C-NMR** (75 MHz, CDCl$_3$) δ (ppm): 155.53 (C), 124.93 (CH), 109.97 (CH), 63.52 (CH$_2$), 62.25 (CH$_2$), 47.45 (CH), 42.80 (CH$_2$), 28.85 (CH$_2$), 27.96 (CH), 19.86 (CH$_3$), 19.73 (CH$_3$). **LRMS** (*m/z*, ESI): 236.12 [M+Na]$^+$, 220.15, 201.04, 157.07, 127.11, 109.10. **HRMS** Calculated for C$_{11}$H$_{19}$NNaO$_3$: 236.1257, found 236.1257.

(E)-2-methyl-5-(2-oxopyrrolidin-1-yl)-2-phenylpent-4-enal (19ca)
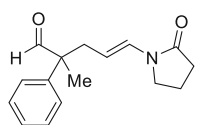
Procedure A: colorless oil, 52% yield. **^{1}H-NMR** (500 MHz, CDCl$_3$) δ (ppm): 9.51 (s, 1H), 7.40 – 7.35 (m, 2H), 7.31 – 7.27 (m, 1H), 7.23 (dd, *J* = 8.3, 1.3 Hz, 2H), 6.88 (d, *J* = 14.4 Hz, 1H), 4.62 (dt, *J* = 14.7, 7.6 Hz, 1H), 3.39 – 3.33 (m, 2H), 2.66 (dd, *J* = 7.5, 1.2 Hz, 2H), 2.48 – 2.41 (m, 2H), 2.09 – 1.99 (m, 2H), 1.43 (s, 3H). **^{13}C-NMR** (126 MHz, CDCl$_3$) δ (ppm): 202.12 (CH), 173.04 (C), 139.57 (C), 129.04 (CH), 127.53 (CH), 127.17 (CH), 126.48 (CH), 106.22 (CH), 54.20 (C), 45.31 (CH$_2$), 37.30 (CH$_2$), 31.29 (CH$_2$), 19.01 (CH$_3$), 17.44 (CH$_2$). **LRMS** (*m/z*, ESI): 280.13 [M+Na]$^+$, 230.13, 147.06, 124.07. **HRMS** Calculated for C$_{16}$H$_{19}$NNaO$_2$: 280.1308, found 280.1311.

(*E*)-N-(5-hydroxy-4-methyl-4-phenylpent-1-en-1-yl)-4-methyl-N-phenylbenzenesulfonamide (20da)
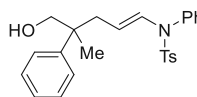
Procedure B: colorless oil, 47% yield. **^{1}H-NMR** (300 MHz, CDCl$_3$) δ (ppm): 7.42 (d, *J* = 8.3 Hz, 2H), 7.34 – 7.12 (m, 10H), 6.89 – 6.70 (m, 3H), 4.20 (dt, *J* = 14.0, 7.8 Hz, 1H), 3.68 (d, *J* = 10.9 Hz, 1H), 3.51 (d, *J* = 10.9 Hz, 1H), 2.44 (s, 3H), 2.31 (qdd, *J* = 13.8, 7.8, 1.2 Hz, 2H), 1.57 (br s, 1H), 1.20 (s, 3H). **^{13}C-NMR** (75 MHz, CDCl$_3$) δ (ppm): 144.53 (C), 143.80 (C), 137.03 (C), 136.00 (C), 131.13 (CH), 130.04 (CH), 129.65 (CH), 129.40 (CH), 128.85 (CH), 128.53 (CH), 127.55 (CH), 126.68 (CH), 126.34 (CH), 108.35 (CH), 71.35 (CH$_2$), 43.95 (C), 39.27 (CH$_2$), 21.81 (CH$_3$), 21.75 (CH$_3$). **LRMS** (*m/z*, ESI): 422.17 [M+H]$^+$, 266.14, 157.07. **HRMS** Calculated for C$_{25}$H$_{28}$NO$_3$S: 422.1784, found 422.1786.
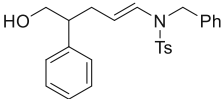
(*E*)-N-benzyl-N-(5-hydroxy-4-methyl-4-phenylpent-1-en-1-yl)-4-methylbenzenesulfonamide (20ea)
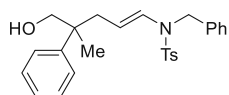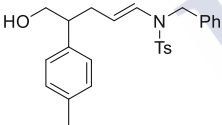
Procedure B: colorless oil, 51% yield. **^{1}H-NMR** (500 MHz, CDCl$_3$) δ (ppm): 7.62 (d, *J* = 8.2 Hz, 2H), 7.33 – 7.24 (m, 7H), 7.24 – 7.17 (m, 1H), 7.17 – 7.06 (m, 4H), 6.59 (d, *J* = 14.2 Hz, 1H), 4.48 – 4.38 (m, 2H), 4.31 (d, *J* = 15.6 Hz, 1H), 3.55 (d, *J* = 10.9 Hz, 1H), 3.41 (d, *J* = 10.9 Hz, 1H), 2.45

(s, 3H), 2.36 (ddd, *J* = 13.9, 7.1, 1.2 Hz, 1H), 2.20 (ddd, *J* = 13.9, 8.1, 1.0 Hz, 1H), 1.13 (br s, 1H), 1.05 (s, 3H). **¹³C-NMR** (126 MHz, CDCl₃) δ (ppm): 144.30 (C), 143.80 (C), 136.04 (C), 135.54 (C), 129.90 (CH), 128.64 (CH), 128.51 (CH), 127.47 (CH), 127.41 (CH), 127.15 (CH), 127.04 (CH), 126.64 (CH), 126.27 (CH), 109.50 (CH), 71.26 (CH₂), 49.45 (CH₂), 43.64 (C), 39.75 (CH₂), 21.70 (CH₃), 21.59 (CH₃). **LRMS** (*m/z*, ESI): 458.17 [M+Na]⁺, 168.05. **HRMS** Calculated for C₂₆H₂₉NNaO₃S: 458.1760, found 458.1768.
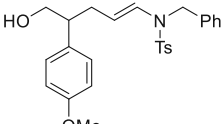
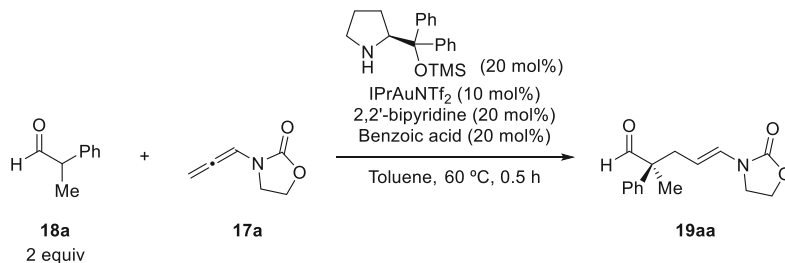### (*E*)-N-benzyl-N-(5-hydroxy-4-phenylpent-1-en-1-yl)-4-methylbenzenesulfonamide (20eg)

Procedure B: colorless oil, 99% yield. **¹H-NMR** (300 MHz, CDCl₃) δ (ppm): 7.55 (d, *J* = 8.3 Hz, 2H), 7.29 – 7.21 (m, 8H), 7.19 – 7.14 (m, 2H), 6.99 – 6.92 (m, 2H), 6.60 (d, *J* = 14.1 Hz, 1H), 4.55 (dt, *J* = 14.4, 7.3 Hz, 1H), 4.37 (d, *J* = 3.2 Hz, 2H), 3.58 (s, 2H), 2.69 – 2.56 (m, 1H), 2.43 (s, 3H), 2.39 – 2.28 (m, 1H), 2.30 – 2.13 (m, 1H), 1.26 (br, 1H). **¹³C-NMR** (75 MHz, CDCl₃) δ (ppm): 143.75 (C), 141.52 (C), 136.07 (C), 135.62 (C), 129.89 (CH), 128.70 (CH), 128.63 (CH), 128.07 (CH), 127.46 (CH), 127.08 (CH), 127.00 (CH), 126.79 (CH), 110.76 (CH), 66.49 (CH₂), 49.50 (CH₂), 48.96 (CH), 33.31 (CH₂), 21.68 (CH₃). **LRMS** (*m/z*, ESI): 422.17 [M+H]⁺, 300.10, 279.08. **HRMS** Calculated for C₂₅H₂₈NO₃S: 422.1784, found 422.1787.

(*E*)-N-benzyl-N-(5-hydroxy-4-(p-tolyl)pent-1-en-1-yl)-4-methylbenzenesulfonamide (20eh)

Procedure B: colorless oil, 99% yield. **¹H-NMR** (300 MHz, CDCl₃) δ (ppm): 7.56 (d, *J* = 8.3 Hz, 2H), 7.31 – 7.22 (m, 5H), 7.20 – 7.13 (m, 2H), 7.06 (d, *J* = 7.6 Hz, 2H), 6.85 (d, *J* = 8.0 Hz, 2H), 6.60 (d, *J* = 14.2 Hz, 1H), 4.57 (dt, *J* = 14.5, 7.4 Hz, 1H), 4.38 (d, *J* = 3.0 Hz, 2H), 3.56 (d, *J* = 6.7 Hz, 2H), 2.68 – 2.49 (m, 1H), 2.43 (s, 3H), 2.33 (s, 3H), 2.41 – 2.26 (m, 1H), 2.32 – 2.12 (m, 1H), 1.27 (s, 1H). **¹³C-NMR** (75 MHz, CDCl₃) δ (ppm): 143.72 (C), 138.37 (C), 136.23 (C), 136.06 (C), 135.61 (C), 129.85 (CH), 129.39 (CH), 128.59 (CH), 127.92 (CH), 127.44 (CH), 127.09 (CH), 127.02 (CH), 127.00 (CH), 110.98 (CH), 66.57 (CH₂), 49.47 (CH₂), 48.50 (CH), 33.30 (CH₂), 21.67 (CH₃), 21.17 (CH₃). **LRMS** (*m/z*, ESI): 458.17 [M+Na]⁺, 436.19 [M+H]⁺, 300.10. **HRMS** Calculated for C₂₆H₂₉NNaO₃S: 458.1760, found 458.1766.
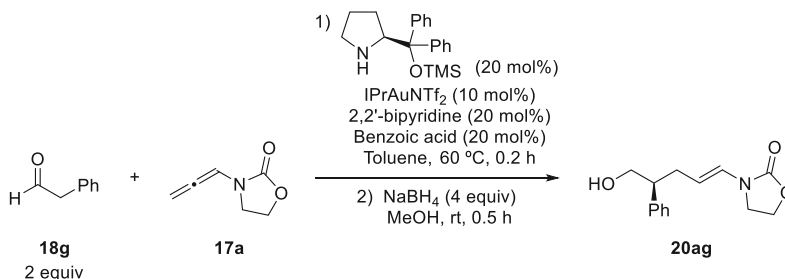
(*E*)-N-benzyl-N-(5-hydroxy-4-(4-methoxyphenyl)pent-1-en-1-yl)-4-methylbenzenesulfonamide (20ei)

Procedure B: colorless oil, 99% yield. **¹H-NMR** (500 MHz, CDCl₃) δ (ppm): 7.57 (d, *J* = 8.2 Hz, 2H), 7.30 – 7.25 (m, 5H), 7.19 (d, *J* = 6.0 Hz, 2H), 6.89 (d, *J* = 8.6 Hz, 2H), 6.84 – 6.78 (m, 2H), 6.61 (d, *J* = 14.5 Hz, 1H), 4.57 (dt, *J* = 14.4, 7.3 Hz, 1H), 4.39 (q, *J* = 15.8 Hz, 2H), 3.82 (s, 3H), 3.57 (dd, *J* = 6.9, 2.6 Hz, 2H), 2.66 – 2.55 (m, 1H), 2.44 (s, 3H), 2.40 – 2.28 (m, 1H), 2.20 (dt, *J* = 15.2, 8.0 Hz, 1H), 1.25 (d, *J* = 6.9 Hz, 1H). **¹³C-NMR** (126 MHz,

CDCl₃) δ (ppm): 158.36 (C), 143.73 (C), 136.01 (C), 135.61 (C), 133.36 (C), 129.85 (CH), 128.97 (CH), 128.58 (CH), 127.41 (CH), 127.05 (CH), 126.99 (CH), 126.95 (CH), 114.08 (CH), 110.83 (CH), 66.61 (CH₂), 55.31 (CH₃), 49.42 (CH₂), 48.08 (CH), 33.40 (CH₂), 21.65 (CH₃). **LRMS** (*m/z*, ESI): 474.17 [M+Na]⁺, 452.18 [M+H]⁺, 353.26 **HRMS** Calculated for C₂₆H₃₀NO₄S: 452.1890, found 452.1892.

(*E*)-N-benzyl-N-(4-(4-fluorophenyl)-5-hydroxypent-1-en-1-yl)-4-methylbenzenesulfonamide (20ej)
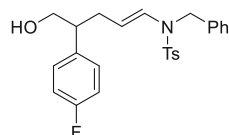
Procedure B: colorless , 99% yield. **¹H-NMR** (300 MHz, CDCl₃) δ (ppm): 7.55 (d, *J* = 8.3 Hz, 2H), 7.34 – 7.18 (m, 5H), 7.18 – 7.10 (m, 2H), 7.03 – 6.80 (m, 4H), 6.57 (d, *J* = 14.2 Hz, 1H), 4.57 – 4.41 (m, 1H), 4.45 – 4.27 (m, 2H), 3.57 (dd, *J* = 6.8, 1.2 Hz, 2H), 2.69 – 2.51 (m, 1H), 2.43 (s, 3H), 2.40 – 2.30 (m, 1H), 2.30 – 2.07 (m, 1H), 1.26 (s, 1H). **¹³C-NMR** (75 MHz, CDCl₃) δ (ppm): 161.67 (d, *J* = 244.4 Hz, C), 143.87 (C), 137.15 (d, *J* = 3.3 Hz, C), 136.03 (C), 135.58 (C), 129.90 (CH), 129.45 (d, *J* = 7.9 Hz, CH), 128.63 (CH), 127.48 (CH), 127.20 (CH), 127.00 (CH), 126.96 (CH), 115.42 (d, *J* = 21.0 Hz, CH), 110.25 (CH), 66.45 (CH₂), 49.48 (CH₂), 48.25 (CH), 33.44 (CH₂), 21.66 (CH₃). **¹⁹F-NMR** (282 MHz, CDCl₃) δ (ppm): -116.31. **LRMS** (*m/z*, ESI): 462.15 [M+Na]⁺, 440.16 [M+H]⁺, 420.14, 300.10. **HRMS** Calculated for C₂₅H₂₇FNO₃S: 440.1690, found 440.1680.

(*E*)-N-benzyl-N-(4-(3-chlorophenyl)-5-hydroxypent-1-en-1-yl)-4-methylbenzenesulfonamide (20ek)
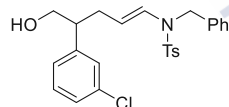
Procedure B: colorless oil, 99% yield. **¹H-NMR** (300 MHz, CDCl₃) δ (ppm): 7.56 (d, *J* = 8.3 Hz, 2H), 7.32 – 7.11 (m, 9H), 6.99 (s, 1H), 6.82 (dt, *J* = 6.3, 1.9 Hz, 1H), 6.59 (d, *J* = 14.2 Hz, 1H), 4.58 – 4.42 (m, 1H), 4.43 – 4.28 (m, 2H), 3.56 (d, *J* = 6.6 Hz, 2H), 2.67 – 2.51 (m, 1H), 2.43 (s, 3H), 2.39 – 2.27 (m, 1H), 2.26 – 2.12 (m, 1H), 1.29 (s, 1H). **¹³C-NMR** (75 MHz, CDCl₃) δ (ppm): 143.88 (C), 143.86 (C), 136.01 (C), 135.50 (C), 134.44 (C), 129.93 (CH), 128.67 (CH), 128.26 (CH), 127.52 (CH), 127.35 (CH), 127.02 (CH), 127.01 (CH), 126.97 (CH), 126.26 (CH), 110.17 (CH), 66.30 (CH₂), 49.52 (CH₂), 48.80 (CH), 33.10 (CH₂), 21.69 (CH₃). **LRMS** (*m/z*, ESI): 478.12 [M+Na]⁺, 456.14 [M+H]⁺, 311.03, 300.10. **HRMS** Calculated for C₂₅H₂₆ClNNaO₃S: 478.1214, found 478.1216.

3. Representative procedure for the enantioselective α-alkylation of aldehydes with allenamides

Procedure C: exemplified for the reaction between **17a** *and* **18a**.

To a solution of IPrAuNTf₂ (13.84 mg, 0.016 mmol), 2,2'-bipyridine (4.99 mg, 0.032 mmol) and benzoic acid (3.90 mg, 0.032 mmol) in Toluene (0.5 ml), was sequentially added a solution of 2-phenylpropanal (**18a**, 42.8 µl, 0.320 mmol) and (*S*)-(-)-α,α-diphenyl-2-pyrrolidinemethanol trimethylsilyl ether (**C1**, 9.95 µl, 0.032 mmol) in Toluene (0.5 ml), followed by addition of a solution of 3-(propa-1,2-dien-1-yl)oxazolidin-2-one (**17a**, 20 mg, 0.160 mmol) in Toluene (0.5 ml; dropwise addition), under Argon atmosphere, in a dried Schlenk tube at 60 °C. The mixture was stirred at that temperature until the allenamide was consumed (the progress of the reaction was easily monitored by tlc) and filtered through a short pad of Florisil®, eluting with EtOAc. The solvent was removed, and the crude residue was dissolved in 0.6 ml of a 1,3,5-trimethoxybenzene 0.0887 M solution in CDCl₃ for ¹H-NMR analysis. The crude mixture was then purified on column chromatography (hexanes/EtOAc 10-40%), affording 28.3 mg of **19aa** (66% yield). For the analysis of the enantiomeric excess, the sample was prepared as follows: 2 mg of **19aa** were dissolved in 20 µl of CH₂Cl₂ (for HPLC), diluted with 1.5 ml of *i*PrOH (for HPLC) and filtered through a syringe filter.

Procedure D: exemplified for the reaction between **17a** *and* **18g**.

To a solution of IPrAuNTf₂ (13.84 mg, 0.016 mmol), 2,2'-bipyridine (4.99 mg, 0.032 mmol) and benzoic acid (3.90 mg, 0.032 mmol) in Toluene (0.5 ml), was sequentially added a solution of 2-phenylacetaldehyde (**18g**, 37.4 µl, 0.320 mmol) and (*S*)-(-)-α,α-diphenyl-2-pyrrolidinemethanol trimethylsilyl ether (**C1**, 9.95 µl, 0.032 mmol) in Toluene (0.5 ml),

followed by addition of a solution of 3-(propa-1,2-dien-1-yl)oxazolidin-2-one (**17a**, 20 mg, 0.160 mmol) in Toluene (0.5 ml; dropwise addition), under Argon atmosphere, in a dried Schlenk tube at 60 °C. The mixture was stirred at that temperature until the allenamide was consumed (the progress of the reaction was easily monitored by tlc). The reaction is quenched by the addition of a solution of NaBH$_4$ (24.21 mg, 0.64 mmol) in MeOH (2 ml), stirred for 0.5 hours and filtered through a short pad of Florisil®, eluting with EtOAc. The solvent was removed, and the crude residue was dissolved in 0.6 ml of a 1,3,5-trimethoxybenzene 0.0887 M solution in CDCl$_3$ for ^{1}H-NMR analysis. The crude mixture was then purified on column chromatography (hexanes/EtOAc 10-40%), affording 39.2 mg of **20ag** (>99% yield). For the analysis of the enantiomeric excess, the sample was prepared as follows: 2 mg of **20ag** were dissolved in 20 μl of CH$_2$Cl$_2$ (for HPLC), diluted with 1.5 ml of *i*PrOH (for HPLC) and filtered through a syringe filter.

(*E*)-2-methyl-5-(2-oxooxazolidin-3-yl)-2-phenylpent-4-enal (19aa)
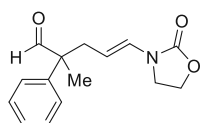
Procedure C: colorless oil, 66% yield, 72% ee. Enantioselectivity was determined by chiral HPLC analysis on Chiralpak® OZ-H at rt, (Hexane : iPrOH = 90:10, 1 ml/min).
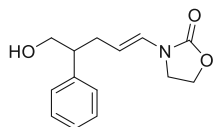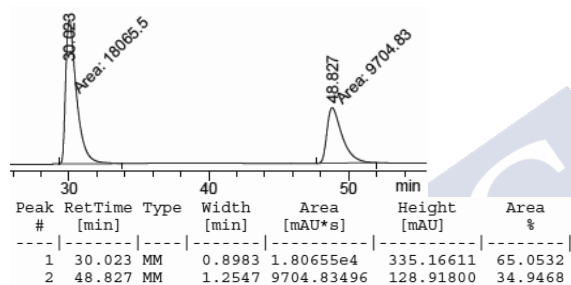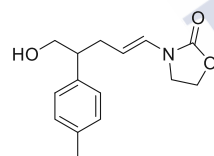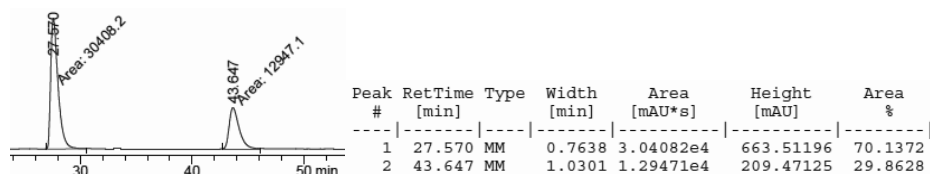
Racemic sample of **19aa**:
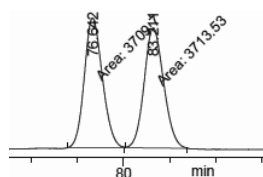
Peak #	RetTime [min]	Type	Width [min]	Area [mAU*s]	Height [mAU]	Area %
1	76.642	MM	2.2606	3709.70435	27.35040	49.9742
2	83.211	MM	2.4434	3713.52856	25.33021	50.0258

Enantioenriched sample of **19aa**, 86:14 er, 72% ee:
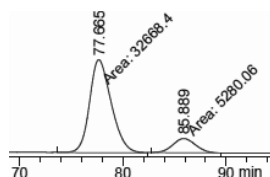
Peak #	RetTime [min]	Type	Width [min]	Area [mAU*s]	Height [mAU]	Area %
1	77.665	MM	2.4446	3.26684e4	222.72377	86.0862
2	85.889	MM	2.5720	5280.05957	34.21497	13.9138

(*E*)-2-(4-methoxyphenyl)-2-methyl-5-(2-oxooxazolidin-3-yl)pent-4-enal (19ab)
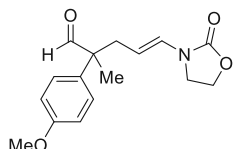
Procedure C: colorless oil, 40% yield, 68% ee. Enantioselectivity was determined by chiral HPLC analysis on Chiralpak® IA at rt, (Hexane : iPrOH = 80:20, 1 ml/min).
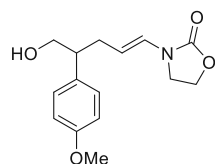
Racemic sample of **19ab**:

Peak #	RetTime [min]	Type	Width [min]	Area [mAU*s]	Height [mAU]	Area %
1	29.923	MM	0.9165	2.28647e4	415.78238	51.0174
2	37.047	MM	1.0549	2.19528e4	346.83911	48.9826
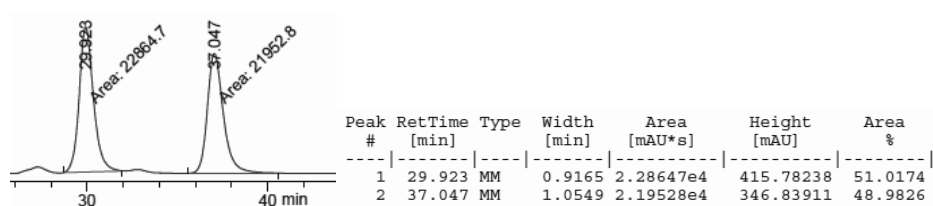
Enantioenriched sample of **19ab**, 84:16 er, 68% ee:

Peak #	RetTime [min]	Type	Width [min]	Area [mAU*s]	Height [mAU]	Area %
1	29.820	MM	0.9028	2.52840e4	466.77127	84.0606
2	36.997	MM	0.9983	4794.30225	80.03907	15.9394
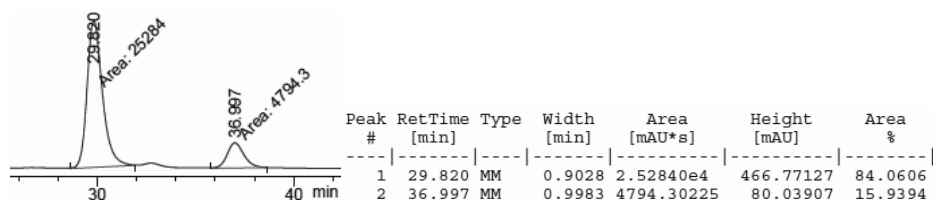
(*E*)-3-(4-(3-chlorophenyl)-5-hydroxy-4-methylpent-1-en-1-yl)oxazolidin-2-one (20ad)
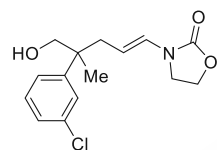
Procedure D:[211] colorless oil, 18% yield, 16% ee. Enantioselectivity was determined by chiral HPLC analysis on Chiralpak® IA3 at rt, (Hexane : iPrOH = 90:10, 1 ml/min).
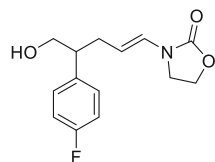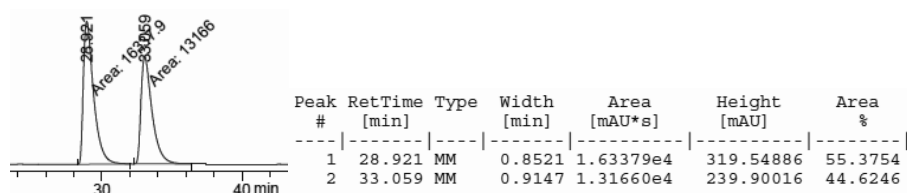
Racemic sample of **20ad**:

Peak #	RetTime [min]	Type	Width [min]	Area [mAU*s]	Height [mAU]	Area %
1	46.499	MM	1.2175	2349.27051	32.16026	49.7352
2	135.036	MM	2.9685	2374.28784	13.33028	50.2648

---
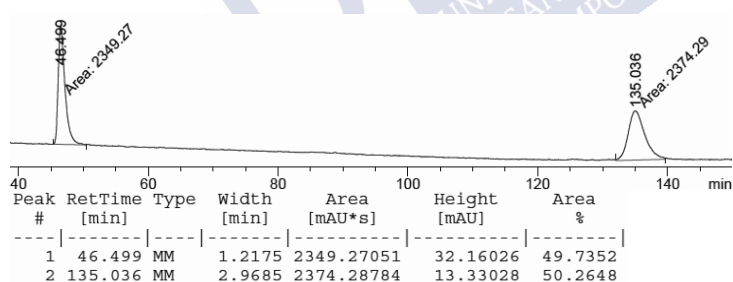
[211] Reaction carried out at 100 °C instead of at 60 °C.

Enantioenriched sample of **20ad**, 58:42 er, 16% ee:
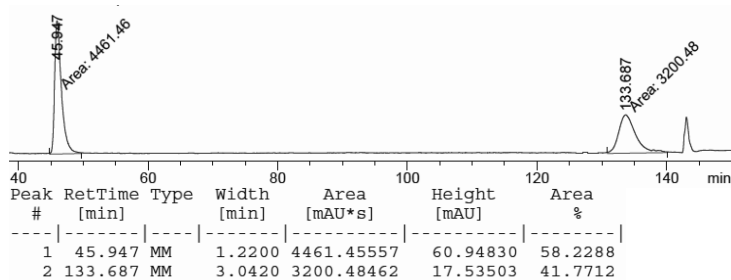
Peak #	RetTime [min]	Type	Width [min]	Area [mAU*s]	Height [mAU]	Area %
1	45.947	MM	1.2200	4461.45557	60.94830	58.2288
2	133.687	MM	3.0420	3200.48462	17.53503	41.7712

(*E*)-2-methyl-5-(2-oxooxazolidin-3-yl)-2-(5,6,7,8-tetrahydronaphthalen-2-yl)pent-4-enal (19af)
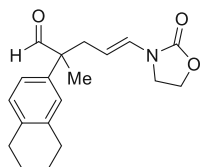
Procedure C: colorless oil, 47% yield, 70% ee. Enantioselectivity was determined by chiral HPLC analysis on Chiralpak® IA3 at rt, (Hexane : iPrOH = 90:10, 1 ml/min).
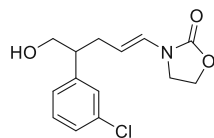
Racemic sample of **19af**:

Peak #	RetTime [min]	Type	Width [min]	Area [mAU*s]	Height [mAU]	Area %
1	21.211	MM	0.6458	1.94195e4	501.18527	50.6963
2	28.894	MM	0.8057	1.88861e4	390.67252	49.3037
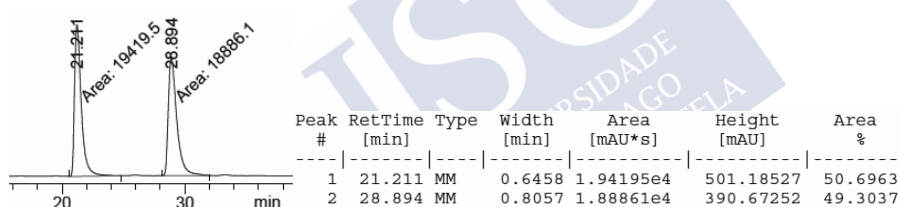
Enantioenriched sample of **19af**, 85:15 er, 70% ee:

Peak #	RetTime [min]	Type	Width [min]	Area [mAU*s]	Height [mAU]	Area %
1	19.950	MM	0.5954	1.37630e4	385.23096	84.5960
2	27.366	MM	0.6980	2506.10303	59.83680	15.4040
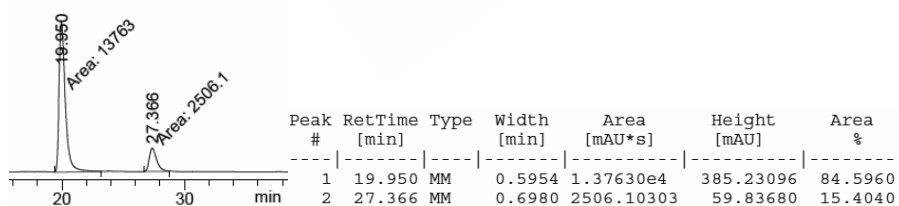
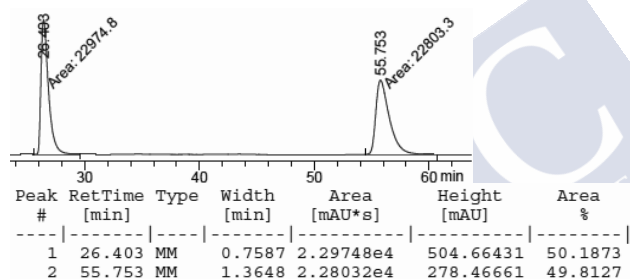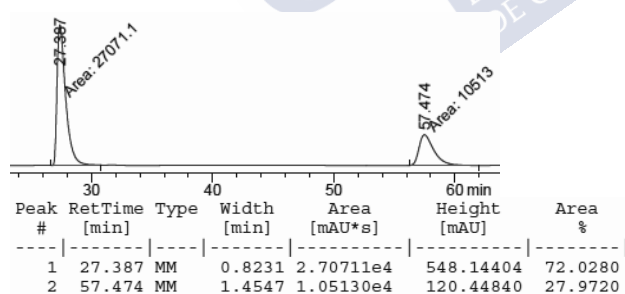## (*E*)-3-(5-hydroxy-4-phenylpent-1-en-1-yl)oxazolidin-2-one (20ag)

Procedure D: colorless oil, 98% yield, 30% ee. Enantioselectivity was determined by chiral HPLC analysis on Chiralpak® IA3 at rt, (Hexane : iPrOH = 85:15, 1 ml/min).
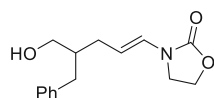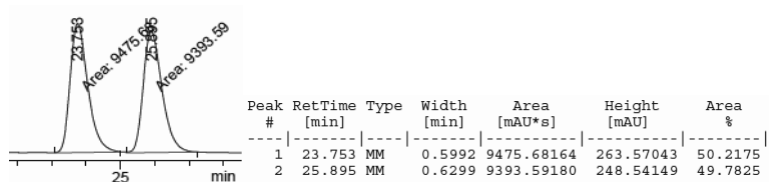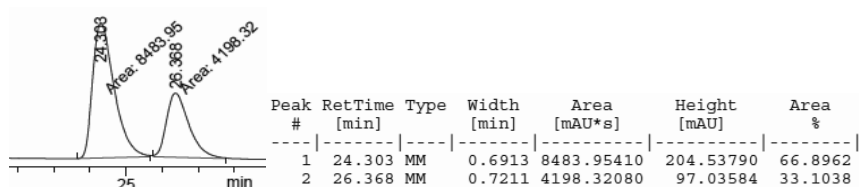
Racemic sample of **20ag**:

Peak #	RetTime [min]	Type	Width [min]	Area [mAU*s]	Height [mAU]	Area %
1	30.339	MM	0.7974	1.48156e4	309.66888	50.2126
2	50.961	MM	1.2468	1.46902e4	196.36877	49.7874
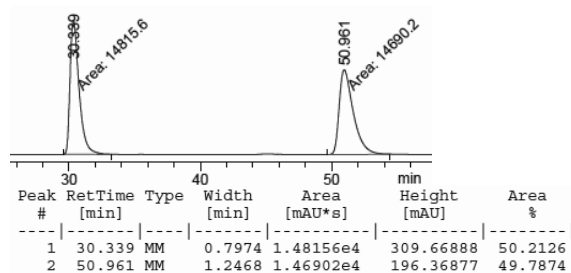
Enantioenriched sample of **20ag**, 65:35 er, 30% ee:

Peak #	RetTime [min]	Type	Width [min]	Area [mAU*s]	Height [mAU]	Area %
1	30.023	MM	0.8983	1.80655e4	335.16611	65.0532
2	48.827	MM	1.2547	9704.83496	128.91800	34.9468

(*E*)-3-(5-hydroxy-4-(p-tolyl)pent-1-en-1-yl)oxazolidin-2-one (20ah)

Procedure D: colorless oil, 96% yield, 40% ee. Enantioselectivity was determined by chiral HPLC analysis on Chiralpak® IA3 at rt, (Hexane : iPrOH = 85:15, 1 ml/min).

Racemic sample of **20ah**:

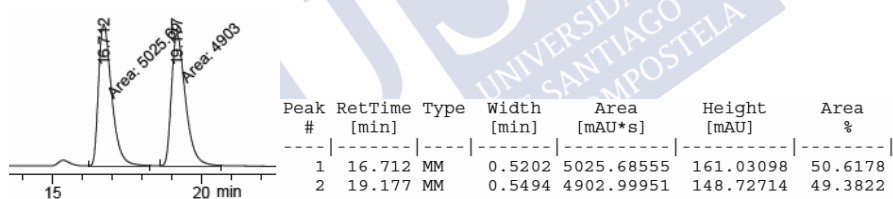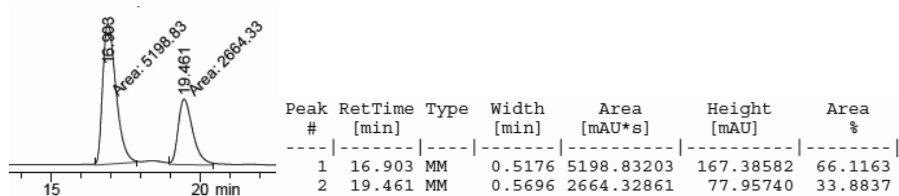| Peak #	RetTime [min]	Type	Width [min]	Area [mAU*s]	Height [mAU]	Area %
1	28.296	MM	0.7015	1.88546e4	447.98538	50.2859
2	45.755	MM	1.0272	1.86402e4	302.43173	49.7141
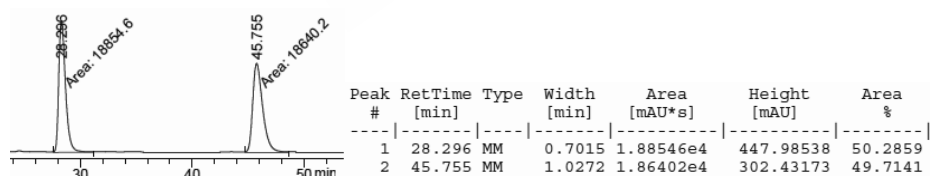
Enantioenriched sample of **20ah**, 70:30 er, 40% ee:

Peak #	RetTime [min]	Type	Width [min]	Area [mAU*s]	Height [mAU]	Area %
1	27.570	MM	0.7638	3.04082e4	663.51196	70.1372
2	43.647	MM	1.0301	1.29471e4	209.47125	29.8628

(*E*)-3-(5-hydroxy-4-(4-methoxyphenyl)pent-1-en-1-yl)oxazolidin-2-one (20ai)

Procedure D: colorless oil, 81% yield, 36% ee. Enantioselectivity was determined by chiral HPLC analysis on Chiralpak® IA3 at rt, (Hexane : iPrOH = 85:15, 1 ml/min).
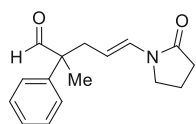
Racemic sample of **20ai**:
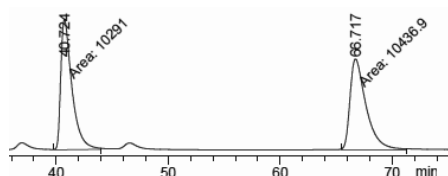
Peak #	RetTime [min]	Type	Width [min]	Area [mAU*s]	Height [mAU]	Area %
1	40.724	MM	1.1530	1.02910e4	148.75505	49.6481
2	66.717	MM	1.6737	1.04369e4	103.93082	50.3519

Enantioenriched sample of **20ai**, 68:32 er, 36% ee:
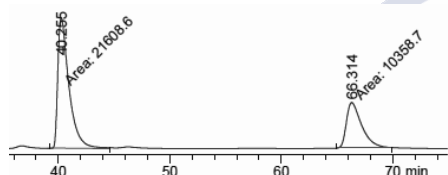
Peak #	RetTime [min]	Type	Width [min]	Area [mAU*s]	Height [mAU]	Area %
1	40.255	MM	1.1602	2.16086e4	310.42313	67.5960
2	66.314	MM	1.5951	1.03587e4	108.23364	32.4040

(*E*)-3-(4-(4-fluorophenyl)-5-hydroxypent-1-en-1-yl)oxazolidin-2-one (20aj)

Procedure D: colorless oil, 99% yield, 10% ee. Enantioselectivity was determined by chiral HPLC analysis on Chiralpak® IA3 at rt, (Hexane : iPrOH = 85:15, 1 ml/min).
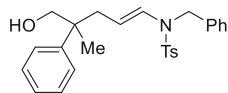
Racemic sample of **20aj**:
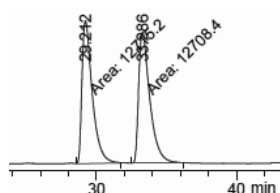
Peak #	RetTime [min]	Type	Width [min]	Area [mAU*s]	Height [mAU]	Area %
1	29.212	MM	0.8534	1.27152e4	248.33220	50.0132
2	33.286	MM	0.9302	1.27084e4	227.70398	49.9868

Enantioenriched sample of **20aj**, 55:45 er, 10% ee:

Peak #	RetTime [min]	Type	Width [min]	Area [mAU*s]	Height [mAU]	Area %
1	28.921	MM	0.8521	1.63379e4	319.54886	55.3754
2	33.059	MM	0.9147	1.31660e4	239.90016	44.6246

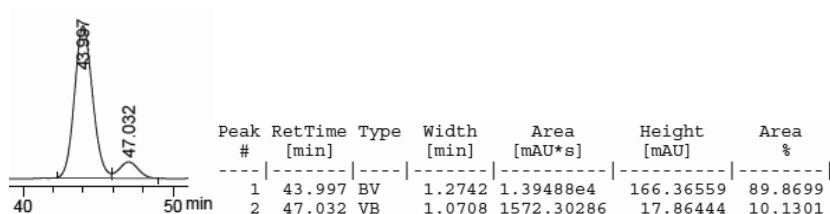**(*E*)-3-(4-(3-chlorophenyl)-5-hydroxypent-1-en-1-yl)oxazolidin-2-one (20ak)**

Procedure D: colorless oil, 99% yield, 44% ee. Enantioselectivity was determined by chiral HPLC analysis on Chiralpak® IA3 at rt, (Hexane : iPrOH = 85:15, 1 ml/min).
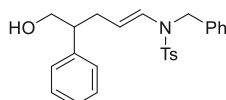
Racemic sample of **20ak**:

Peak #	RetTime [min]	Type	Width [min]	Area [mAU*s]	Height [mAU]	Area %
1	26.403	MM	0.7587	2.29748e4	504.66431	50.1873
2	55.753	MM	1.3648	2.28032e4	278.46661	49.8127

Enantioenriched sample of **20ak**, 72:28 er, 44% ee:

Peak #	RetTime [min]	Type	Width [min]	Area [mAU*s]	Height [mAU]	Area %
1	27.387	MM	0.8231	2.70711e4	548.14404	72.0280
2	57.474	MM	1.4547	1.05130e4	120.44840	27.9720

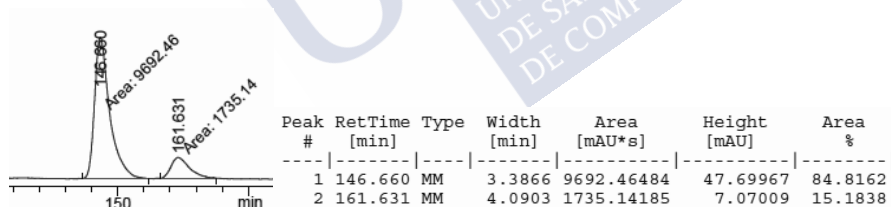**(*E*)-3-(4-benzyl-5-hydroxypent-1-en-1-yl)oxazolidin-2-one (20am)**

Procedure D:[212] colorless oil, 45% yield, 34% ee. Enantioselectivity was determined by chiral HPLC analysis on Chiralpak® IA3 at rt, (Hexane : iPrOH = 85:15, 1 ml/min).
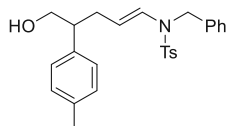
---

[212] Reaction carried out using acetonitrile as solvent instead of toluene.

Racemic sample of **20am**:

Peak #	RetTime [min]	Type	Width [min]	Area [mAU*s]	Height [mAU]	Area %
1	23.753	MM	0.5992	9475.68164	263.57043	50.2175
2	25.895	MM	0.6299	9393.59180	248.54149	49.7825

Enantioenriched sample of **20am**, 67:33 er, 34% ee:

Peak #	RetTime [min]	Type	Width [min]	Area [mAU*s]	Height [mAU]	Area %
1	24.303	MM	0.6913	8483.95410	204.53790	66.8962
2	26.368	MM	0.7211	4198.32080	97.03584	33.1038

(*E*)-3-(4-(hydroxymethyl)-5-methylhex-1-en-1-yl)oxazolidin-2-one (20an)
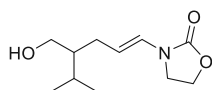
Procedure D:[212] colorless oil, 31% yield, 32% ee Enantioselectivity was determined by chiral HPLC analysis on Chiralpak® IA3 at rt, (Hexane : iPrOH = 85:15, 1 ml/min).
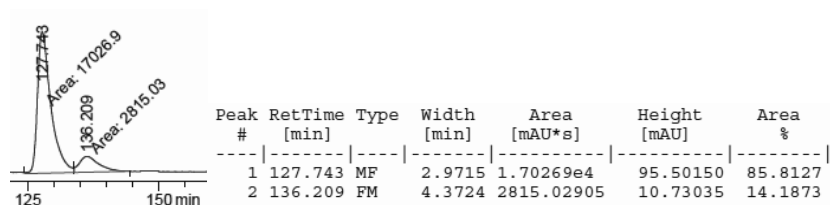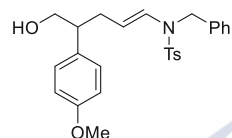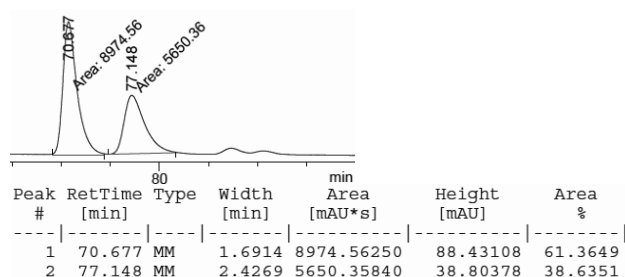
Racemic sample of **20an**:

Peak #	RetTime [min]	Type	Width [min]	Area [mAU*s]	Height [mAU]	Area %
1	16.712	MM	0.5202	5025.68555	161.03098	50.6178
2	19.177	MM	0.5494	4902.99951	148.72714	49.3822

Enantioenriched sample of **20an**, 66:34 er, 32% ee:

Peak #	RetTime [min]	Type	Width [min]	Area [mAU*s]	Height [mAU]	Area %
1	16.903	MM	0.5176	5198.83203	167.38582	66.1163
2	19.461	MM	0.5696	2664.32861	77.95740	33.8837

---

[212] Reaction carried out using acetonitrile as solvent instead of toluene.

(E)-2-methyl-5-(2-oxopyrrolidin-1-yl)-2-phenylpent-4-enal (19ca)

Procedure C: colorless oil, 50% yield, 82% ee. Enantioselectivity was determined by chiral HPLC analysis on Chiralpak® IA3 at rt, (Hexane : iPrOH = 85:15, 1 ml/min).

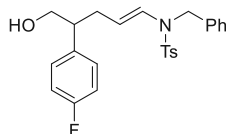Racemic sample of **19ca**:
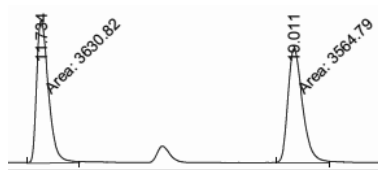
Peak #	RetTime [min]	Type	Width [min]	Area [mAU*s]	Height [mAU]	Area %
1	11.734	MM	0.3953	3630.82056	153.09007	50.4588
2	19.011	MM	0.4863	3564.79321	122.16275	49.5412

Enantioenriched sample of **19ca**, 91:9 er, 82% ee:
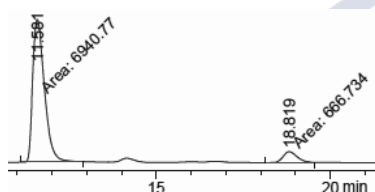
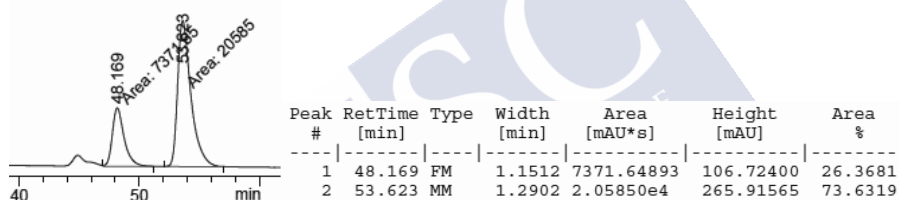| Peak #	RetTime [min]	Type	Width [min]	Area [mAU*s]	Height [mAU]	Area %
1	11.581	MM	0.3933	6940.77100	294.10605	91.2358
2	18.819	MM	0.4873	666.73438	22.80306	8.7642

(*E*)-N-benzyl-N-(5-hydroxy-4-methyl-4-phenylpent-1-en-1-yl)-4-methylbenzenesulfonamide (20ea)

Procedure D: colorless oil, 50% yield, 80% ee. Enantioselectivity was determined by chiral HPLC analysis on Chiralpak OZ-H at rt, (Hexane : iPrOH = 90:10, 0.5 ml/min).
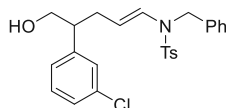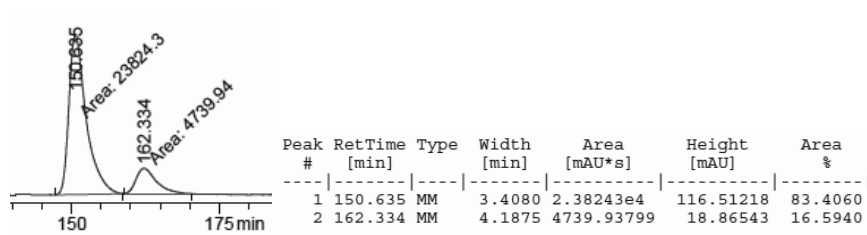
Racemic sample of **20ea**:
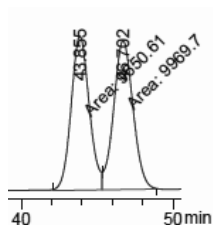
Peak #	RetTime [min]	Type	Width [min]	Area [mAU*s]	Height [mAU]	Area %
1	43.855	MF	1.3876	9650.60547	115.91866	49.1868
2	46.702	FM	1.4827	9969.70312	112.06666	50.8132

Enantioenriched sample of **20ea**, 90:10, 80% ee:

Peak #	RetTime [min]	Type	Width [min]	Area [mAU*s]	Height [mAU]	Area %
1	43.997	BV	1.2742	1.39488e4	166.36559	89.8699
2	47.032	VB	1.0708	1572.30286	17.86444	10.1301

(*E*)-N-benzyl-N-(5-hydroxy-4-phenylpent-1-en-1-yl)-4-methylbenzenesulfonamide (20eg)

Procedure D: colorless oil, 99% yield, 70% ee. Enantioselectivity was determined by chiral HPLC analysis on Chiralpak® IA3 at rt, (Hexane : iPrOH = 95:5, 1 ml/min).

Racemic sample of **20eg**:

Peak #	RetTime [min]	Type	Width [min]	Area [mAU*s]	Height [mAU]	Area %
1	142.482	MM	3.0457	5907.63379	32.32792	50.0369
2	156.064	MM	3.8935	5898.90967	25.25123	49.9631
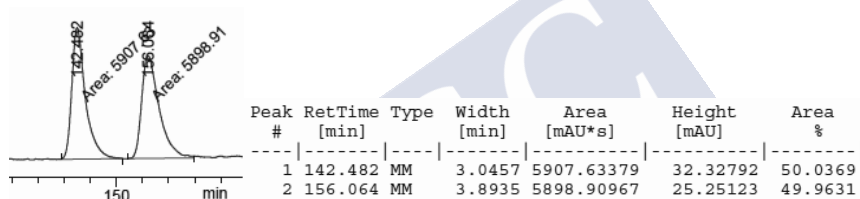
Enantioenriched sample of **20eg**, 85:15 er, 70% ee:

Peak #	RetTime [min]	Type	Width [min]	Area [mAU*s]	Height [mAU]	Area %
1	146.660	MM	3.3866	9692.46484	47.69967	84.8162
2	161.631	MM	4.0903	1735.14185	7.07009	15.1838

(*E*)-N-benzyl-N-(5-hydroxy-4-(p-tolyl)pent-1-en-1-yl)-4-methylbenzenesulfonamide (20eh)

Procedure D: colorless oil, 99% yield, 72% ee. Enantioselectivity was determined by chiral HPLC analysis on Chiralpak® IA3 at rt, (Hexane : iPrOH = 95:5, 1 ml/min).

Racemic sample of **20eh**:


```
Peak RetTime Type  Width     Area     Height   Area
  #   [min]        [min]    [mAU*s]    [mAU]     %
----|-------|----|-------|----------|---------|--------|
  1 130.800 MF   2.9532 9351.25488   52.77546 50.1614
  2 138.252 FM   4.5219 9291.09082   34.24477 49.8386
```
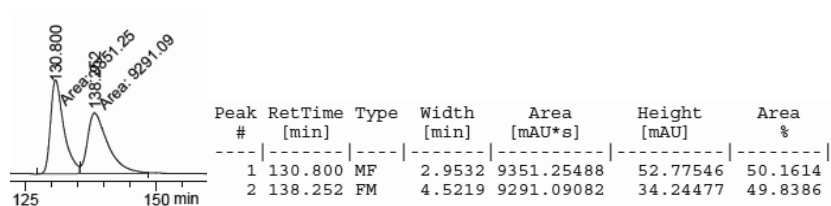
Enantioenriched sample of **20eh**, 86:14 er, 72% ee:


```
Peak RetTime Type  Width     Area     Height   Area
  #   [min]        [min]    [mAU*s]    [mAU]     %
----|-------|----|-------|----------|---------|--------|
  1 127.743 MF   2.9715 1.70269e4    95.50150 85.8127
  2 136.209 FM   4.3724 2815.02905   10.73035 14.1873
```

(*E*)-N-benzyl-N-(5-hydroxy-4-(4-methoxyphenyl)pent-1-en-1-yl)-4-methylbenzenesulfonamide (20ei)

Procedure D: colorless oil, 99% yield, 22% ee. Enantioselectivity was determined by chiral HPLC analysis on Chiralpak® IA3 at rt, (Hexane : iPrOH = 90:10, 1 ml/min).

Racemic sample of **20ei**:


```
Peak RetTime Type  Width     Area     Height   Area
  #   [min]        [min]    [mAU*s]    [mAU]     %
----|-------|----|-------|----------|---------|--------|
  1  70.485 MM   1.6582 5714.65674   57.43891 51.0414
  2  77.200 MM   2.4831 5481.46973   36.79199 48.9586
```
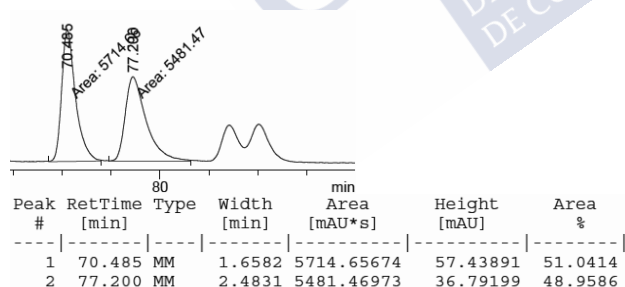
Enantioenriched sample of **20ei**, 61:39 er, 22% ee:


```
Peak RetTime Type  Width     Area     Height   Area
  #   [min]        [min]    [mAU*s]    [mAU]     %
----|-------|----|-------|----------|---------|--------|
  1  70.677 MM   1.6914 8974.56250   88.43108 61.3649
  2  77.148 MM   2.4269 5650.35840   38.80378 38.6351
```

(*E*)-N-benzyl-N-(4-(4-fluorophenyl)-5-hydroxypent-1-en-1-yl)-4-methylbenzenesulfonamide (20ej)

Procedure D: colorless oil, 99% yield, 48% ee. Enantioselectivity was determined by chiral HPLC analysis on Chiralpak® IA3 at rt, (Hexane : iPrOH = 90:10, 1 ml/min).

Racemic sample of **20ej**:

Peak #	RetTime [min]	Type	Width [min]	Area [mAU*s]	Height [mAU]	Area %
1	47.376	FM	1.1112	1.09596e4	164.37982	50.0251
2	52.895	MM	1.2291	1.09486e4	148.46262	49.9749
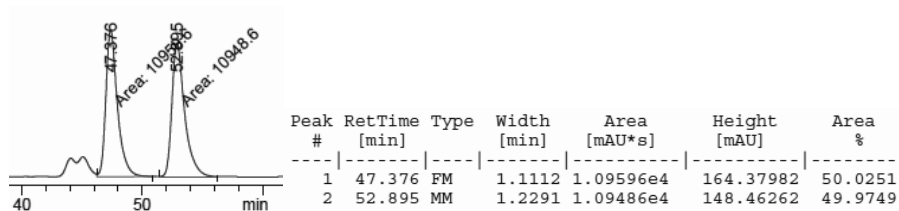
Enantioenriched sample of **20ej**, 26:74 er, 48% ee:

Peak #	RetTime [min]	Type	Width [min]	Area [mAU*s]	Height [mAU]	Area %
1	48.169	FM	1.1512	7371.64893	106.72400	26.3681
2	53.623	MM	1.2902	2.05850e4	265.91565	73.6319

(*E*)-N-benzyl-N-(4-(3-chlorophenyl)-5-hydroxypent-1-en-1-yl)-4-methylbenzenesulfonamide (20ek)

Procedure B: colorless oil, 99% yield, 66% ee. Enantioselectivity was determined by chiral HPLC analysis on Chiralpak® IA3 at rt, (Hexane : iPrOH = 95:5, 1 ml/min).

Racemic sample of **20ek**:

Peak #	RetTime [min]	Type	Width [min]	Area [mAU*s]	Height [mAU]	Area %
1	150.487	MF	3.4345	1.75565e4	85.19675	50.1688
2	160.723	FM	4.2543	1.74383e4	68.31705	49.8312
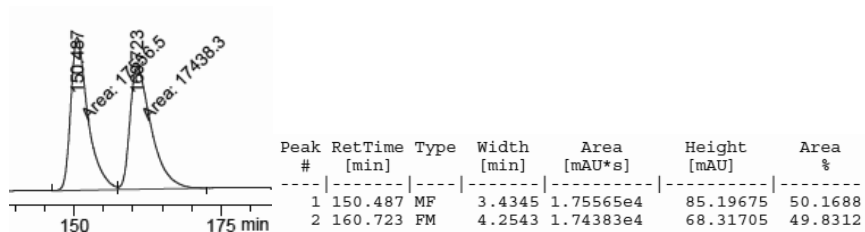
Enantioenriched sample of **20ek**, 83:17 er, 66% ee:

Peak #	RetTime [min]	Type	Width [min]	Area [mAU*s]	Height [mAU]	Area %
1	150.635	MM	3.4080	2.38243e4	116.51218	83.4060
2	162.334	MM	4.1875	4739.93799	18.86543	16.5940

4. ^{31}P-NMR and ESI-MS experiments

4.1. General considerations

^{31}P-NMR experiments were carried out in VARIAN innova-500 (202 MHz for ^{31}P) using toluene-d_8 and in the presence of a sealed capillary containing 85% H_3PO_4 in D_2O. All the experiments were carried out at 60 °C. After running the ^{31}P-NMR experiment, and aliquot was taken to do ESI-MS experiments, which were carried out in an UHPLC-Mass with Bruker AmaZon SL IT-MS detector.

4.2. Ph$_3$PAuNTf$_2$

Ph$_3$PAuNTf$_2$ (2:1) toluene adduct (12,55 mg, 0.008 mmol) was dissolved in toluene-d_8 and added to a NMR tube containing a sealed capillary of 85% H_3PO_4 in D_2O. An aliquot was diluted with CH_2Cl_2 (for HPLC) and filtered through a syringe filter for ESI-MS analysis.

Ph$_3$PAuNTf$_2$ (toluene-d_8 complex, 2:1): ^{31}P-NMR: 31.12 ppm; ESI-MS (M$^+$): 559.14.
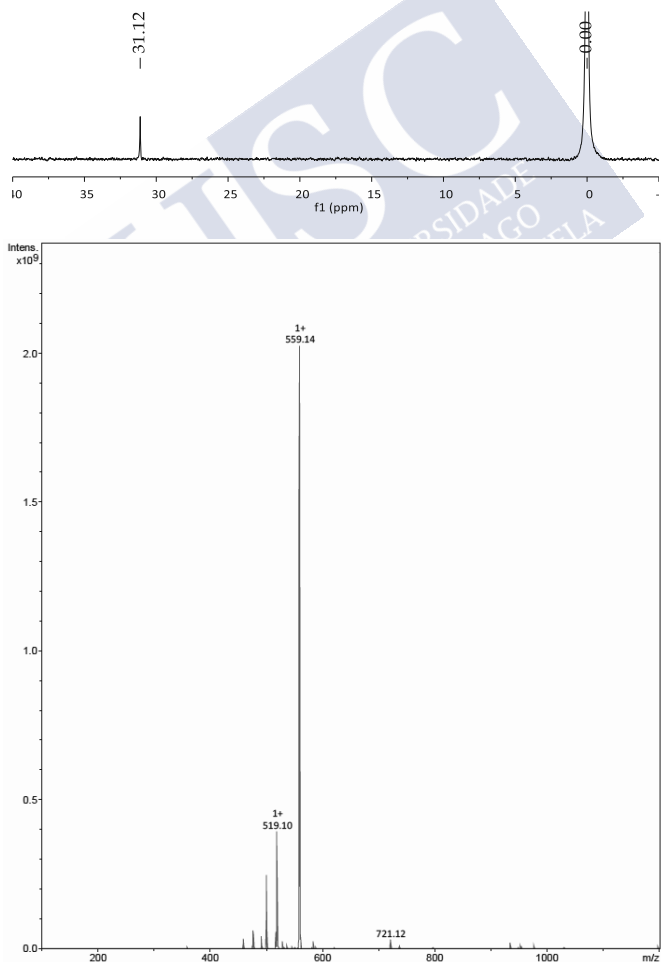
4.3. Ph₃PAu(bpy)NTf₂

Ph₃PAuNTf₂ (2:1) toluene adduct (12.55 mg, 0.008 mmol) was dissolved in toluene-d_8, followed by a subsequent addition of 2,2′-bipyridine (2.5 mg, 0.016 mmol), leading to the quantitative formation of Ph₃PAu(bpy)NTf₂ and added to a NMR tube containing a sealed capillary of 85% H_3PO_4 in D_2O. An aliquot was diluted with CH_2Cl_2 (for HPLC) and filtered through a syringe filter for ESI-MS analysis.

Ph₃PAu(bpy)NTf₂ (prepared by mixing bpy and Ph₃PAuNTf₂, ratio 1:1): ³¹P-NMR: 31.52 ppm; ESI-MS (M⁺): 615.17.
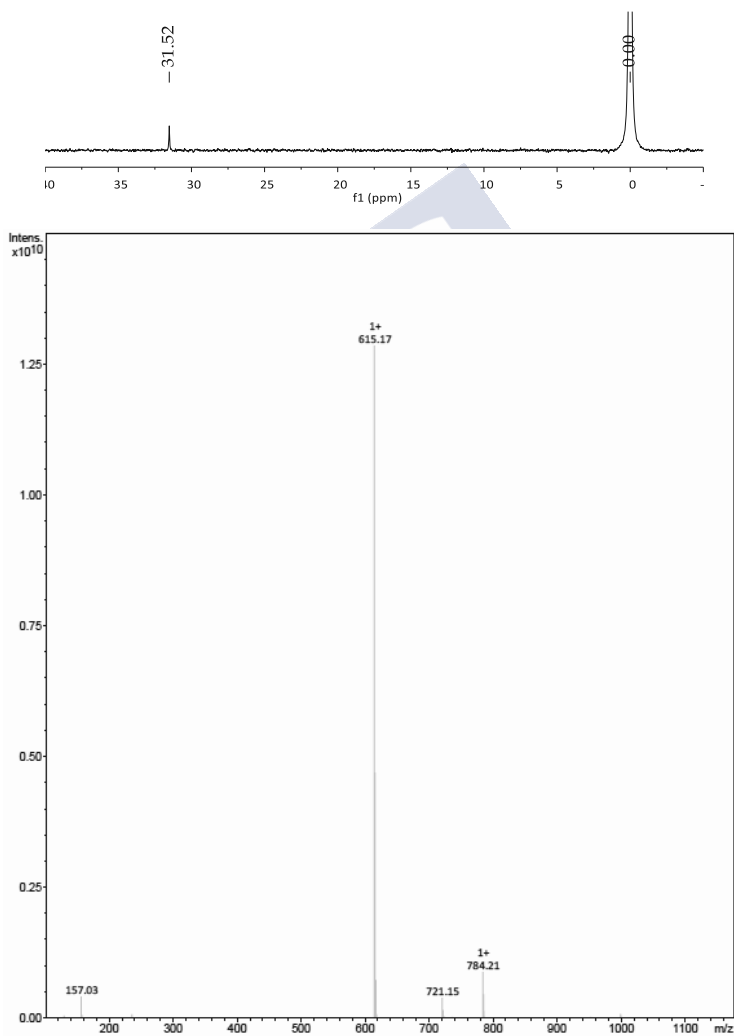
4.4. Ph₃PAu(C1)NTf₂

Ph₃PAuNTf₂ (2:1) toluene adduct (12.55 mg, 0.008 mmol) was dissolved in toluene-d_8, followed by a subsequent addition of (*S*)-(-)-α,α-diphenyl-2-pyrrolidinemethanol trimethylsilyl ether (**C1**, 5 μl, 0.016 mmol), leading to the quantitative formation of Ph₃PAu(C1)NTf₂ and added to a NMR tube containing a sealed capillary of 85% H₃PO₄ in D₂O. An aliquot was diluted with CH₂Cl₂ (for HPLC) and filtered through a syringe filter for ESI-MS analysis.

Ph₃PAu(C1)NTf₂ (prepared by mixing C1 and Ph₃PAuNTf₂, ratio 1:1): ³¹P-NMR: 30.55 ppm; ESI-MS (M⁺): 784.43.
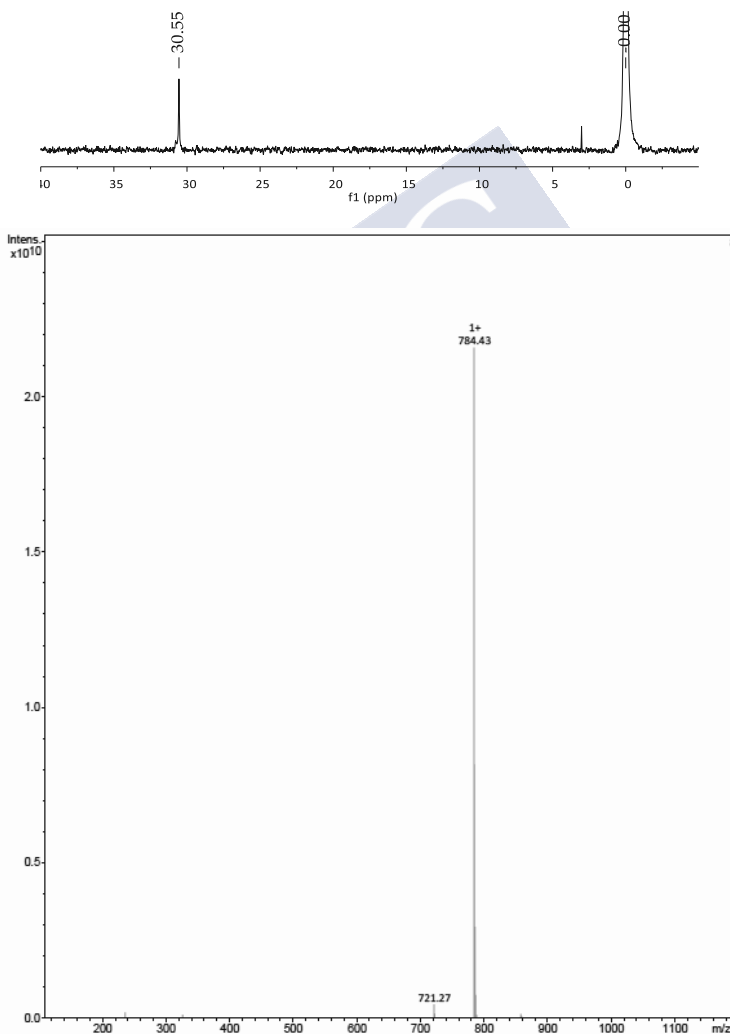
4.4. Ph₃PAu(C1)NTf₂ + 2,2'-bipyridine

To the preformed $Ph_3PAu(C1)NTf_2$ was added 2,2'-bipyridine (2.5 mg, 0.016 mmol) and transferred into a NMR tube containing a sealed capillary of 85% H_3PO_4 in D_2O. After doing the ^{31}P-NMR experiment, a subsequent addition of 2,2'-bipyridine (2.5 mg, 0.016 mmol, overall ratio $Ph_3PAu(C1)NTf_2$: bpy = 1:2) was added to the NMR tube and we measured the ^{31}P chemical shift. Finally, another addition of 2,2'-bipyridine (5 mg, 0.032 mmol, overall ratio $Ph_3PAu(C1)NTf_2$: bpy = 1:4). All the aliquots were taken at every step and diluted with CH_2Cl_2 (for HPLC) and filtered through a syringe filter for ESI-MS analysis.

a) $Ph_3PAu(C1)NTf_2$: bpy (ratio 1:1): ^{31}P-NMR: 30.58 ppm; ESI-MS (M⁺): 784.40.
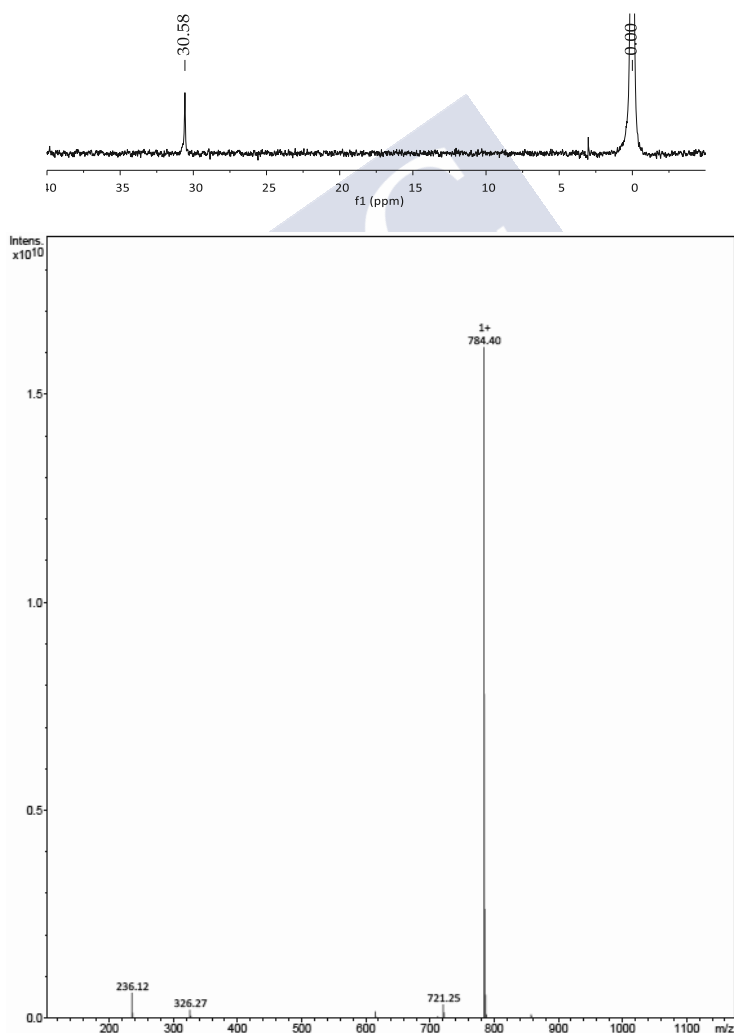
b) Ph$_3$PAu(C1)NTf$_2$: bpy (ratio 1:2): ^{31}P-NMR: 30.60 ppm; ESI-MS (M$^+$): 615.23; 784.40.
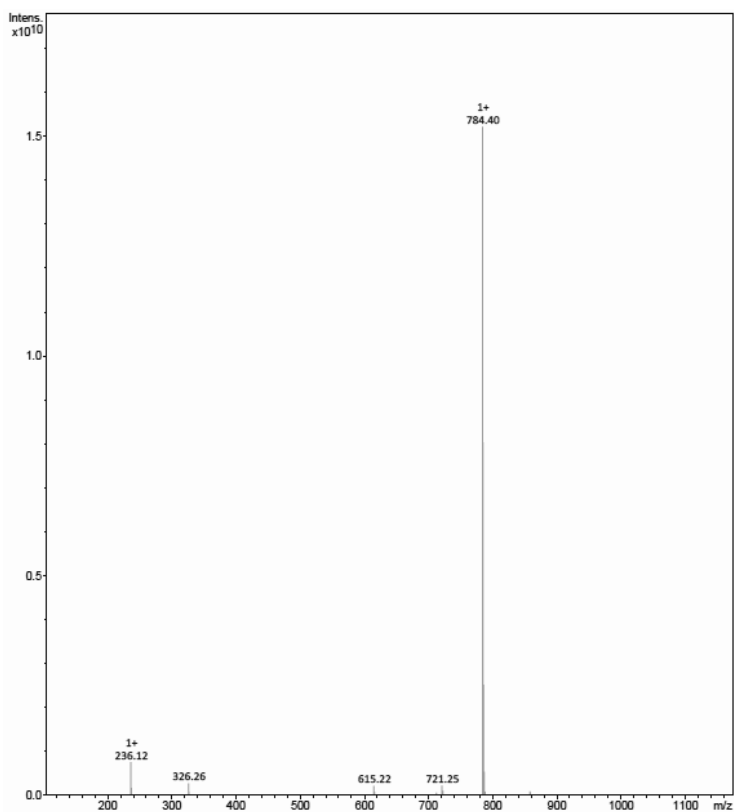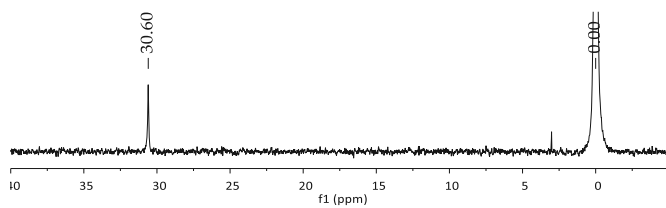
c) Ph$_3$PAu(C1)NTf$_2$: bpy (ratio 1:4): ^{31}P-NMR: 30.65 ppm; ESI-MS (M$^+$): 615.22; 784.42.
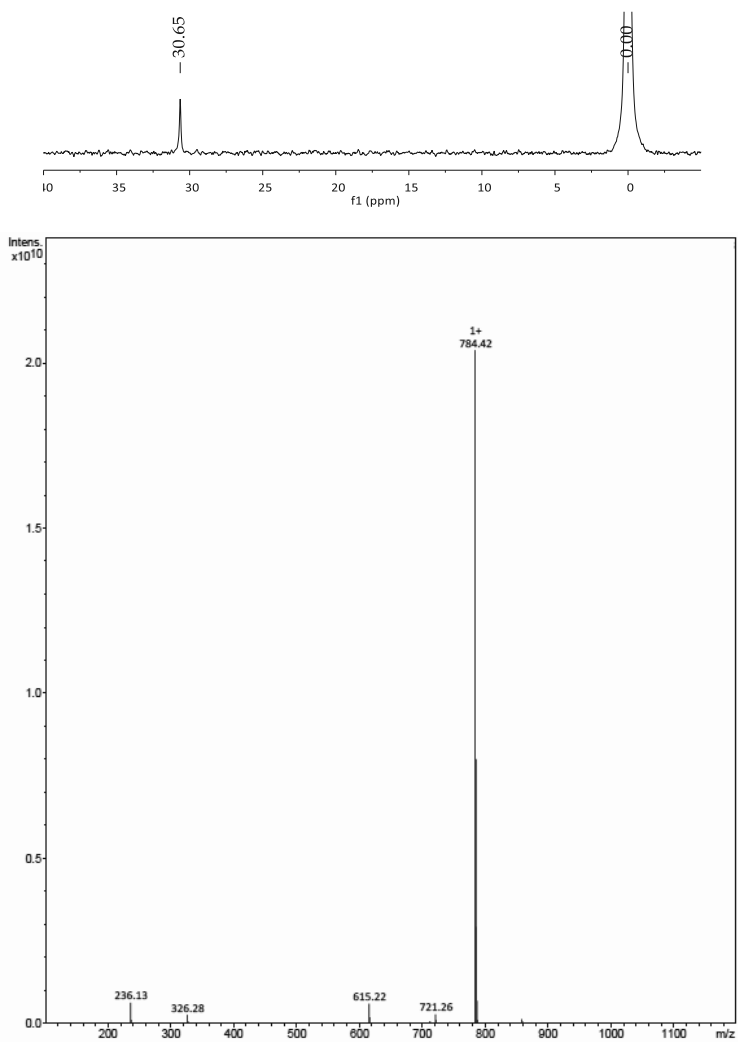
4.5. Ph₃PAu(bpy)NTf₂ + (S)-(-)-α,α-diphenyl-2-pyrrolidinemethanol trimethylsilyl ether (C1)

To the preformed Ph₃PAu(bpy)NTf₂ was added (*S*)-(-)-α,α-diphenyl-2-pyrrolidinemethanol trimethylsilyl ether (**C1**, 5 µl, 0.016 mmol) and transferred into a NMR tube containing a sealed capillary of 85% H_3PO_4 in D_2O. After doing the ^{31}P-NMR experiment, a subsequent addition of phenylacetaldehyde (9.36 µl, 0.080 mmol) was added to the NMR tube and we measured the ^{31}P chemical shift. All the aliquots were taken at every step and diluted with CH_2Cl_2 (for HPLC) and filtered through a syringe filter for ESI-MS analysis.

a) Ph₃PAu(bpy)NTf₂ : C1 (ratio 1:1): ^{31}P-NMR: 30.57 ppm; ESI-MS (M⁺): 784.40.
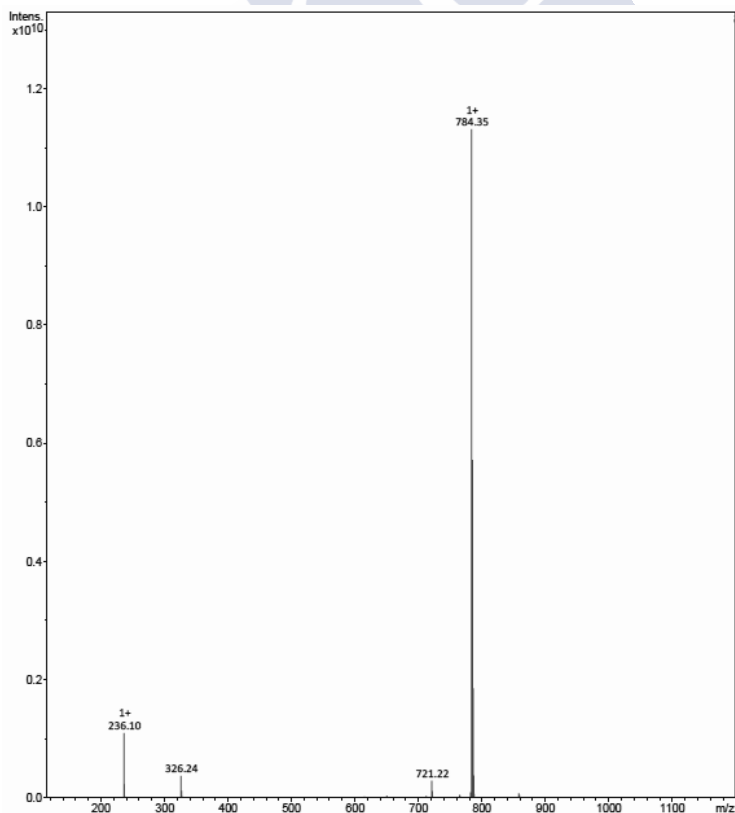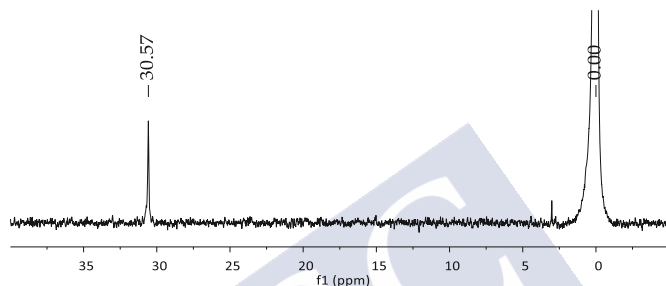
b) Ph$_3$PAu(bpy)NTf$_2$: C1 : phenylacetaldehyde (ratio 1:1:5): ^{31}P-NMR: 30.77 ppm; ESI-MS (M$^+$): 784.40.
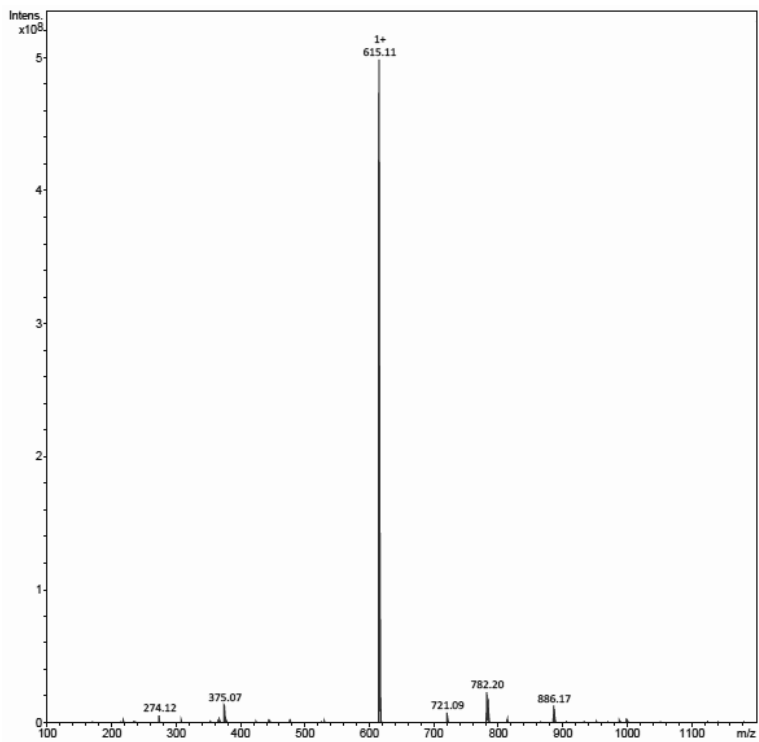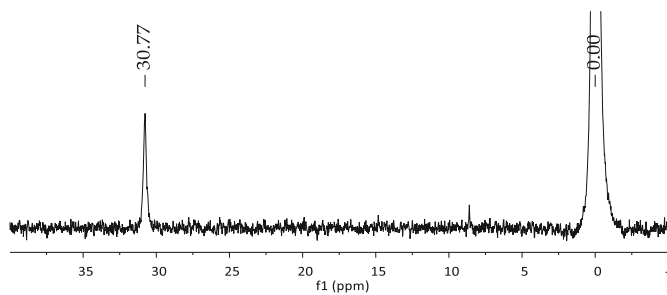
Chapter II: Asymmetric formal (2+2+2) cycloaddition between allenamides and alkenyl-oximes. Straightforward access to azabridged medium-sized carbocycles

Selected NMR spectra[216]

---

[216] In this section we only include the NMR spectra of the most representative compounds. In the attached CD-ROM, the corresponding NMR spectra of all the compounds of this thesis can be found.

Selected NMR spectra from Chapter I

19ab

20ag

20aj

20da

HO

Me

N—Ts

Ph

20ea

20eg